Design and analysis of a Robotic Tentacle arm using aMechanical multiplexer and Bowden cable system

Submitted in partial fulfilment of the requirements of the degree of

Bachelor of Technology in Mechanical Engineering

By

Bhavika Chawla	111810014
Aditya Potnis	111810071
Rohit Khadilkar	111810109
Kaushik Kunale	111813024

Project Guide:

Dr N K Chougule

Department of Mechanical Engineering,

College of Engineering Pune

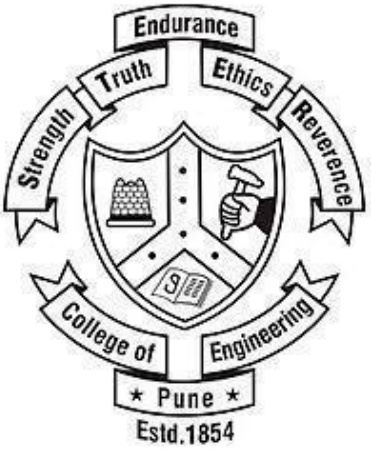

College of Engineering Pune

Department of Mechanical EngineeringAY 2021-22

Project Report

Group 31

Design and analysis of a Robotic Tentacle arm using a Mechanical multiplexer and Bowden cable system

Group Members-

Bhavika Chawla 111810014

Aditya Potnis 111810071

Rohit Khadilkar 111810109

Kaushik Kunale 111813024

Project Guide:

Dr N K Chougule

Department of Mechanical Engineering,College of Engineering Pune

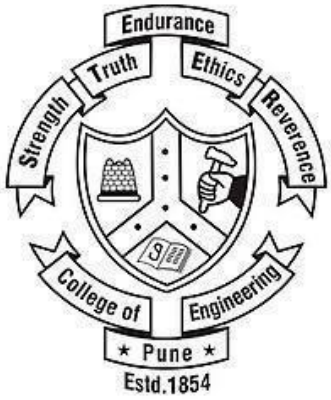

College of Engineering Pune

Department of Mechanical Engineering

AY 2021-22

Department of Mechanical Engineering

AY 2021-22

CERTIFICATE

This is to certify that the report titled **Design and analysis of a Robotic Tentacle arm using a Mechanical multiplexer and Bowden cable system** is submitted in the partial fulfillment of the requirement for the award of Bachelor of Technology of COEP, affiliated to Savitribai Phule Pune University, by

1. Bhavika Chawla 111810014
2. Aditya Potnis 111810071
3. Rohit Khadilkar 111810109
4. Kaushik Kunale 111813024

Dr. N.K. Chougule, Professor,
Department of Mechanical Engineering, COEP

Dr. M.R. Nandgaokar, Professor and Head,
Department of Mechanical Engineering, College of Engineering Pune

Date:

Place:

This report entitled

Design and analysis of a Robotic Tentacle arm using a Mechanical multiplexer and Bowden cable system

By

111410014	Bhavika Chawla
111810071	Aditya Potnis
111810109	Rohit Khadilkar
111813024	Kaushik Kunale

is approved for the degree of

Bachelor of Technology

Of

Department of Mechanical Engineering

College of Engineering Pune (An autonomous institute of Govt. of Maharashtra)

Examiners	Name	Signature
1. Internal Examiner	_____	
2. Supervisor (s)	_____	
	_____	
	_____	

Date:

Place:

Date:

Declaration

We declare that this written submission represents our ideas in our own words and where others' ideas or words have been included, we have adequately cited and referenced the original sources. We also declare that we have adhered to all principles of academic honesty and integrity and have not misrepresented or fabricated or falsified any idea/data/fact/source in our submission. We understand that any violation of the above will be cause for disciplinary action by the Institute and can also evoke penal action from the sources which have thus not been properly cited or from whom proper permission has not been taken when needed.

Signature

111810014 Bhavika Chawla _____

111810071 Aditya Potnis _____

111810109 Rohit Khadilkar _____

111813024 Kaushik Kunale _____

Place:

Abstract

This project report presents the overview of a tendon driven robotic arm which is maneuverable and compact. A distinctive feature of this arm is its mechanical multiplexer, which allows it to have a significant reduction in the number of motors required for its actuation. A Bowden cable mechanism is used to actuate the joints of the assembly. In this report, the three stages of development of the robotic arm are discussed in depth along with the design and methodology that was adopted for the three stages and the inverse kinematics which govern the arm's movement. The three stages of the design were-design of the arm assembly, design of the mechanical multiplexer and prototyping of the entire assembly. All the components of this assembly were printed using PLA(Polylactic Acid) on a 3D printer and proceeded with the assembly of the multiplexer and the arm. Testing was then done to verify the accuracy of the arm. This innovative design ensured that the assembly was both light and sturdy, with most of the components being readily available in the market as well as being cost efficient. This report also provides insight into the possible applications of this robotic arm in real life situations.

Contents

List of Figures **Page Nos**

Chapter 1 - Introduction to the project

Chapter 2- Literature review

Chapter 3 - Design overview

s

CHAPTER 1 - Introduction to the project

Aim

We propose the design of a redundant multi degrees of freedom tendon actuated robotic tentacle arm using a Bowden cable assembly for joint actuation with a mechanical multiplexer module to allow actuation joint selection and motor count reduction.

The novelty of the design is the mechanical multiplexers which can select joints and change the relative angle between the selected joints. The joints preserve angles passively until a mechanical multiplexer actuates them again.

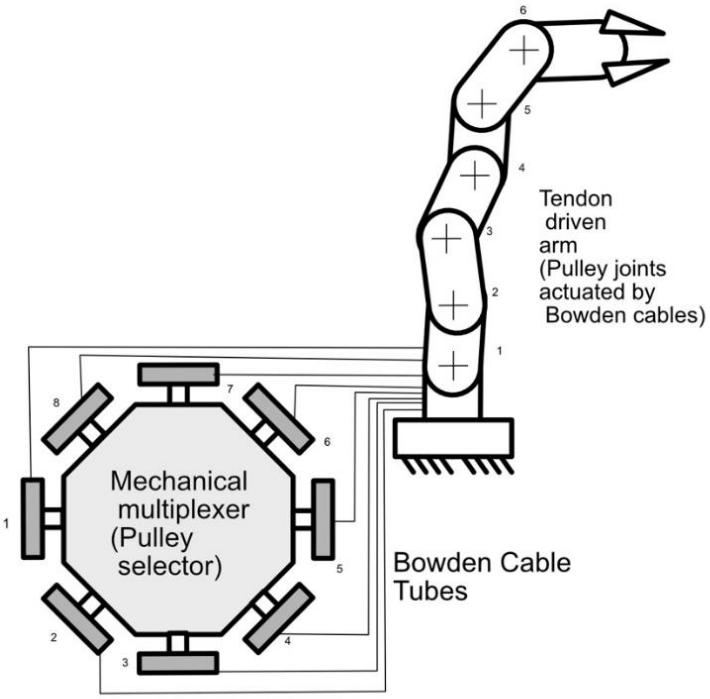

Figure 1 Concept block drawing

Introduction-

From elephant trunks to octopus' arms and human tongues, nature abounds with tentacles that are adept at manipulation. The use of tendons for the transmission of the forces and the movements in robotic devices has been investigated by several researchers all over the world. The interest in this kind of actuation is based on the possibility of optimizing the position of the actuators with respect to the moving part of the robot, in the reduced weight, high reliability, simplicity in the mechanical design and, finally, in the reduced cost of the resulting kinematic chain.

An ideal tentacle is a non-conventional robotic arm with infinite mobility. It has the capability of taking sophisticated shapes and of achieving any position and orientation in a 3D space. Recently, tendon driven robots have been used in many industrial fields. Especially, cable-driven parallel robots have been used in specialized industrial applications where dynamical features such as high accuracy in systems requiring quick transitions. Because of high sensitivity, low inertia, and large workspace, they have been even used in specialized industrial fields where dynamical features such as high speed and accuracy are required, as well as in systems requiring quick transitions between moving states and high positional accuracy, for example, surgical robots and pick-and-place robots.

History-

The concept of robotic arms isn't a new one. It dates to the late 1400s. In the 1950s, researchers studying Leonardo da Vinci's notebooks found drawings and sketches of everything from robotic arms to complete humanoid figurines that could have theoretically run on the clockwork technologies available at the time. These devices used pulleys, weights, and gears to provide semi-autonomous motion, centuries before we ever imagined using them for assembly or manufacturing.

Unimate introduced the first industrial robotic arm in 1961, it has subsequently evolved into the PUMA arm. The Rancho arm was designed; Minsky’s Tentacle arm appeared a few years later, Scheinman’s arm in 1969, and MIT’s Silver arm right after. Aird became the first cyborg human with a robotic arm in 1993.

Motivation and Necessity

The territory of robotic arms is still fairly new and many new improvements are being made to increase rigidity and accuracy of these arms. We hope to go deeper into this topic while analyzing and fixing real life problems with the help of our robot.

Generally, contemporary designs of robotic arms meant for repetitive actions or tasks are both expensive as well as bulky and heavy. We aim to create a design which is precise but also affordable, lightweight and compact.

Scope

Since our model is extremely light, sturdy, flexible and maneuverable; it has the following applications:

1. It could be used along with a camera to get a visual inspection of disaster-stricken areas like the aftermath of earthquakes, which are inaccessible to human intervention. These robots could help find humans and other life forms trapped under debris.

2. It has the potential to be used underwater to explore the ocean and its various mysteries, or for biological research.

3. It could be used for mining applications, such as metal detection, finding cracks, faults in metals and detecting poisonous gasses in mines.

4. If fitted with the appropriate equipment, it could be used in the construction of tunnels and underground passageways.

5. Used for pick and place applications at minimum costs.

Need for mechanism

Articulated robotic arms have undergone considerable developments in specific manufacturing environments. Yet, some significant opportunity for research exists in the development of highly redundant obstacle-constrained arm mechanisms. These arms generally require lower accuracy and much higher flexibility than typical articulated arms, along with the small size necessary to travel in highly constrained areas.

Objectives

To design and analyze a compact and sensitive robotic tentacle mechanism with multiple degrees of freedom and a mechanical multiplexer to allow motor count reduction.

1. Design of light components of arm with High structural integrity.
2. Designing system with Bowden cable and pulley to improve accuracy and reduce cable slack.
3. Using high tensile strength Kevlar cables with low stretching.
4. Simulation of static system performance.
5. Test of system performance.

Action Plan

Gantt Chart is created using Notion.so. All relevant file tracking and Task tracking is done using Notion.

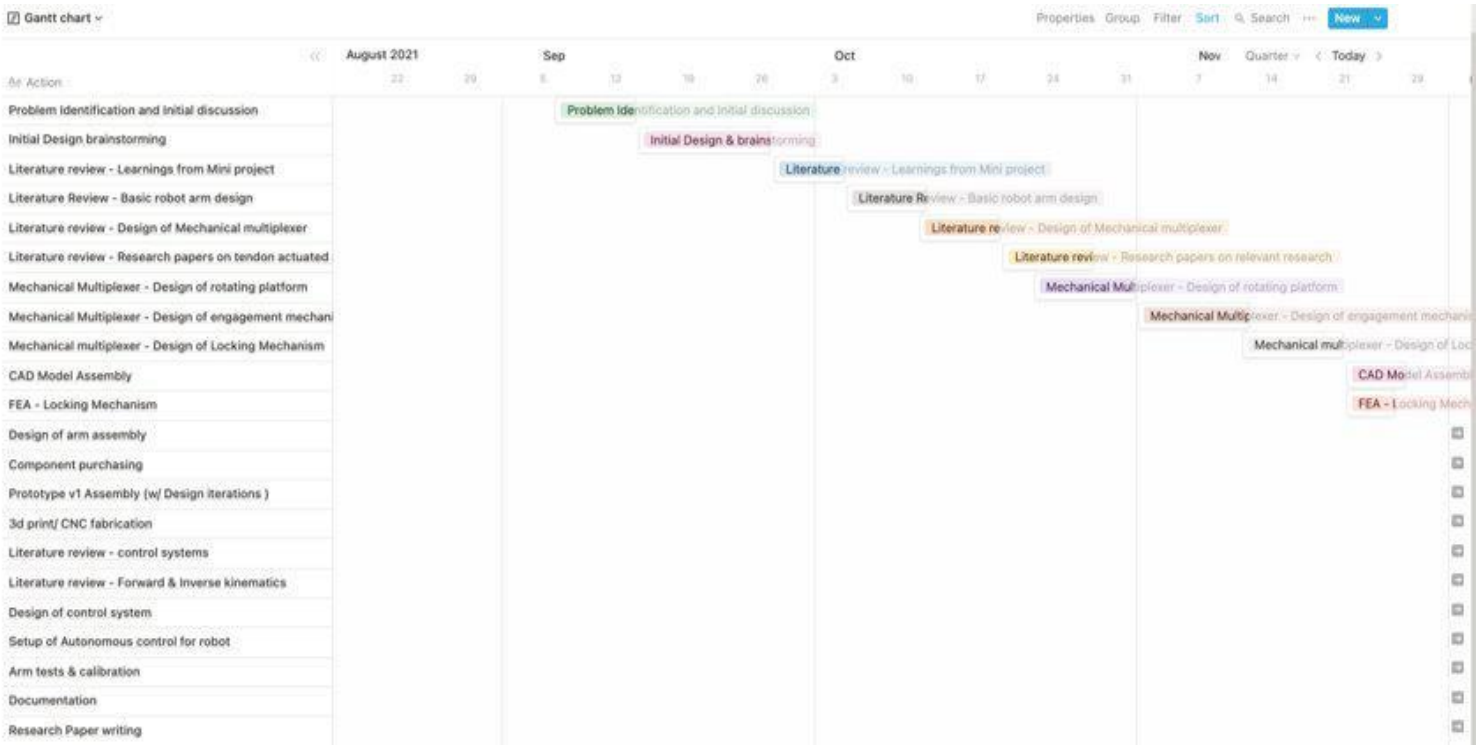

Figure 2 Gantt chart Phase 1

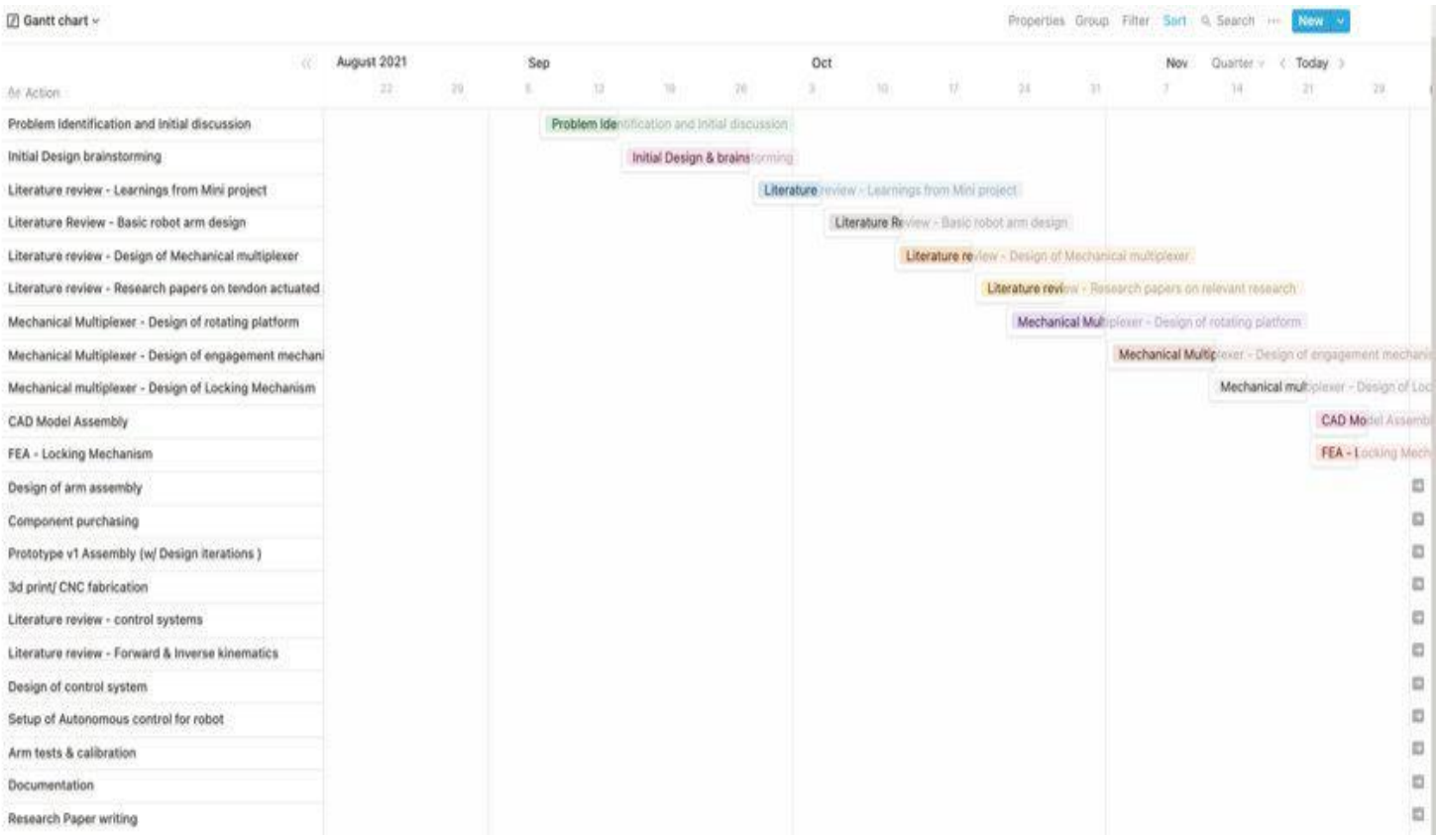

Figure 3 Gantt chart Phase 2

Methodology

1. Literature review of current technology.
2. Identification of structural parameters.
3. Design in CAD software.
4. FEA static structural analysis.
5. DH parameter arm calculation and forward kinematics for arm using Python.
6. Arm motion study in simulation.
7. Mechanical multiplexer design for redundant arm.
8. Control system design for robot motion.
9. Motor selection & part selection.
10. 3D printing components and prototyping.
11. Assembly and Functional testing.

Initial Idea was developed with a different design in the **Mini** project.

AIM AND NECESSITY OF THE PROJECT:

1. During natural disasters, early response is crucial to rescue survivors. Assistive devices which are compact and easy to transport are valuable for rescue purposes.

2. This device can be used to inspect for survivors in a natural disaster affected area.

3. Robotic arms with motors fixed on linkages tend to have higher cost & size as the degree of freedom increases.

4. The problem is two-fold:
   Motor, harmonic drive, pulley etc. are required to drive each joint, each adding weight to the previous joint.

5. Arm must be designed to be larger to accommodate for this greater weight.

6. This increases cost due to the requirement of larger motors and components.

Mini Project -Solution

A. Using a modular 2 Degree of freedom knuckle joint based system which is driven by tendons (cables) which are located remotely.

B. Design of the knuckle joint is hollow, allowing passage of additional movement of tendons in the next segments.

C. As motors and components are remote, the arm does not require waterproofing and can be used in places with risk of radiation as well.

Figure4 Miniproject arm CAD model

Fig 5 Pictures of the Mini Project

Figure 5 Photos of miniproject prototype with 1 and 2 joints

CHAPTER 2- Literature Review

Paper 1- Design and Modelling of a Minimally Actuated Serial Robot

By Yotam Ayalon, Lior Damti and David Zarrouk

This paper demonstrates a serial robot featuring minimally actuated extremely redundant actuators (MASR). The robot consists of a planar arm with ten passive rotational joints and a single mobile actuator that traverses the connections to arrive at the required joints. It then rotates the ones that have been assigned. The joints are locked using a worm gear configuration. After the movable actuator advances to another link, a gripper is linked to the movable actuator, enabling it to carry objects along with the links to reduce the actuation of the joints and the working period. A linear stepper motor controls the robot's vertical mobility in 3D space. The paper presents the mechanical design throughout the study of serial robots with ten passive joints and automatic joint actuation rotatable actuator. Also described is an optimization technique and simulations to reduce the mobile actuator's running time and travelled distance. Multiple trials utilising a robotic prototype demonstrate the MASR robot's advantages: its relatively low weight compared to similar robots, its exceptional modularity, and the simplicity with which its parts may be exchanged as there is no cabling along the arm.Conventional serial robots comprise many inflexible links that are coupled together via actuated joints. Most commercially available three-dimensional serial robots have between four and seven degrees of freedom. Traditional serial robots are frequently insufficient for tasks that require mobility in confined spaces. In some sectors, the inability to do specific activities due to restricted access has significant commercial implications. The capability of hyper redundant robots (also known as snake robots) to maneuver around obstacles and in highly tight places is the primary reason for their invention. 10 to 20 motors generally control them.

Extensive research over the last several decades has resulted in a variety of designs and mechanisms for a wide range of applications, including search and rescue operations and maintenance and medical uses for minimally invasive treatments. These robots and continuum robots are potential candidates for planetary exploration and space satellite maintenance because of their low weight. Despite this, control and motion planning with serial robots provide serious hurdles in terms of high dimensionality analysis. Numerous academics have addressed the planning problem using various optimization methodologies, resulting in significant gains.

The paper proposes a minimally actuated customizable tracks robot and a preliminary design conception serial robot with a mobile actuator MASR that moves along the links to rotate the joints in previous works to simplify the kinematics and actuation and decrease the dynamic modelling. The MASR combines many traits and benefits of minimally actuated and highly redundant robots. Because of the lower number of motors and the simplicity of the design, better durability, reduced weight, cheaper costs, and high modularity are possible.

Fig 6- MASR

Paper 2- Super Dragon: A 10 m-long Coupled Tendon-driven Articulated Manipulator By- Gen Endo1, Atsushi Horigome2 and Atsushi Takata1

In Japan, the decommissioning of the Fukushima Daiichi Nuclear Power Plants was a national priority.To safely collect the fuel debris inside the nuclear reactor, the distribution and properties of the waste must be determined. The paper discusses a ten-meter-long articulated manipulator used for research inside the principal container vessel. We used a linked tendon-driven mechanism and a gravity adjustment system based on synthetic fiber ropes to create a lightweight and thin articulated manipulator. Following a discussion of the underlying theory and control algorithm, we will concentrate on the precise mechanical design of a prototype model. Through simple motion experiments, we validated its viability.

In Japan, the Fukushima Daiichi Nuclear Power Plants (NPPs) decommissioning is a national priority. Each nuclear reactor contains more than 100 tonnes of nuclear fuel waste, including melted atomic fuels and structural elements. In July 2017, the International Research Institute of Nuclear Decommissioning (IRID) obtained visual photos of fuel debris in the Primary Container Vessel (PCV) of the No. 3 reactor for the first time utilising a small-sized remotely controlled underwater vehicle produced by Toshiba . However, the photos collected were incomplete and confined to the No. 3 reactor; consequently, more research is required to comprehend the fuel debris distribution and characteristics completely.

To probe within it, a long-reach manipulator is necessary.In the future, PCV will be used to retrieve fuel debris. IRID and Mitsubishi Heavy Industry collaborated to create a prototype model of a 6-degree-of-freedom (DoF) massive hydraulic manipulator to remove fuel debris and interior structures .The arm's length and weight were 7.1 m and 3500 kg, respectively. Despite having a considerable output force of 2000 kgf, it was difficult to deploy due to its great size and weight.Previous research on the long-reach articulated manipulator has been published in peer-reviewed journals. They designed a remote handling system with an eight m-long horizontally extensible manipulator dubbed Octant 1 to maintain an experimental tokamak nuclear fusion reactor.

The Octant 1 consisted of six segments that were serially joined by five yaw joints and could mechanically sustain a 100 kg weight at the end. All actuators were fitted at the joints, and the total weight was estimated to be over 7000 kg, which was rather considerable.
The CEA LIST created an 8.2 m long multi-link manipulator with five modules, each measuring 160 mm in diameter [7]. The payload weighed 10 kilogrammes. Each module contained pitch and yaw joints, and the arm had a total of 10 degrees of freedom.

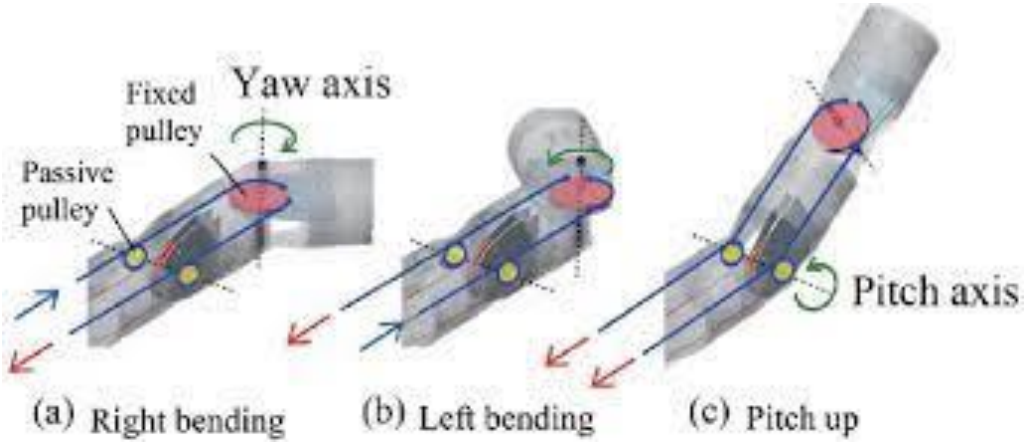

Fig 7- Super Dragon

Paper 3 Design of Tendon-Driven Manipulators

By Lung-Wen Tsai Professor, Mechanical Engineering Department and Institute for Systems Research, University of Maryland, College Park, MO 20742 Fellow ASM

This study provides an overview of the current state-of-the-art in tendon-driven manipulator design. Tendons can only apply tension, not compression, a unique feature of tendon-driven manipulators. The fundamental mechanics related to the construction of tendon-driven manipulators are reviewed based on this distinguishing feature. Structure categorization, kinematics, statics, dynamics, and control are all covered in the review.
Open-loop kinematic chains are familiar in multi-degree-of-freedom (DOF) manipulators. An actuator is fitted on each link of a conventional open-loop manipulator to drive the following link through a speed reduction device. As a result, actuators and speed reducers installed at the distal end serve as the load for actuators located at the proximal end.
As a result, an individual joint driven manipulator is often significant and heavy. Mechanical power transmission systems can minimize the size and inertia of a manipulator.
A well-designed transmission system allows the actuators to be positioned close to or at the base. As a result, lightweight and small manipulators may be developed.

Transmission systems can be used in many forms, such as gear trains, bar linkages, and tendon drives (cables, belts, tapes, chains, or ropes). The transmission mechanism selected is determined by the application and other design factors. The power-to-weight ratio must be maximized, backlash and vibration must be decreased, and friction must be reduced.

Among the many transmission systems, tendon drives offer the benefits of being lightweight, having little backlash, having low friction, being compact, and absorbing stress. Tendon drives have two advantages: (1) actuators may be mounted on the base, and (2) a correctly pre tensioned tendon-driven system has negligible backlash. Because of these advantages, tendons are more suited than other transmission systems in applications like dexterous hands, where minimal space and lightweight are required.

Tendon-driven manipulators' kinematic structures are categorised into various groups based on the kind and quantity of tendons utilised. The fundamental kinematic and static force transformations between the tendon, joint, and end-effector space have been characterised. Admissible conditions for arranging tendon routings and pulley sizes are specified. The concept of isotropic transmission is introduced, and a theory for achieving such transmission characteristics is presented. Finally, the dynamics and control of tendon-driven manipulators are discussed. Two methods of resolving redundant tendon forces and maintaining positive tensions are outlined.

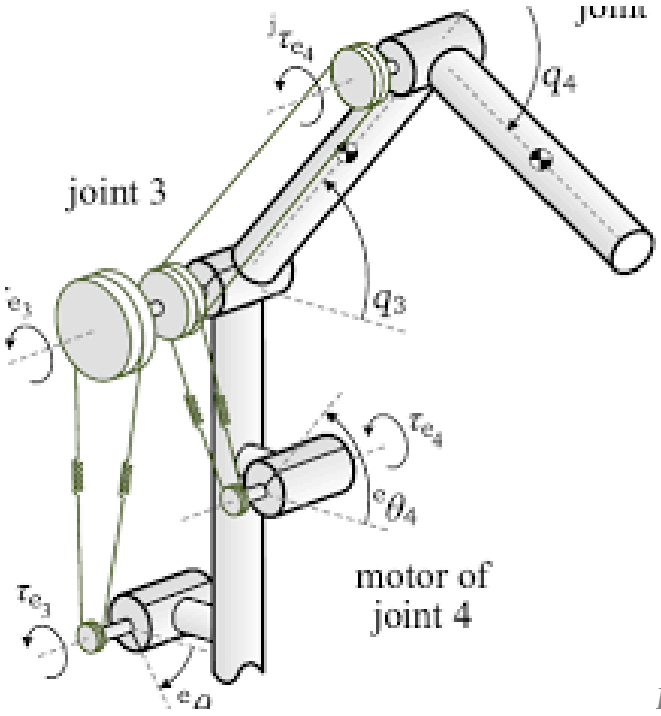

Fig 8- Tendon Driven Manipulator

Paper 4- Kinematic comparison of surgical tendon-driven manipulators and concentric tube manipulators

By-Zheng Lia,, Liao Wub , Hongliang Renc , Haoyong Yuc

Robot manipulators are becoming more popular in minimally invasive surgery (MIS). When working in a limited surgical cavity, they must have a compact size, a large workspace, appropriate dexterity, and payload capability. Snake-like flexible manipulators are ideal for these tasks. However, typical fully actuated snake-like flexible manipulators are difficult to miniaturise, and the payload is highly restricted even after shrinking. The alternative is to utilise snake-like flexible manipulators that are underactuated. Tendon-driven continuum manipulators (TCM), tendon-driven serpentine manipulators (TSM), and concentric tube manipulators (CTM) are the three most common designs (CTM). In this work, the three designs are compared at the mechanism level in kinematics. The workspace and distal end dexterity for TCM, TSM, and CTM with one, two, and three parts are compared. Other features of these designs are explored, such as sweeping motion, scaling, force sensing, stiffness control, and so on. According to the findings, tendon-driven and concentric tube designs complement each other in terms of workspace, which is impacted by the number of sections and the length distribution among branches. Tendon-driven designs provide more distal end dexterity while generating greater sweeping motion in areas near the shaft.

Manipulators or robot arms are increasingly being employed in tight space applications. Minimally invasive surgery (MIS) techniques such as laparoscopic surgery, Single Port Access surgery (SPA), Natural Orifice Transluminal Endoscopic Surgery, and industrial endoscopic non-destructive inspection are typical examples. The manipulator must enter and work in limited locations with numerous barriers in these applications. As a result, the manipulator is often snake-like, i.e. slim and with a high degree of freedom (DOFs). This enables the manipulator to access the target while maintaining appropriate mobility around it. These manipulators are mounted on a robotic platform, with their flexible bending parts introduced into the surgical cavity through a trocar. The surgeons direct the manipulator to access the surgical target and complete the procedure. Traditional snake-like manipulators are serial robot arms with a high number of completely articulated joints. Depending on the kind of joint, one or two integrated motors operate it. As a result of this design, the robot is enormous and sophisticated in mechanical construction and control. Another technique for actuating all the joints is to remove the actuators from the robot framework, such as the tensor arm. In this configuration, the motors are located at the robot's base, and motion is conveyed to the manipulator through tendons. The size of the manipulator may be lowered to some amount with this design, but the number of tendons required is enormous, limiting the downscaling of the manipulator. These snake-like robots generally have a cross-sectional size of 102 mm. They must be miniaturised before they can be used in MIS. However, massive efforts are required to reduce the size of these robots. As a result, thoroughly articulated designs in surgical manipulators are unusual. The SPRINT robot has two arms, each with three entirely operated joints [11]. It is not, in any way, snake-like. The i-Snake [12] resembles a snake. It features seven adjustable joints and a 12.5 mm diameter. The iSnake's payload, on the other hand, is quite restricted. This severely limits its uses in MIS.

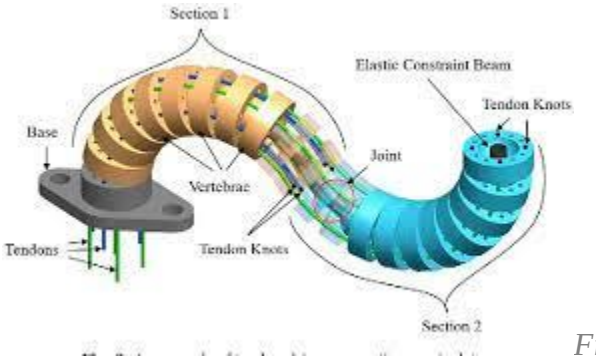

Fig 9- concentric tube manipulator

Paper 5- A Review of Motion Planning Algorithms for Robotic Arm Systems By- Shuai Liu and Pengcheng Liu

Motion planning is critical in the realm of robotics. This article presents the most recent advances in the study and development of various algorithms and motion planning methods during the last five years, with a heavy emphasis on robotic arm systems. Most contemporary motion planning methods rely on random sampling techniques—enhanced algorithm performance such as those based on optimization and Probabilistic Movement Primitives (ProMPs).
And physics-based approaches are viable research paths to investigate to increase efficacy. The benchmarking of the algorithm for assessment is a worthwhile research path. Model-based solutions have the potential to increase the efficiency of
The work, but it is less capable of dealing with mishaps. Modelfreed approaches, on the otherhand, can fix this problem, but it takes a long time. to calculate This
The research also delves into the robotic handling of stiff and non-rigid objects.
(deformable) things are investigated. The report summarises various obstacles and future research directions and specific algorithms and techniques are proposed for the best usage of the robotic arms,The advancement and widespread deployment of robot technology has increased the country's production and the improvement of society as a whole. Robots and robot goods are rapidly infiltrating individuals' lives. Work. Welding, installation, and inspection are examples of jobs that robot technology can undertake. Even in hazardous circumstances, robots may perform admirably.Even deal with some unforeseen occurrences. With the market revolution, robots are getting increasingly popular
The robotic arm is a model of the earliest robots utilised in realising life and social production. Many activities, such as lifting important things or assembling mating pieces require the coordinated functioning of two or more robotic arms. The working system of the robotic arm is quite intricate in the entire work process, and there may be numerous barriers outside. When many robot arms are required to execute a task simultaneously, mutual obstacle avoidance between the robot arms must also be addressed.

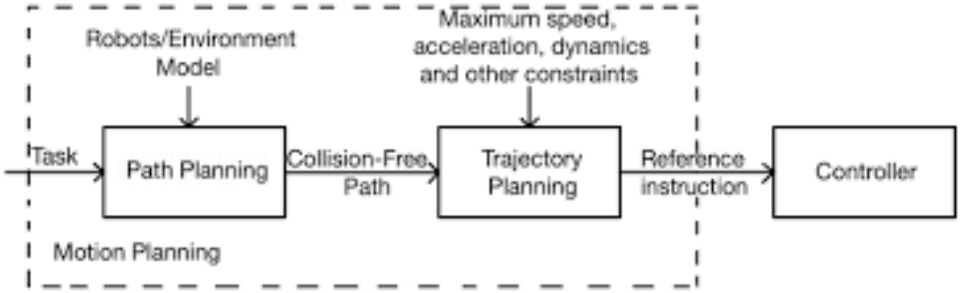

Fig 9- Motion planning diagram

Paper 6- A General Mechanical Model for Tendon-Driven Continuum

Manipulators

By Federico Renda, Student Member, IEEE and Cecilia Laschi, Member, IEEE

Although the robotic community has recently shown a lot of interest and work in continuum manipulators, control and modelling of such manipulators remain a difficult job, mainly because they require a continuum approach. This work presents a generic mechanical model with a geometrically accurate technique for tendon-driven continuum manipulators. Because of the flexibility of the parameters that may be specified, this model can be used for a wide range of manipulators. The suggested technique might also be a valuable instrument for establishing the control plan. The model can also accurately replicate the linked tendon drive since it considers the torsion of the robot arm instead of ignoring it, as is customary in other existing models.

The endeavour to improve the performance of robot manipulators has resulted in a greater focus on continuum manipulators, particularly biologically-inspired continuum manipulators [1][2]. A continuum manipulator is a (continuous) bending robot made of elastic parts with preferably limitless degrees of freedom. They include hyper-redundant manipulators, which are many short, stiff linkages [3]. Biological systems, like elephant trunks [4][5] and squid tentacles [2], have inspired continuum robots. Controlling and modelling continuum manipulators is problematic since it necessitates a continuum approach and provides varying degrees of non-linearity in terms of material and geometry. Many researchers are now involved in this stimulating challenge, but there is a problem.
They include the hyper-redundant class, which is still far from being solved. Most existing techniques are limited to piecewise-constant-curvature approximation [6-8] or kinematic analysis [9]. Jones and Gray [10] recently published a steady-state model of a continuous robot that ignores

actuation. The dispersed force and torque operating on the robot are approximated in the exquisite work of Boyer and Perez [11]. Still, no consideration is made of the actuators that may create them. Zheng and Branson [12] developed a spring-mass technique rather than a continuum approach, which is too complicated to apply in an embedded system.

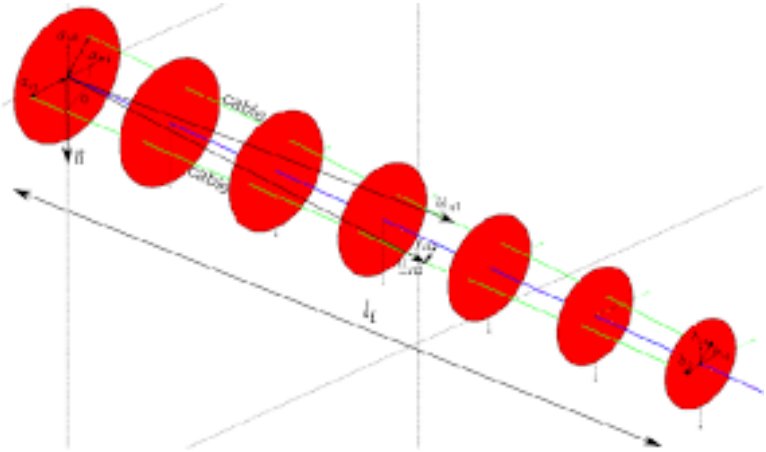

Fig. 3. Tendon kinematic parameters in the reference configuration.

Fig 10- Continuum Robot

Paper 7- Coupled tendon-driven multijoint manipulator

ByS. Hirose, Dept. of Mech. Sci., Tokyo Inst. of Technol., Japan S. Ma

CT arm, a linked tendon-driven manipulator, is introduced, and its control is explained. The CT arm has a unique tendon traction force transmission mechanism in which a pair of tendons used to drive a joint is pulled from base actuators through pulleys installed on the base-side joints. The instrument makes use of the coupled driving function of the tendon traction forces and hence has the potential to increase payload capability.

Because of its mechanical simplicity, the CT arm has the attributes of being robustly constructed and economically manufactured. A preliminary discussion of its control is also held, which is the control algorithm.

Introduced, and its management is also described. The CT is created to reduce the square sum of the traction force of tendons while meeting stated constraints. Computer simulation is used to demonstrate the validity of the control approach.

Multijoint manipulators with high degrees of freedom will be employed efficiently in an endeavour to robotise inspections, checks, and machinery assembly.in complex situations, such as a nuclear reactor or a chemical factory, where numerous machines and equipment are crowded, These swindleshould have a lengthy arm like an elephant's trunk. This enables for simple avoidance of obstacles. However, in practice, there are two options.major technological issues and the multijoint manipulator are not commonly used.

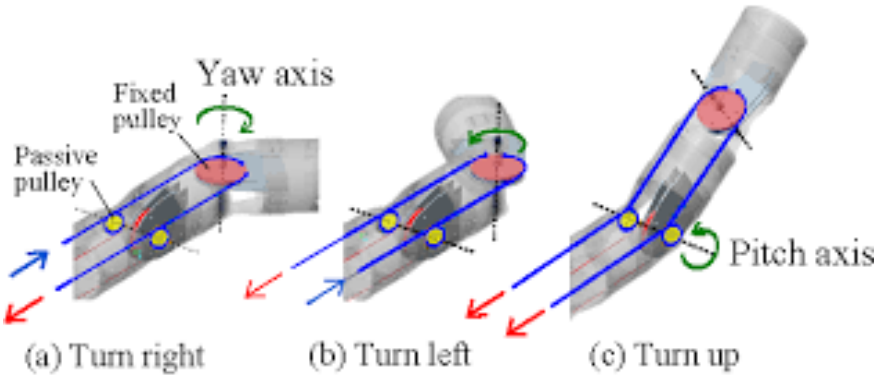

Fig. 5. 3D motion of 3D CT-Arm

Fig 11- multijoint manipulator

Paper 8- SIMBA: Tendon-Driven Modular Continuum Arm with Soft Reconfigurable Gripper

By- Anand Kumar Mishra1,2*, Emanuela Del Dottore1,2, Ali Sadeghi1, Alessio Mondini1 and Barbara Mazzolai1

In this article, they explain the conceptual design and execution of the Soft Compliant Manipulator for Broad Applications (SIMBA) manipulator, which was created and built to compete in the RoboSoft Grand Challenge 2016. They suggested in our new design:

1. A modular continuum arm with separate actuation units for each module promotes maintainability.
2. A soft reconfigurable hand for better finger adaptation to objects of diverse shapes and sizes.
3. A movable base to expand workspace.

They used a hybrid approach in designing and manufacturing, integrating soft and hard components in both materials and actuation, to provide high lateral stiffness in the arm via flat springs, soft joints in fingers for more compliance, and a tendon-motor actuation mechanism that provides flexibility while also providing precision and speed. The SIMBA manipulator has exhibited remarkable gripping and manipulation skills by grasping varying fragility, shape, and size items. Lifting things weighing up to 2 kg has also proven to be resilient and dependable. The experimental results indicated that our design and technique could lead to the development of robots capable of acting in unfamiliar and unstructured situations in collaboration with people for several purposes.

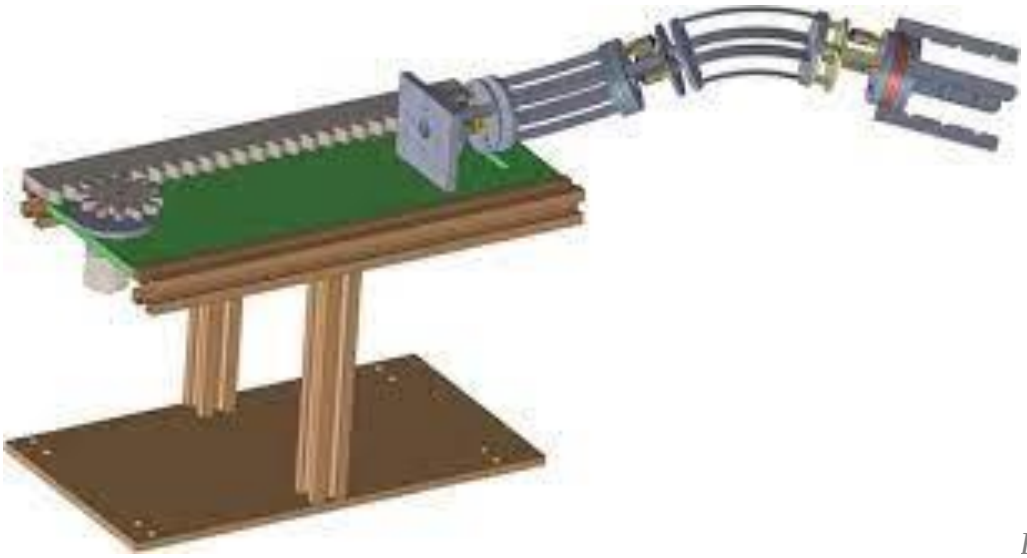

Fig 12-Soft Grip

Paper 9- Design of a Weight-compensated and Coupled Tendon-driven Articulated Long-reach Manipulator

By- Atsushi Horigome1, Gen Endo2, Koichi Suzumori2 and Hiroyuki Nabae2

A weight-compensated and linked tendon-driven mechanism is presented, and a mixture of the current two systems and their static control is addressed. This system enables a long-reach manipulator with very tiny actuators by attaching one thick tendon to a connected tendon-driven mechanism. Static tension management was examined, and a plan was presented that derives the tension of the joint regulating tendons and the weight-compensating tendon from the arm position. Furthermore, in six postures, tendon strain on three types of the suggested mechanism is simulated. Weight compensation occasionally necessitates high tension in the tendons that govern the joints; nevertheless, it often decreases tendon tension to less than 2 kN.

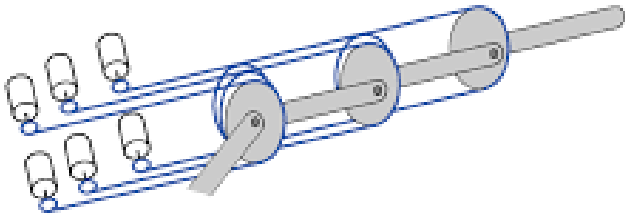

(a) A coupled tendon-driven mechanism model

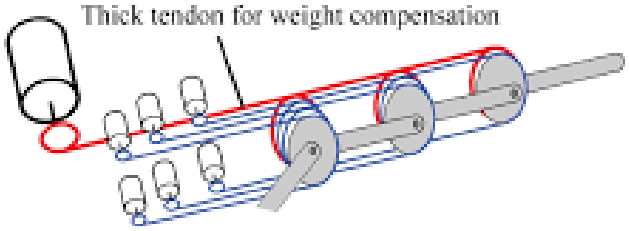

(b) A coupled tendon-driven mechanism model with weight-compensation mechanism.

Fig 13 – Articulated Manipulator

Paper 10- Design of Modular Reconfigurable Robotic System for Construction and Digital Fabrication

By-Milica Vujović,Aleksandar Rodić,Ilija Stevanović

The design of an innovative robotic system for building construction is presented in this research. The suggested robotic system has a modular structure and is reconfigurable, allowing it to adapt to various building needs. The robotic technology described in this research is used in low-rise residential structures (ground floor plus three floors and attic). The reconfigurable system described in this work allows for the use of three different types of robots: parallel SCARA, construction Delta robots, and redundant, hyper articular robots for infrastructure inspection. The modular construction allows for quick assembly, disassembly, and system operation even if one of the module's components fails.

The mechanical system design is based on 3D printer models, with the ability to easily swap multiple end effectors to control the material throughout building, assembly, installation, and final processing of the facade and walls. In the paper's conclusion, a brief comparative comparison of traditional building methods will be provided and a discussion of the unique technique of utilizing robots in highly automated building construction processes.

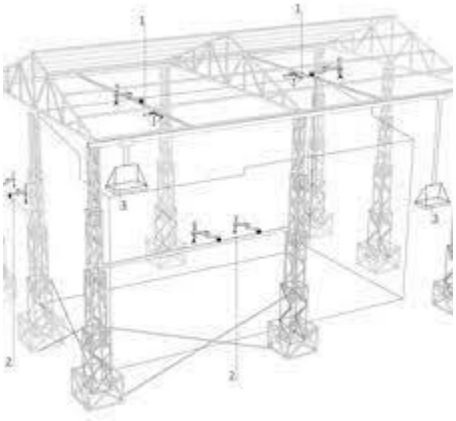

Learnings from the Mini Project- Summary

1) The Universal joint restricts angular movement to +/- 60 degrees due to forks restricting travel.

2) Nylon tendons undergo large extension in tension leading to inaccurate angles.

3) Tendon is slack on one side reducing accuracy of angles of joints and lead to oscillations.

4) Each joint requires 1 stepper motor, thus increasing the overall cost of the system.

5) Open loop control system leads to low accuracy of arm.

6) Average accuracy of +/- 4 degrees

Improvements Possible in the mini project

a) Usage of Bowden system to ensure fixed length of cable required

b) Usage of Mechanical Multiplexer to reduce motor count

c) Addition of encoder/ potentiometer for control system

CHAPTER 3 – Design Overview

Overall Design Specifications of the System

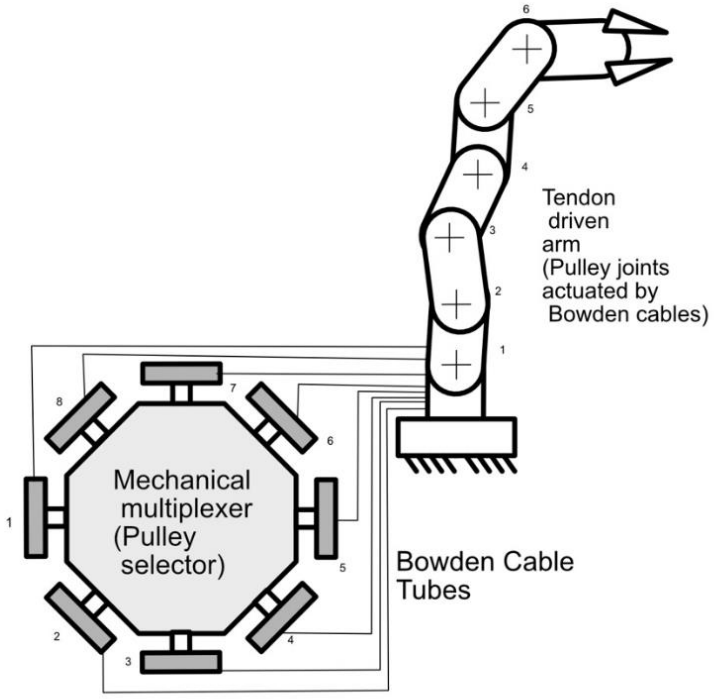

- Resolution of the system = 2 Degrees
- Least Count of Input Stepper based on slot allowance = 180 Degrees

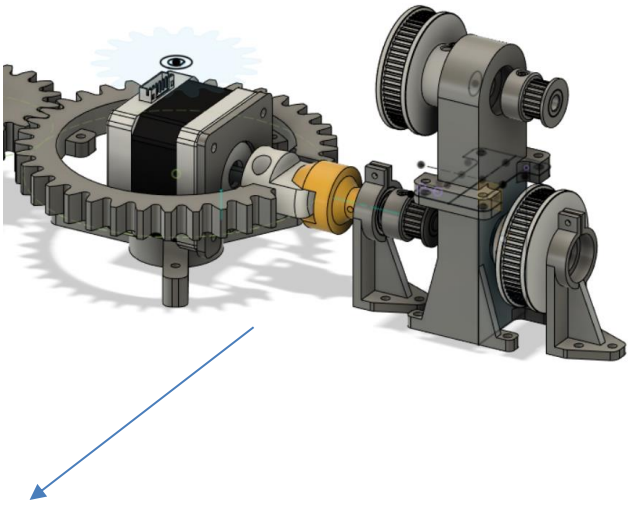

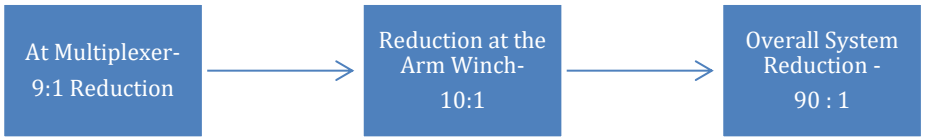

- Payload (Camera/Gripper) = 120gms

- Length of the Arm = 0.7m
- Max Diameter of the Arm (Octagon)= 56mm

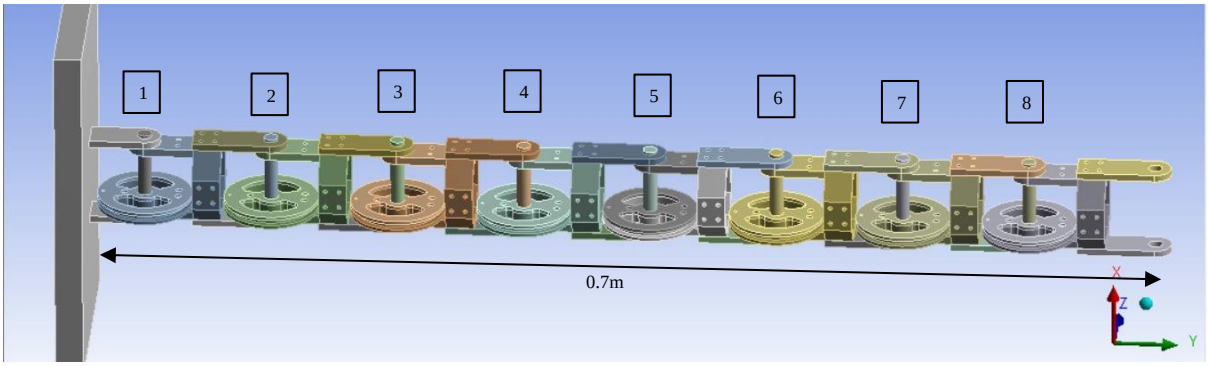

Manhole cover dimensions for reference-

- Standard rectangular manhole covers have dimensions 1200 x 900 mm and are used for covering most of the manholes seen in city infrastructure.

- No of Segments = 8
- DOF = 8

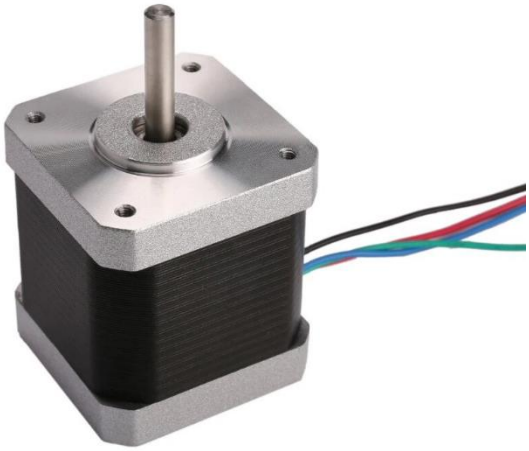

- Nema 17 Input Stepper Motor –
- Step Angle = 1.8 degrees (200 steps/rev)
- Max Speed = 600 rpm
- Power provided to the system = 5 watt
- Torque = 5.6 kgf-cm

Stage 1- Mechanical Multiplexer

The design underwent 2 iterations after design improvements before final prototyping of the system.

The first iteration consisted of a circular mechanical multiplexer mounted on a turntable. The mechanical multiplexer had spring loaded clutch plates, which would be engaged and disengaged and then rotated for a concurrent movement in the tension cables. Following is a detailed look at the mechanism-

First Design-

Design of the system-

Following are main components of the system:

1. Mechanical Multiplexer
2. Bowden cables
3. Arm assembly
4. CNC motor controller for stepper motors

The Mechanical Multiplexer is used to select the pulley that is required to be driven. The Bowden cable pair attached to the corresponding selected pulley is actuated to the required angle. The spring-loaded lock is used to lock it when the motor is disengaged.
The Bowden cable pair is attached on the other end to the arm joint pulley which is to be actuated. The diameter of the driving pulley on the multiplexer to the driven pulley at the joint is kept in a ratio of around 1:10 to increase torque. And achieve smaller angular resolution.

A CNC controller is used to interface motors to the software.

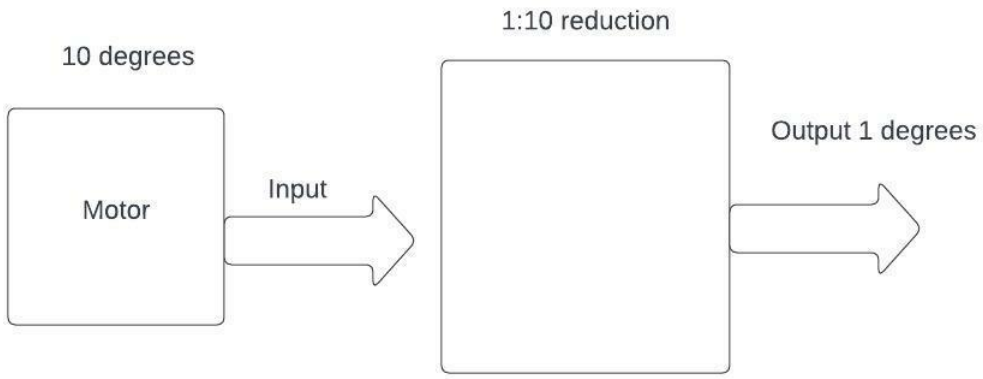

Fig 14- Gear reducers

Specifications : Number of divisions (teeth): 36
Quantized step angle : 360/ 36 = 10 degree
Driving Motor : NEMA 23 stepper
Selecting Motor NEMA 17 stepper
Engaging Motor: Servo ES08A

- Multiple iterations were reviewed for simplicity and utility and circular layout was selected.
- Design analysis and FEA of parts related to mechanism will be done
- Following parts/ assemblies are needed for Multiplexer:
- Tooth lock and clutching module for locking pulley at fixed angle deviations when motor is disconnected.
- Selector assembly for selecting and driving lock/ clutch module by rotating motor to required position.
- Engagement mechanism to connect and disconnect from clutch module using linear actuation
- Circular housing frame for holding clutching mechanism
- Pulley to be attached to Bowden cable system.

Figure 15 Proposed design of the Mechanical Multiplexer

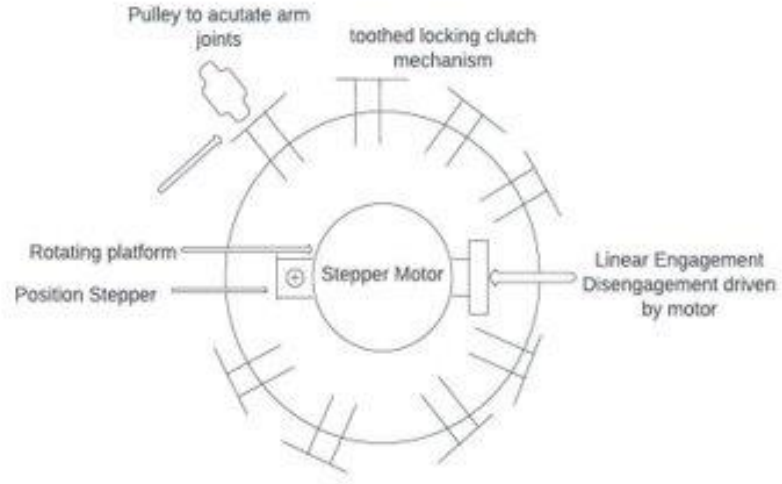

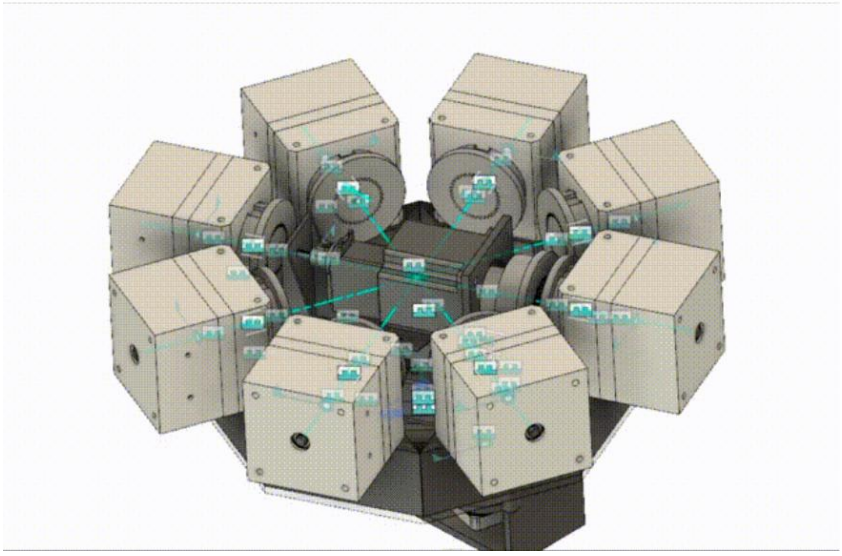

Figure 16 CAD model of Mechanical multiplexer

Main mechanisms and their working
The important mechanisms used in the assembly and working of the mechanical multiplexer are :

(I) Rotating Selector Mechanism
(II) Engagement Disengagement Mechanism
(III) Locking Mechanism

(I) Rotating selector mechanism

Components: NEMA 17 stepper motor, Spur gear pair, Rotating Platform,
Working: The engagement mechanism is mounted on an octagonal platform which is rotated by a spur gear pair (with a chosen reduction ratio of 4:1; limited by dimensional constraints). The gear pair is supplied with power from the NEMA 17 stepper motor which is placed below the platform. It selects the port to output rotation to.

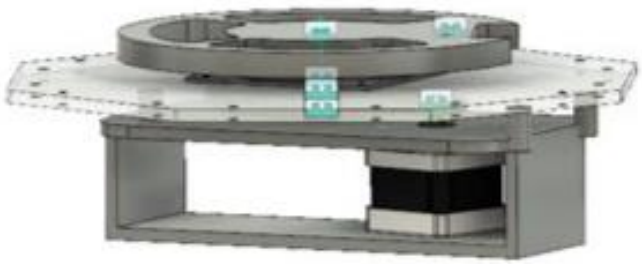

Figure 17 Rotating platform subassembly

(II) Engagement Disengagement Mechanism
Components: Internally splined ring, NEMA 23 Stepper motor, Servo motor, Straight rod with sliding bearings, Power screw.
Working: The end of the power screw is fixed in the end support. Hence, when the servo motor rotates, the entire set of the motors along with the ring slides forward and backward on the rod. Once the desired position is reached, the splined ring engages with the splined shaft to deliver power.

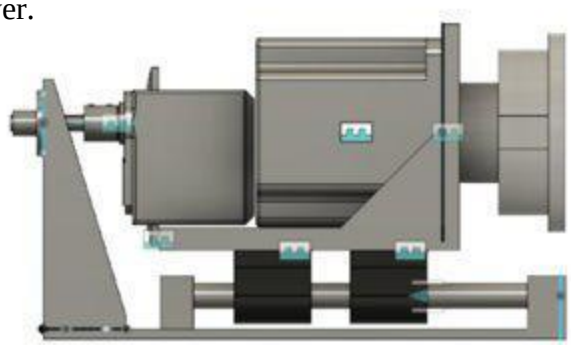

Figure 18 Engagement mechanism subassembly

(III) Locking Mechanism

Components: Externally splined shaft (on which winches will be mounted), Internally splined ring cover lock, springs

Figure 19 Locking mechanism section views

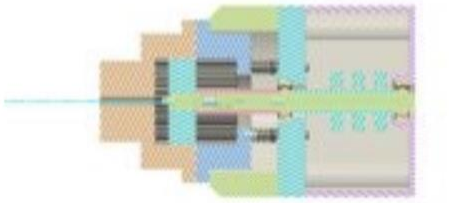

Working: When the internally splined shaft is pushed by the power screw mechanism, it displaces the internally splined cover lock ring which in normal position is engaged with the externally splined shaft and prohibits any movement. Now this lock ring is spring loaded. When it is displaced from its position and is pushed back, the shafts engage. After the power screw mechanism withdraws the engaging shaft, the lock ring engages with the externally splined shaft and regains normal position by the virtue of springs.

Toothed locking and clutch module-

Current locking mechanism is in process of design which uses spring loaded locking. When required to be unlocked, the selector will actuate and push lock to disengage, thus allowing it to be rotated. When selector retracts, spring loaded lock will re engage.

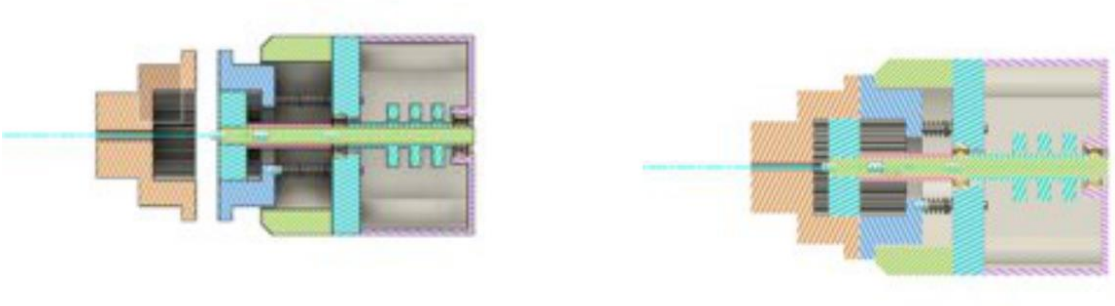

Figure 20 Section view Locking assembly partly engaged

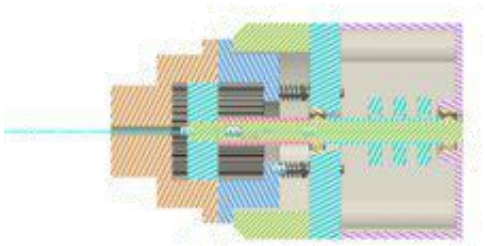

Figure 21 Locking assembly engaged (Teeth unlocked)

CAD of Mechanical Multiplexer with 8 engaging disengaging modules

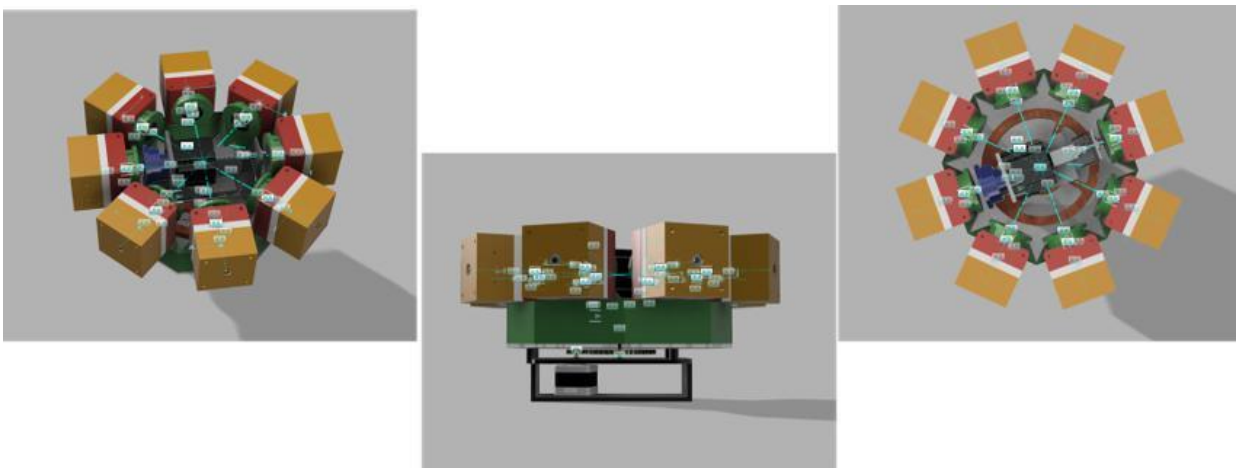

Figure 23 Views of model

Parametric modelling of components

All parts are created with parametric modelling to accommodate for future design changes

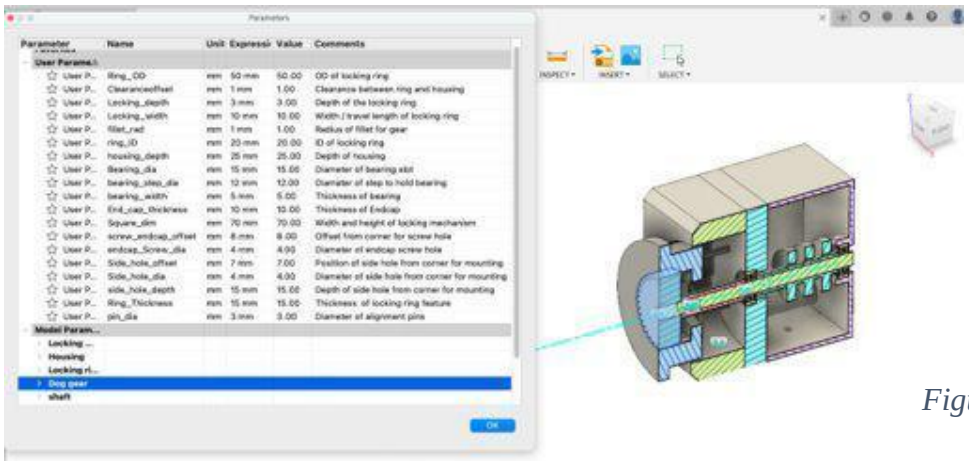

Figure 24 modelling of locking module

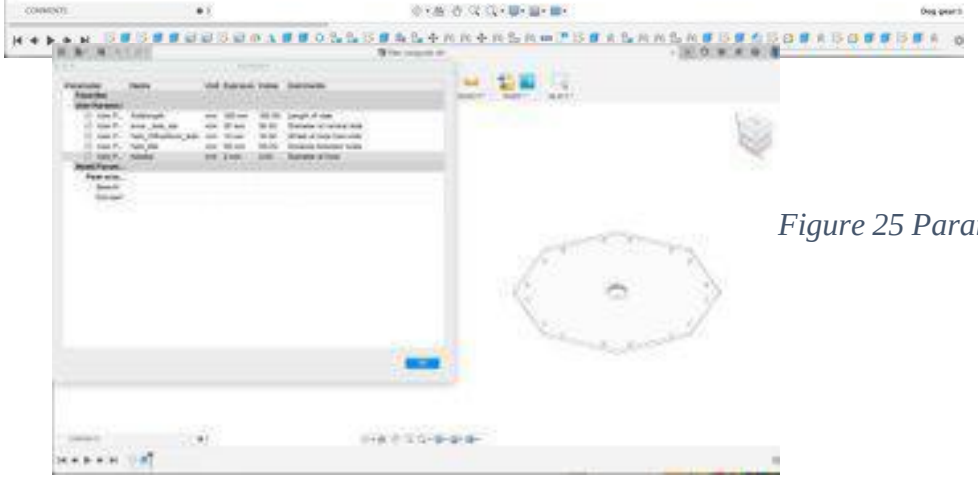

Figure 25 Parametric modelling of octagonal base

Figure 26 Linear Actuator CAD and Exploded View

Linear Actuator

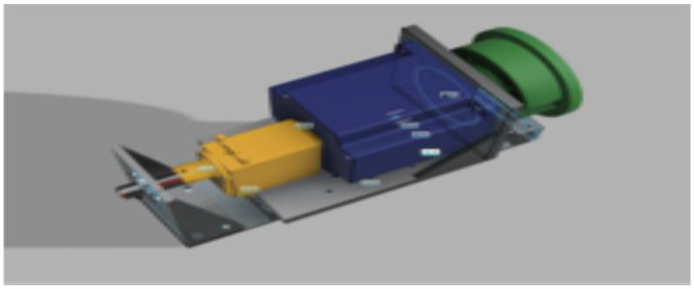

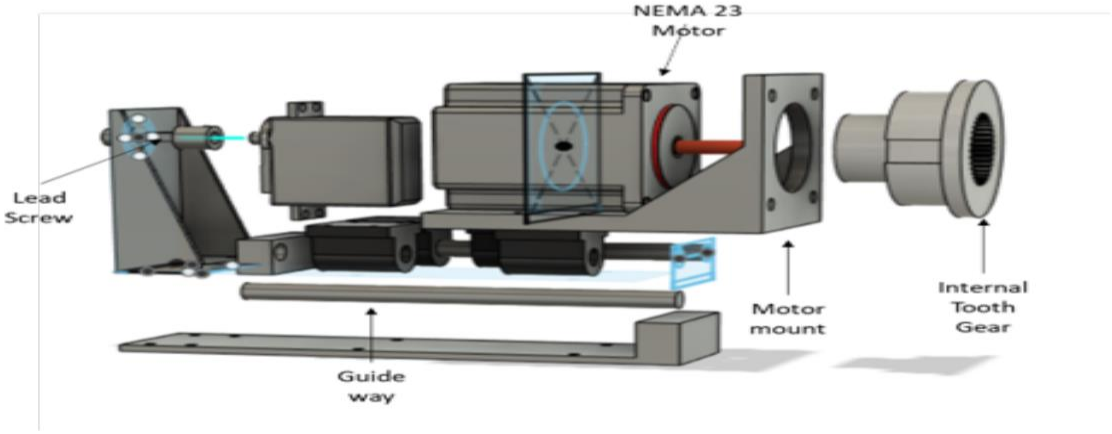

Dog Clutch with locking mechanism

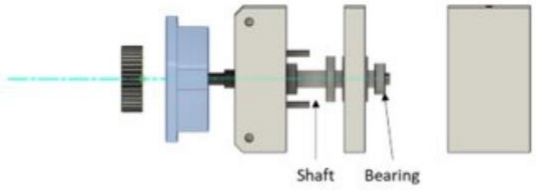

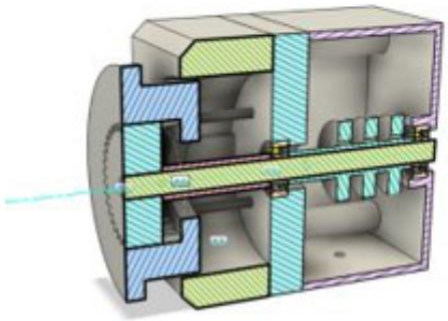

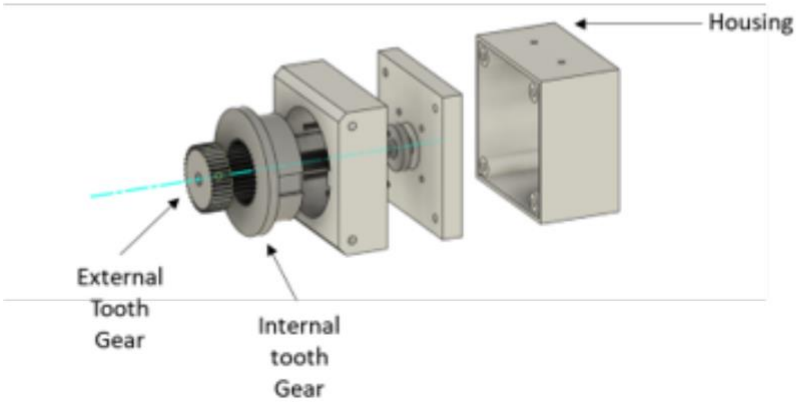

Turn table exploded view

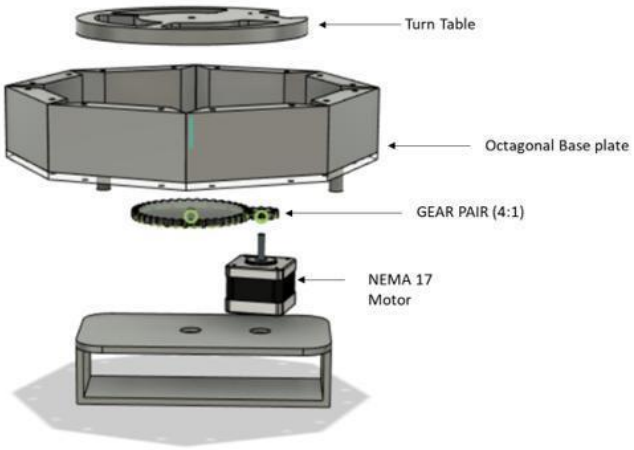

Figure 26 Locking mechanism exploded view

Finite Element Analysis-Structural Analysis

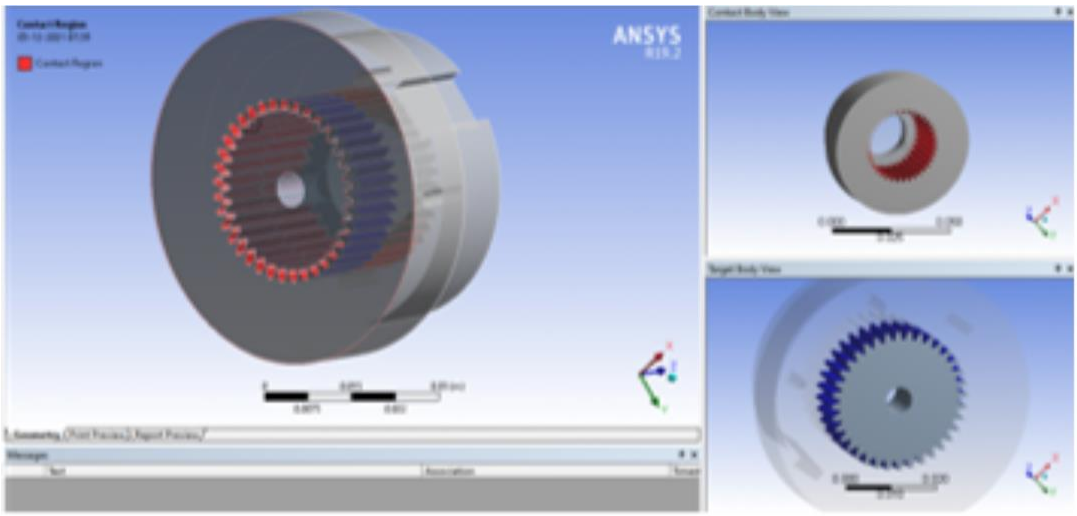

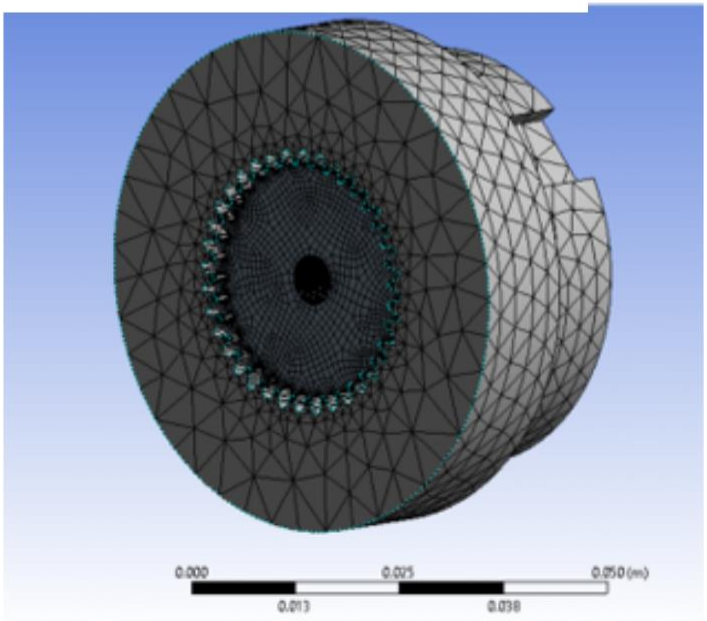

Figure 29 Contact points

After modelling the entire system in Fusion 360 using parts and assemblies, the Finite Element Analysis on the multiplexer mechanism was performed. The Static structural approach was adopted in Ansys to analyze the dog clutch, which is one of the most critical motion transformation components.

The pieces were allocated to the material, which was PLA (Polylactic acid), and the material attributes were defined to the geometry as indicated. The two meshing gears' contact zone was then specified.
Other pre-processing steps included allocating supports and creating a Fine mesh. And, as required, the model was solved for a torque moment of 0.412 Nm.
The system, together with the selected material, was found to be in a safe range, with maximum deflection and equivalent stresses of 0.8 Microns and 1.3MPa, respectively.

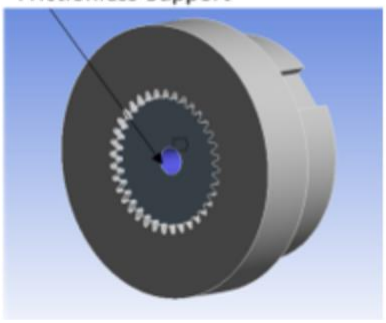

Figure 30 Shaft fixing

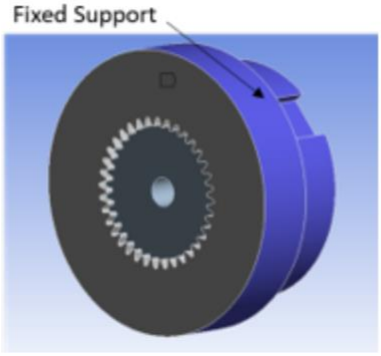

Figure 31 Fixed support

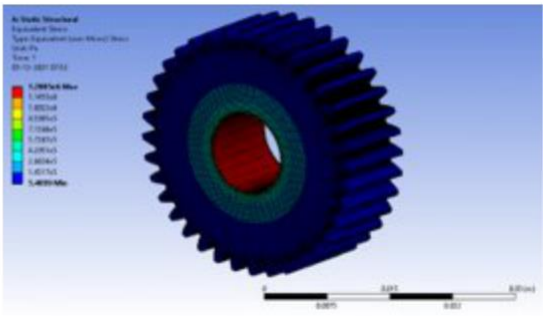

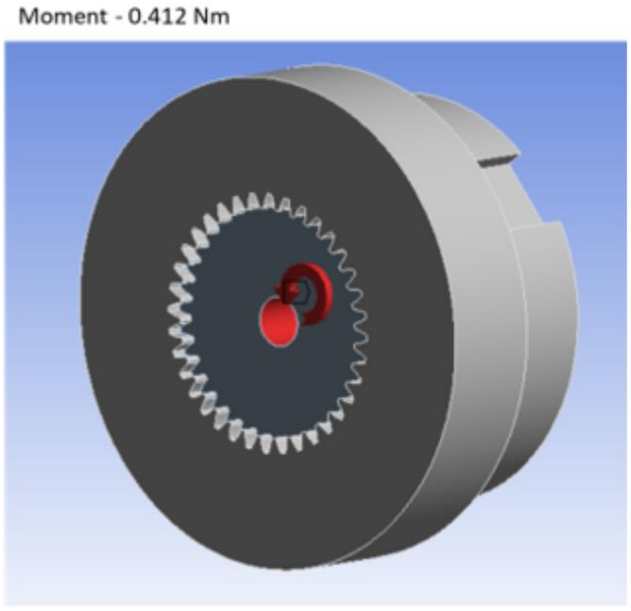

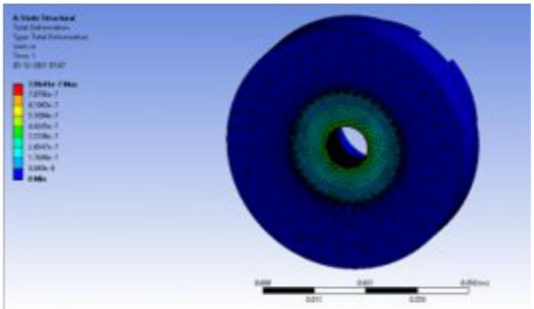

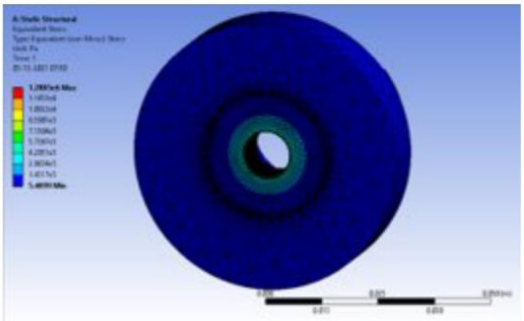

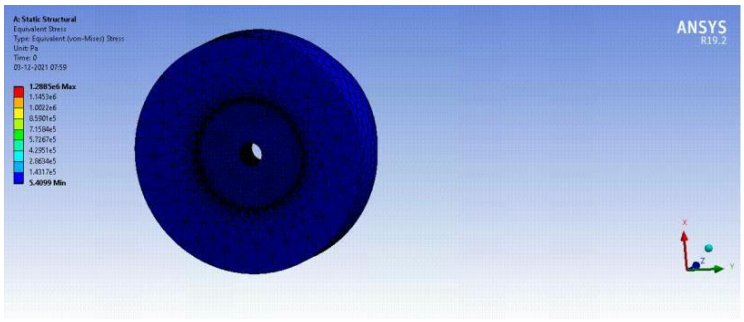

Figure 32 Output of static structural analysis

Figure 33 Moment setup

INPUT

SPECIFICATION	**VALUE**
Material	PLA(Polylactic Acid)
Contacts	Teeth of meshing Internal and External Dog Gears
Mesh Type	Fine, Tetrahedral
Frictionless Support	At shaft hole of Internal gear
Fixed Support	External surface of the external gear
Moment Position	At frictionless support
Moment Magnitude	0.412 Nm

OUTPUT

SPECIFICATION	**VALUE**
Max. Deformation	0.8 Microns
Equivalent Stress	1.3MPa

Problems with the first version and the subsequent solution-

We realized early into the first prototyping stage of our first iteration that there were some flaws with the actual model-

1. Constraints of accuracy involving the limited functionality of the 3D printer caused our printed prototype to have an irregular surface finish. The flank and the surface of the printed gears were uneven and the gear teeth, being very small, also lacked surface finish.
2. Since this version of the arm depended on the interlocking of the multiplexer for actuation, the poor surface finish meant that we could not rely on this design to give 100% satisfactory working. There was a very high chance of mismatching or misalignment of the multiplexer and the gears, which could lead to machine failure.
3. Even slight vibrations in this design could have potentially caused severe misalignment.
4. Furthermore, we concluded that this design would also be very expensive, given the eight modules of the locking mechanism, along with the arm cost.
5. Due to these unforeseen conditions, we also observed that the given model could not smoothly operate with the available torque from the NEMA 23 stepper motor, used for driving the system. This meant that we could not use this design for any applications requiring even slightly higher values of torque- like gripping or holding.
6. The angular alignment was not accurate in engagement because the stepper motor did not have sufficient level of accuracy. The accuracy required for proper alignment and engagement would have led to higher cost and manufacturing complexity.

Fig 33- Mismatch of assembly

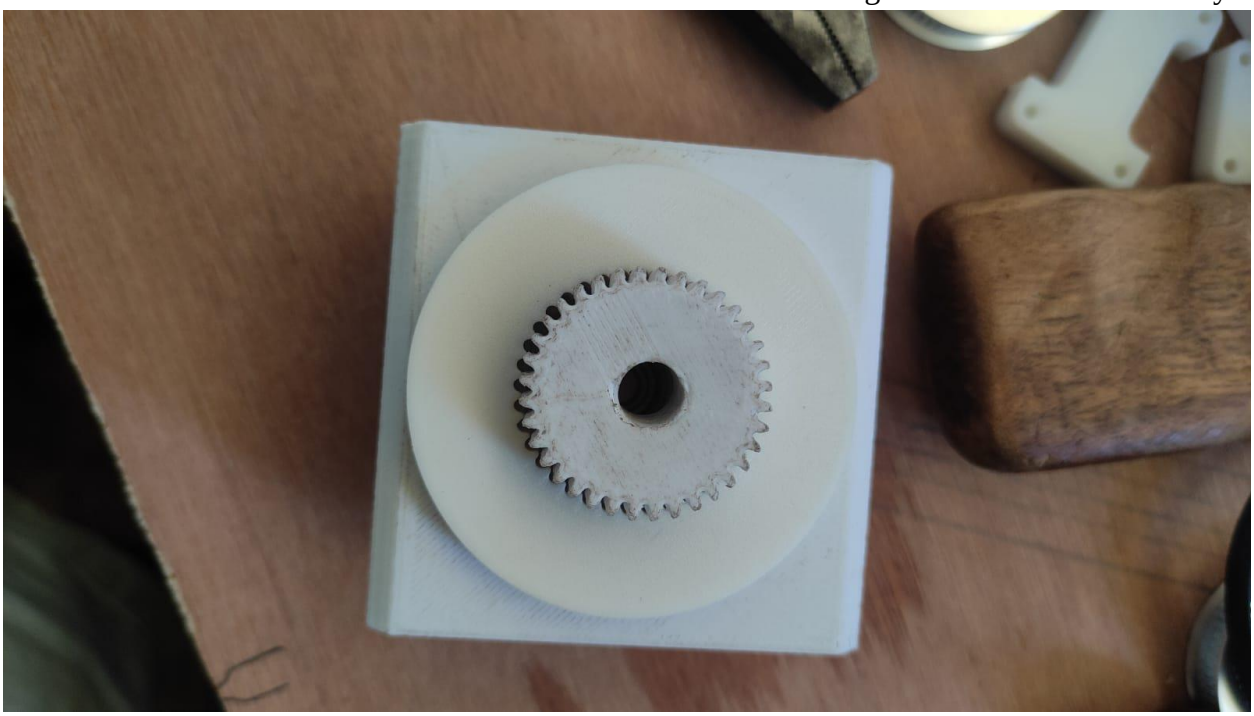

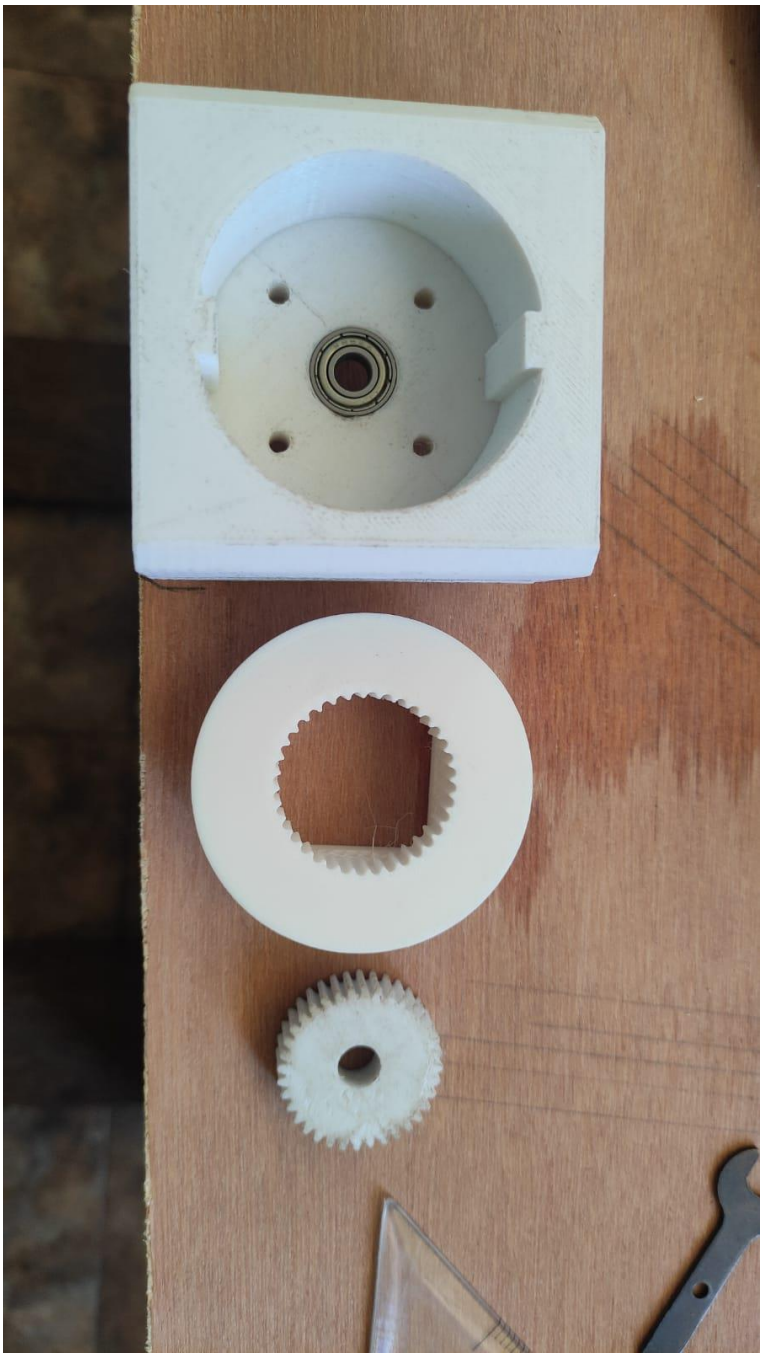

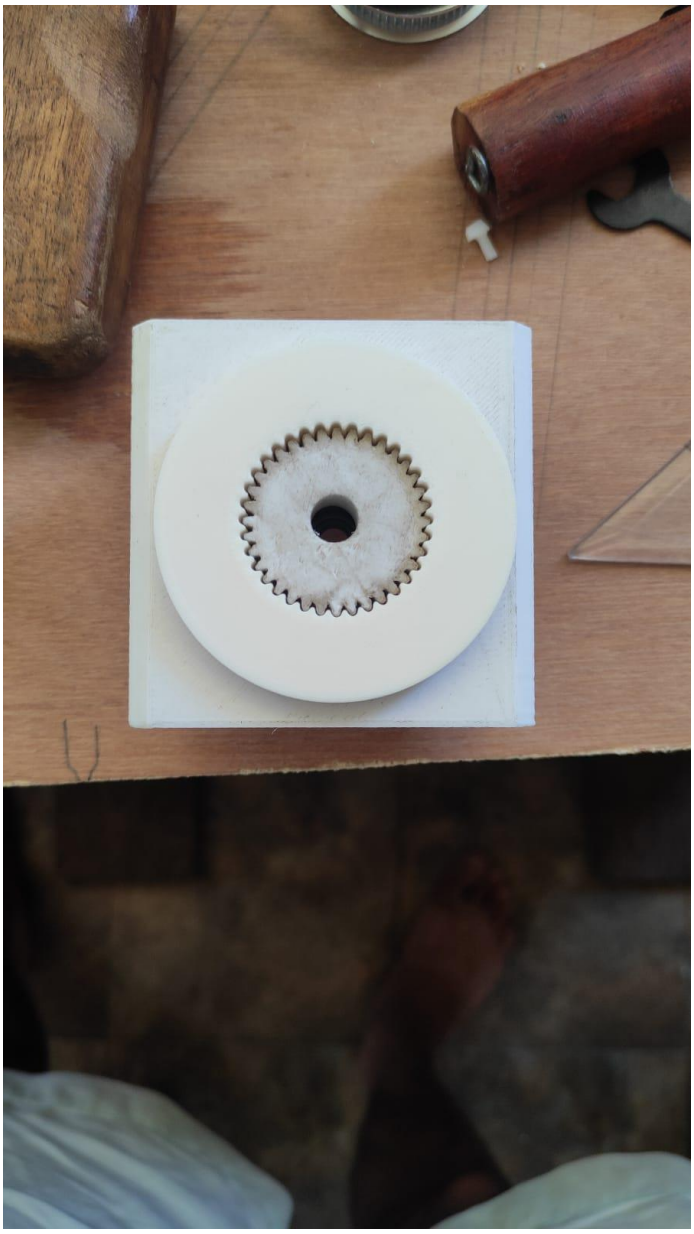

Given all these factors, we decided to reiterate our process and start working on a different mechanism, with simpler components and a much higher chance of success.

Second Design

Specifications:

Driving Motor : Nema 17, 5.6 kgf-cm

Selecting Motor NEMA 17 stepper

Timing belt reduction ratio= 1:9

Quantized output angle : 180/ 9 = 20 degrees

In the second design revision, changes were made to the existing mechanical multiplexer to make the design suitable for our requirements-

We made two notable changes to the design of the mechanical multiplexer-

1. We changed the engaging/disengaging mechanism to a more simple system consisting of a hole and shaft.
2. Addition of two reducers per multiplexer module.

In this mechanism, the torque input from the motor revolves the locking mechanism to the required multiplexer module to be actuated. The shaft on the rig will then enter the hole of the module and be rotated by 180 degrees to be put into a locked position. In this locked position, the stepper motor now provides a torque input , which; by means of the two reducer pairs is converted to output torque in step sizes of 2 degrees. This torque is then used to add or remove tension to the bowden mechanism so as to actuate the arm.

CAD MODEL OF THE SECOND ITERATION OF THE MULTIPLEXER

Fig 34- Front view CAD model of revised mechanical multiplexer

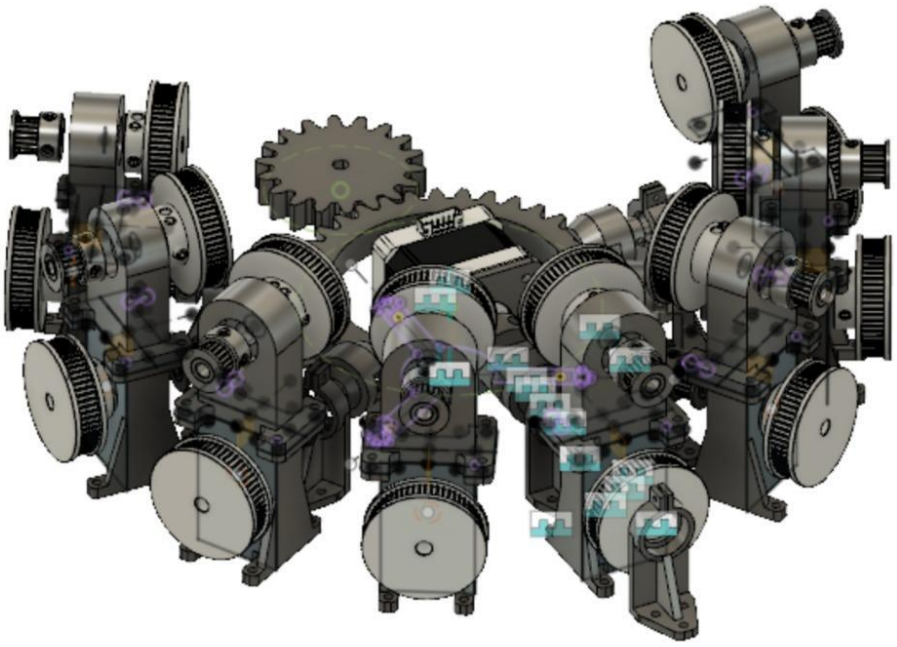

Fig 35- Side view of CAD model of revised mechanical multiplexer

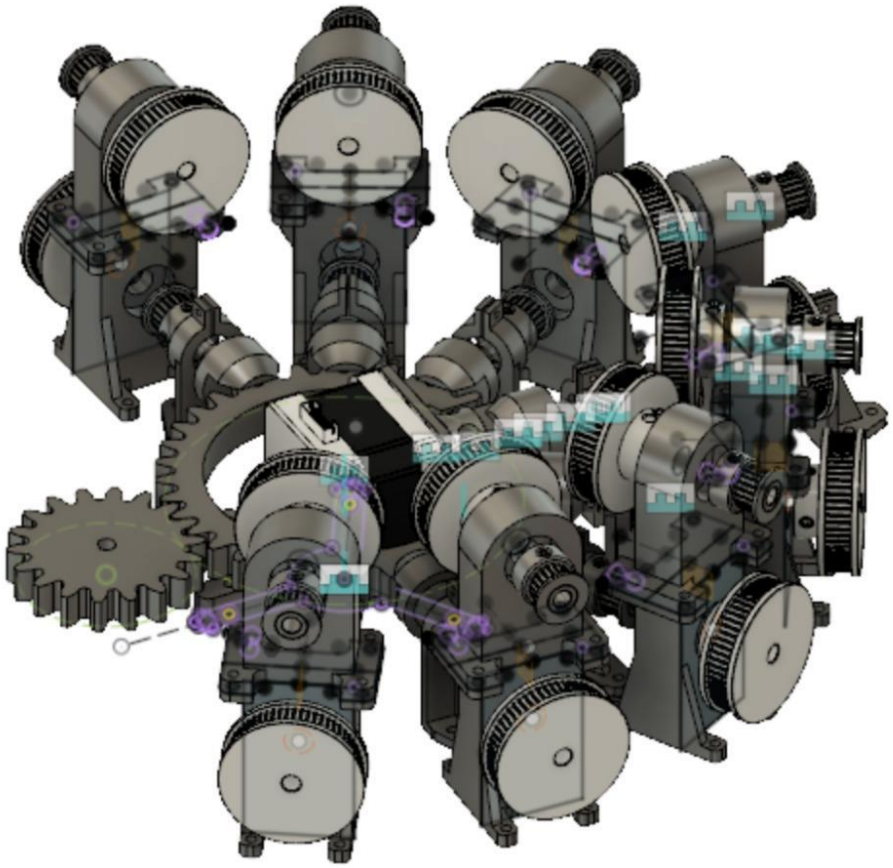

Fig 35- Left Side view of CAD model of revised mechanical multiplexer

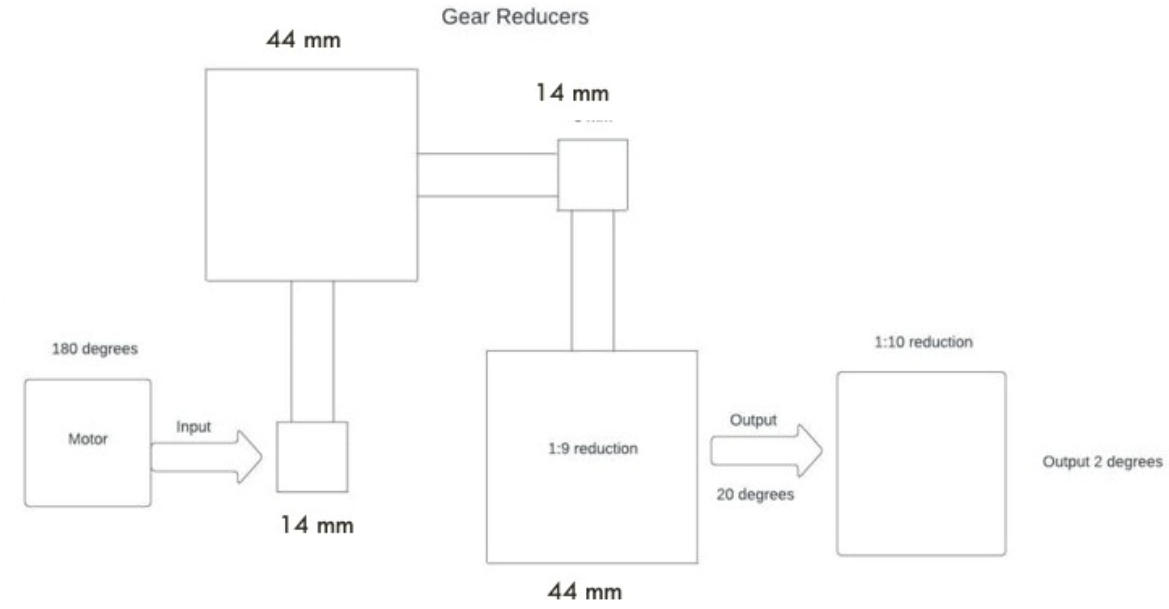

Fig 36- Block diagram of gear reduction

Design Calculations for Multiplexer

A) *Safety of Slot Design*
B) *Timing Belt Selection*
C) *Gear Design and Motor Selection*
D) *Safety of Shaft Mount*

A) Slot Design

Slot design is done assuming that the slot for engagement/disengagement is similar to that of an Oldham coupling. Following is the process adopted in the design of Oldham coupling and hence in slot calculation for Torque.

Oldham coupling

The Oldham coupling is used to connect shafts with lateral misalignment shafts which are parallel but not collinear. The misalignment of about 5 mm is taken care of by this coupling. It consists of two flanges with a diametral rectangular groove and a central floating part with the mating projections called *tongues* at right angles as shown in Figure 15.17. This central disc slides in the grooves of the flanges and needs the lubrication to avoid noise, wear and tear and improves efficiency of power transmission. The Oldham coupling can transmit high torque at low speed as high speed will produce dynamic unbalance due to center of gravity of central disc does not coincide with the axis of rotation of shafts.

Step-1 and 2 are same as discussed in the case of muff coupling and give us shaft diameter

$$d = \sqrt[3]{\frac{16M_{td}}{\pi\tau_{dshaft}}}$$

Input Parameters:
Current Torque Available at motor: 5.6kgcm = 5.6*9.81*10= 549.36Nmm
Torque at the slot= Motor torque*Reduction ratio = 549.36*9=4944.23
d is taken to be 5 mm as trial as it is a standard size bolt available. Checking for safety in shear:

- d (of shaft) =5=$\sqrt[3]{\frac{16*Mtd}{pi*Torque}} = \sqrt[3]{\frac{16*4944.23}{3.14*Shear}} => Shear$ =201N/mm^2

This value of shear is much lesser than the shear stress limit of steel, the design is safe for failure in shear.

- d (of slot) =22=$\sqrt[3]{\frac{16*Mtd}{pi*Torque}} = \sqrt[3]{\frac{16*4944.23}{3.14*Shear}}$=>Shear=2.36N/mm2

Since Shear is lesser than shear stress limit for PLA, design is safe.

Step-3: Coupling proportions

Considering *c* as the parallel misalignment between two shafts, we can set all the dimensions of the coupling using the empirical relation in the given table.

Table 6: Proportions of Oldham's coupling

Diameter of hub	$d_1 = 1.8d + 20\ mm$	Thickness of tongue	$t_1 = 0.4d + 0.15c\ mm$
Diameter of flange	$d_2 = 3d + c\ mm$	Width of tongue	$b = 0.25d + 0.1c\ mm$
Length of hub	$l = 0.75d + 12.5\ mm$	Thickness of flange	$t_2 = 0.6d + 0.25c\ mm$

The design of the Oldham coupling is based on the bearing pressure consideration because the groove of the driver's shaft applies the force on the tongue and develops pressure between the bearing areas. The pressure may be assumed zero near centre and maximum at the outer periphery as shown

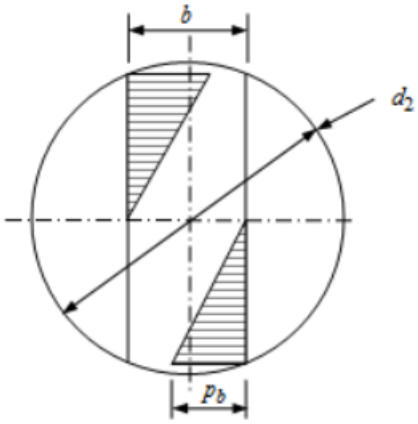

Pressure distribution on the tongue on central disc of the Oldham coupling

Torsional capacity of the tongue (PLA)

$$M_t = \frac{1}{6} P_b d^2 t$$

t is taken to be 10 mm for trial basis.

Mt=$\frac{P_b * d^2 * t}{6} == \frac{25 * 20^2 * 10}{6} = 16666.67 Nmm$

Allowable pressure *Pb*= 25N/mm^2 (for Shear)

We need not to find the torsional capacity of the flange as the thickness of the flange is more than the thickness of the tongue.

Since, M_t (Torsional Capacity) is greater than current torsion, the design is safe.

Thickness of tongue	t	10	mm
Allowable Pressure	Pb	25	N/mm^2
Torsion	Mtd	4944.24	N mm
Polar Moment of Inertia	J	15700	mm^4
Diameter of Shaft	d	20	mm
Torsional Capacity	Mt	16666.67	N mm
Torsional Shear	Tau	0.105441	N mm

$$\tau = \frac{M_t \, r}{J}$$

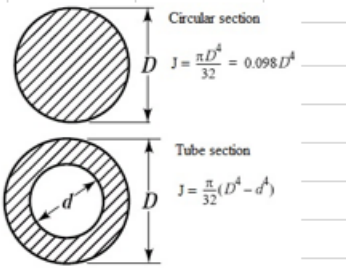

B)Timing Belt Selection

Multiplexer has an output of 180-degree quantized step angle. This angle requires to be reduced to smaller value for better resolution of robot arm joint angles.

A 1:9 ratio is required for compound timing belt for torque increase and step angle reduction.

Smallest step at Input= 180 degrees
Compound timing belt reduction= 1: 9
Output at end of compound = 180 / 9 = 20 degrees.

Reduction at winch 1:10 using capstan drives (driving and driven winch),

Input winch is connected to output of mechanical multiplexer with and Outer Diameter of 6 mm.
Output winch has outer diameter of 60 mm.

Cables are routed through constant length Nylon Bowden tubes.

Hence final output is (180/ 9) / 10 = 2 degrees

The arm is able to have an output resolution of 2 degrees.

For the timing belt selection:

Motor holding torque of NEMA 17 motor = 5.6 kgf-cm = g x 5.6 kgf-cm = 9.81 m/s^2 x 5.6 x 10
Motor holding torque of NEMA 17 motor = 549.36 N-mm = 0.549 N-m

Maximum torque is in second pair in the compound timing belt reducers.
Same pulleys are used for cost reduction and simpler part selection (as availability timing belt of parts is limited). Second pair timing belts will have maximum tension force as a result of maximum torque.

Pair 1:

Torque at driving timing pulley = 0.549 N-m
Torque at smaller timing pulley = 0.549 x 3 N-m = 1.647 N-m

Pair 2:

Torque at driving timing pulley = 1.647 N-m
Torque at smaller timing pulley = 1.647 N-m x 3 N-m = 4.941 N-m

Upper limit for Motor speed on NEMA 17 motor is 100 rpm i.e. 100 x 0.10472 rad/s = 10.47rad/s (for the stepper CNC speed control).

Hence,
Power = T x W / 1000 kW = 4.941 x 10.47 = 0.0517 kW

Here,
T = Torque (N-m)
W = Max angular speed (rad/s)
From Misumi selection guide for driving belts,
Power = 0.0517 kW

Table 23. Selection Guide Table (2GT·3GT series)

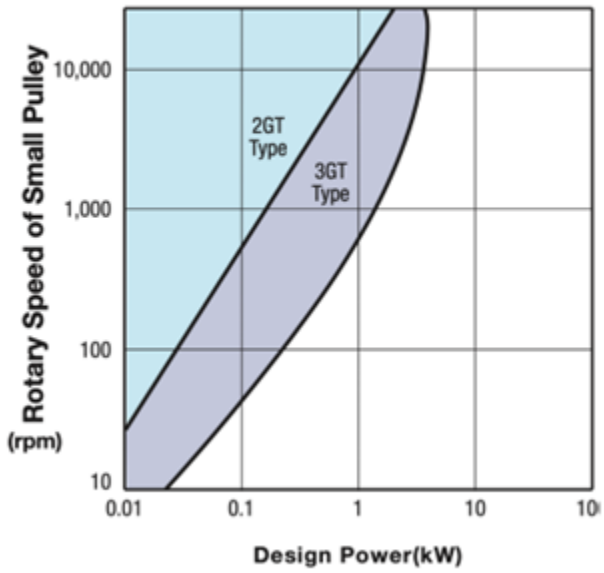

Belt

2GT Belt is suitable for selection.

Available belt width for 2GT is 6mm.

Pulley

Driving timing pulley specifications:

- Aluminum GT2 Timing Pulley
- 20 Tooth
- 5mm Bore
- Outer Diameter: 16 mm.
- Inner Diameter: 5mm.

Driving timing pulley specifications:

- Aluminum GT2 Timing Pulley
- No. of teeth: 60
- Bore Diameter(mm): 5
- Outer Diameter(mm): 44

Hence 1:3 ratio is achieved (20/ 60).

Closed loop length is selected as 200 mm. for timing belt.

Distance between the Centers:

Length of the belt: 200

Diameter of pulley 1: 16

Diameter of pulley 2: 44
X: distance between the centers of 2 pulleys

L= (pi/2) (d1+d2) +2x+ ((d1-d2)2 / 4x)
= (3.14/2) (16+44) + 2x + ((44-16)2 / 4x)
200 = 94.2+2x+729/x
105.8 = 2x + 729/x
2x2 -105.8x + 729=0

X1=44.75
X2=8.14 (Value is discarded as it doesn't fit dimensions)

Centre distance is 44.75 mm.

The timing pulley mounts are made to be height adjustable using variable height shims.

C)Gear Design and Motor Selection
Speed: 40 rpm (min 15) (max 70)
Ꮳ: 4.1866667 rad/sec

Input Gear Parameters:
Pressure angle: 20 Degrees
Number of teeth: 18
Module: 2mm (Step angle is 1.8 degree. To achieve higher accuracy, i.e., a smaller step angle using the module of 2 mm which gives step angle of 1:2. Lowest possible printer resolution is +-0.3mm. Sufficient accuracy. cannot be obtained with m<2. Hence module is chosen to be 2 here.)

Table 17.1 *Proportions of standard involute teeth (in terms of module m)*

	14.5° full depth system	*20° full depth system*	*20° stub system*
Pressure angle	14.5°	20°	20°
Addendum	m	m	0.8 m
Dedendum	1.157 m	1.25 m	m
Clearance	0.157 m	0.25 m	0.2 m
Working depth	2 m	2 m	1.6 m
Whole depth	2.157 m	2.25 m	1.8 m
Tooth thickness	1.5708 m	1.5708 m	1.5708 m

Output Gear Parameters:
Pitch Circle Diameter: 36 mm
Addendum: 2mm
Dedendum: 2.5mm
Clearance: 0.5mm
Working depth: 4mm
Whole Depth: 4.5mm
Tooth thickness: 3.1418mm
Tooth Space: 3.1418mm
Fillet radius: 0.8

For the motor to transmit rotational motion, the torque by the motor must be greater than that of the resistance offered by the rotational inertia of the Knob engaged in the hand of the multiplexer.
Hence finding rotational inertia = I

Inertia:
Mass of the motor = 0.5 kgs
Length = b = 47mm
Breadth = d = 42mm

Shape	Image	Equation
Cuboid	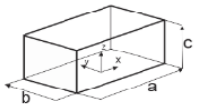	$I_{G_{xx}} = \frac{1}{12} m\,(b^2 + c^2)$ $I_{G_{yy}} = \frac{1}{12} m\,(a^2 + c^2)$ $I_{G_{zz}} = \frac{1}{12} m\,(a^2 + b^2)$

With reference to the above table, the case for cuboid is chosen as that of the Slot shape
$I_{G_{zz}} = \frac{1}{12} m\,(a^2 + b^2)$
I = 165.542 kg. mm^2 =0.00017 kg.m2

w= 40 rpm = 0.6667 rps
(As speed is not a primary feature, we have taken this to be 40rpm in the work area)

w=$\frac{2*pi*40}{60}$=4.176rad/sec

Therefore,
Power= I*w=0.00017*4.176=0.00069Watt

The Torque = $\frac{P}{w} = \frac{0.00069}{2*pi*nrps} = \frac{0.00069}{2*3.14*0.6667} = 0.16554Nm = 165.542Nmm$

Reduction Ratio = 2 (To have better precision of almost 1 degree)

Therefore, net opposing torque at the slot: Torque*Reduction ratio=165.542*2=331.083Nmm

Thus, the Nema 17 motor is chosen as it offers a net holding torque of 5kgcm that is 392.266N-mm.

Checking Safety of Gear

ESTIMATION OF MODULE BASED ON BEAM STRENGTH				ESTIMATION OF MODULE BASED ON WEAR STRENGTH		
$m=\left[\frac{60\times10^6}{\pi}\left\{\frac{(\mathrm{kW})C_s(fs)}{znC_v\left(\frac{b}{m}\right)\left(\frac{S_{ut}}{3}\right)Y}\right\}\right]^{1/3}$				$m=\left[\frac{60\times10^6}{\pi}\left\{\frac{(\mathrm{kW})C_s(fs)}{z_p^2n_pC_v\left(\frac{b}{m}\right)QK}\right\}\right]^{1/3}$		
Module	m	2		Pitch Line vel v	0.07536	m/s
Power		6.93068E-07		K	1.1664	
Number of teeth		18				
n(rpm)		40	rpm			
Cv		1.300660736				
b		8	mm			
Q		1.333333333				
K		1.1664				
Sut		50	Mpa			
Cs		3.25				
(A higher value is taken to compensate for printing flaws)		Driving Mc:Heavy shock Driven Mc:Heavy Shock				
Y		0.308				
Factor of Infill		1				
Fos(for beam strength)				Fos (For Wear Strength)		
15.28933				23.85135		

(i) For ordinary and commercially cut gears made with form cutters and with $v < 10$ m/s,

$$C_v = \frac{3}{3+v} \qquad (17.20)$$

$$v = \frac{\pi d' n}{60\times10^3}$$

$$K = 0.16\left(\frac{\mathrm{BHN}}{100}\right)^2$$

$$Q = \frac{2z_g}{z_g + z_p}$$

Table 28- Excel calculations of Safety of Gear

E) Stand Design

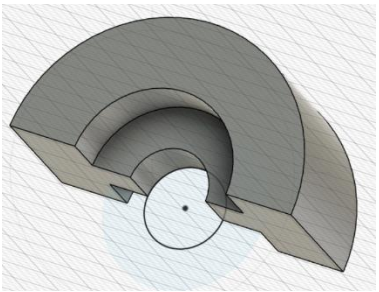

Area under tension: 124.50 mm^2

Tension in belt: $\frac{Torque}{Radius}$

T1=$\frac{1.647}{0.008}$=205.87N

T2=$\frac{4.941}{0.008}$=616N

Total tension: 2T1+2T2=1643.75N

FOS: $\frac{Sut}{Tensile\ Stress} = \frac{Sut}{\frac{Tension}{Area}} = \frac{50}{\frac{1643.75}{124.50}} = 3.78$

Pair 1: Torque at smaller timing pulley = 0.549 x 3 N-m = 1.647 N-m
Pair 2: Torque at smaller timing pulley = 1.647 N-m * 3 = 4.941 N-m
Radius of smaller pulley:8mm

G) Bearing Selection

Stage 2- Arm Design

1. Stage 2 is the design of Arm Assembly
2. Arm Assembly consists of Bowden cable and the Joint pulley.
3. Initial tests using simulations for multibody analysis
4. FEA and Design analysis of arm members.

Stage 3- Design Calculations-

Design Calculations for Arm Module

A) The Winch

The Diameter of the winch of the arm is taken to 60 mm as the pair of 60mm(winch) and 6mm at the output shaft gives a reduction of 1:10**.**

B) The Fork

The base of the fork is taken to be in an octagonal shape (Because the design is parametric in which you can use it for planar and non-planar as well. Manufacturing is easier and mounting components is easier as well) The input parameters for the design of the arms of the fork are:

(i) Circumcircle diameter of Octagon

The diameter is taken to be 56mm given the dimensional constraint. This value was arrived at by logic and trial-error method with the aim of limiting the side of octagon to less than 25mm. This value of diameter aids accommodation of Bowden cables and does not hinder the flexibility of nylon tube.

(ii) Height of the Octagon

The height of the octagonal base is taken to be 20mm. Again, the same was arrived at by trial and error and verification of safety in ANYSYS FEA. This height not only provides sufficient structural integrity of mounting points of the fork but also ensures proper accommodation of Bowden cables and flexibility of nylon tube.

(iii) Length/Breadth ratio the fork

The ratio is taken as 7. Various cases were check in excel sheet using the WHAT-IF analysis for safety in various types of failures. The ratio of 7 gives satisfactory safety without increasing dimensions. Used Goal Seek.

(iv) Diameter of the Eye

Diameter of the eye is taken to be 6mm. This was decided based on optimum material usage. Using a lower diameter would have increased material and bigger diameter would have resulted in shear failure.

(v) Tension in cable

The tension is cable is assumed to be 20N for first link which is going to exp highest tension. Because calculation of exact tension is not possible given the complex nature of the system. We tried multiple ways of finding tension in the string like balancing moments or using basic rotational dynamics, but ended up having at least one more unknown parameter in either way.20N is the reaction force of the entire system.

(vi) Weight of the arm

The total weight of the arm including the end effector (if used) is limited to 25N.

Design Calculations:

- Side of Octagon:

Side of the octagon= $\frac{\text{Diameter of the circumcircle of Octagon}}{2*1.307}$

$=\frac{56}{2*1.307}$ = 21.42mm

- Dimensions of Fork

Length = 15mm

Breadth = $\frac{Length}{\text{Ratio (Length/Breadth)}}=\frac{15}{7} = 2.1mm$

Area of rectangular Cross Section= Length* Breadth = 15*2.2=31.5mm^2

- Projected Area of the Eye= Breadth* Diameter of the eye= 2.2*12 = 25.2mm^2
- Critical area for tension = Area of rectangular cross section-Projected area of the eye

=33-26.4=6.30mm^2

- Length of Fork under shear: $\sqrt{Outer\ Radius^2-Inner\ Radius^2}$=$\sqrt{7.5^2-6^2}$=4.5mm
- Distance between the centre of eye and base: 36 mm

Calculation for Factor of Safety

- Safety in Compression

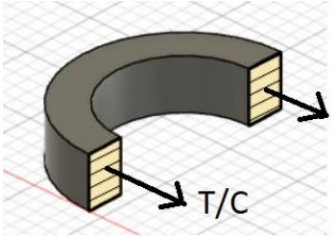

FOS in Compression= $\frac{Compressive\ strenth}{(\frac{Compressive\ Force}{Area})}=\frac{95}{(\frac{45}{2*6.30})} \approx 26.6$

- Safety in Tension

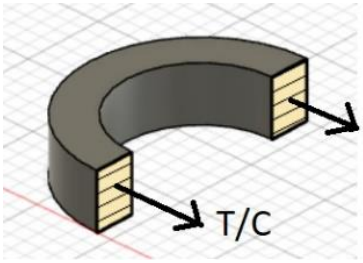

FOS in Tension= $\frac{Yield\ strenth}{(\frac{Tensile\ Force}{Area})}=\frac{50}{(\frac{45}{2*6.3})} \approx 14$

- Safety in Shear

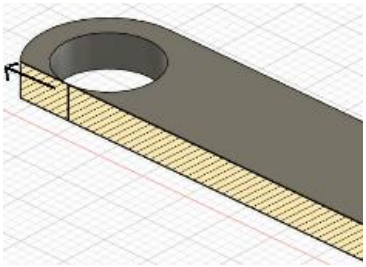

FOS in Shear= $\frac{Shear\ strenth}{(\frac{Shear\ Force}{Area})}=\frac{50}{(\frac{45}{4*\text{Length of Fork under shear}*breadth})} \approx \frac{50}{(\frac{35}{4*4.5*2.1})} \approx 47.25$

- Safety in Bending

Effective Bending Moment due to weights of all modules and end effector = 360 N.mm
(Centre of Gravity Calculations done in subsequent part)
Case 1: Bending force perpendicular to length

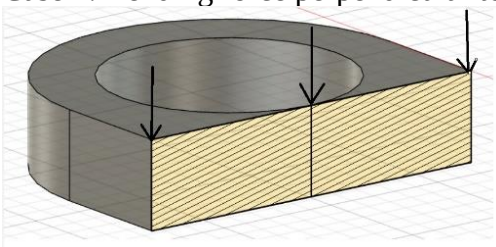

$$\sigma_b = \frac{M}{I} \cdot y$$

I: Moment of Inertia about center

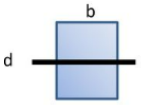

$$I_{cc} = \frac{bd^3}{12}$$

I = $\frac{15*2.2^3}{12} = 24.31mm4$

y: Distance between neutral axis and extreme edge = d/2=$\frac{Breadth}{2} = 1.05mm$

Factor of Safety = $\frac{360*1,1}{13.31} = 2.09$

Case 2: Bending force perpendicular to breadth

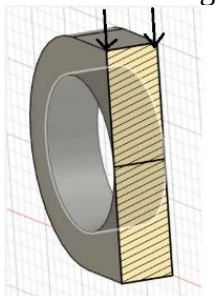

$$\sigma_b = \frac{M}{I} \cdot y$$

I: Moment of Inertia about center

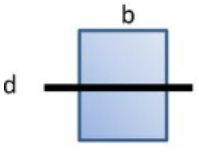

$$I_{cc} = \frac{bd^3}{12}$$

$I = \frac{2.2*15^3}{12} = 590.62mm4$

y: Distance between neutral axis and extreme edge = d/2=$\frac{Length}{2} = 7.5mm$

Factor of Safety = $\frac{360*7.5}{618.75} = 7.11$

Note :	*Values in cells highlighted in yellow can be varied for different outputs.*						
Basic Dimension for Fork Base							
Circumcircle Diameter for Octagon	56	mm					
Side of Octagon	21.42	mm					
Octagon height	20						
Winch Diameter	60	mm					
# Design of Fork					# Material Properties		
Dimensions :					Material Chosen :	Polylactic Acid Filament	
Ratio Length(OD)/Breadth(thickness)			7				
Rectangular Cross Section			Breadth(b)	Depth(d)	Comressive Strength :	95	Mpa
Dimensions (in mm)			15	2.1	Yield Strength (Syt)	50	Mpa
Area			31.50	mm^2	Flexural Strength	65	Mpa
					Shear Strength	25	N
Diameter of the eye			12	mm			
Projected Area of Eye			25.2	mm^2			
Area for compression and tension			6.30	mm^2			

Table 24- Excel calculations for Fork Base

	Area for compression and tension			6.30	mm^2	
	Length of fork under shear			4.5	mm	
	Distance between centre of eye and base			36	mm	
(i)	**Safety in Compression**					
	Tension in Cable			20	N	
	Weight			25	N	
	FOS :			*26.6*		
(ii)	**Safety in Tension**					
	Tension Force (Due to subsequent winch)			20	N	
	Weight			25	N	
	FOS			*14*		
(iii)	**Safety in Shear**					
	Area for Shear :	37.8	mm^2			
	FOS	*47.25*				

Type	FOS
Compression	26.6
Tension	14
Shear	47.25
Bending	2.09
Minimum FOS	**2.09**

(iv)	**Safety in Bending**				
	Force causing bending	20	N		
	Bending Moment	720	N-mm		
	I (right pov)	590.625			
	y (right pov)	7.5	mm		
	Bending Stress	9.142	N/mm^2	*FOS*	*7.11*
	I (top pov)	24.31			
	y (top pov)	1.05	mm		
	Bending Stress	31.098	N/mm^2	*FOS*	*2.09*

Table 29- Safety Calculations

FINITE ELEMENT ANALYSIS

Analysis of a Single Joint:

Joint:

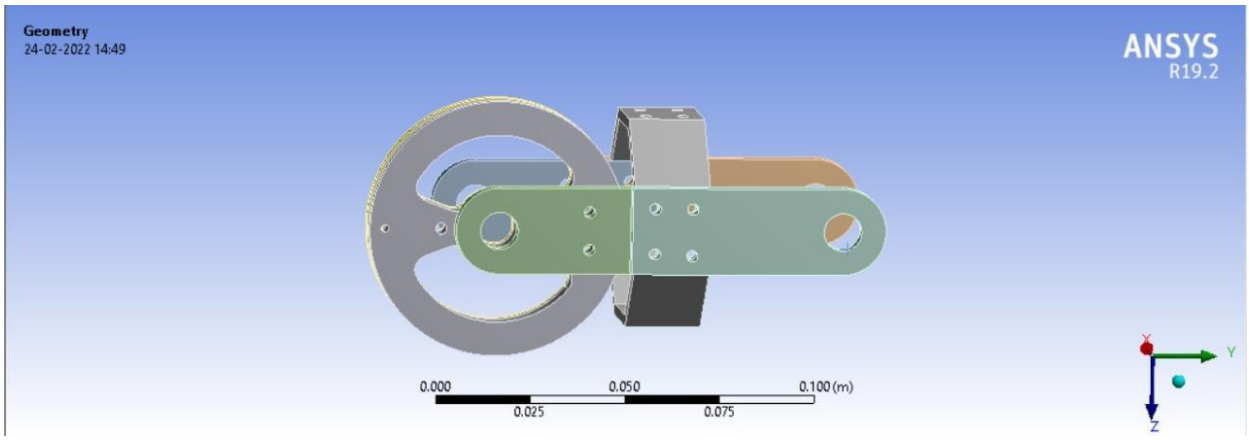

Fig 38- Joint FEA

Assigning Material Properties:

Material	
Material Name	PLA
Fluid	**False**
Density	**0.00125 g/mm^3**
Ultimate Strengtl	**55000000 Pa**
Elastic Modulus (	**3.5000E+9 Pa**
Shear Modulus (I	**2.4000E+9 Pa**
Poisson's Ratio	**0.3**
Thermal Conduct	**0.2 W/m-K**

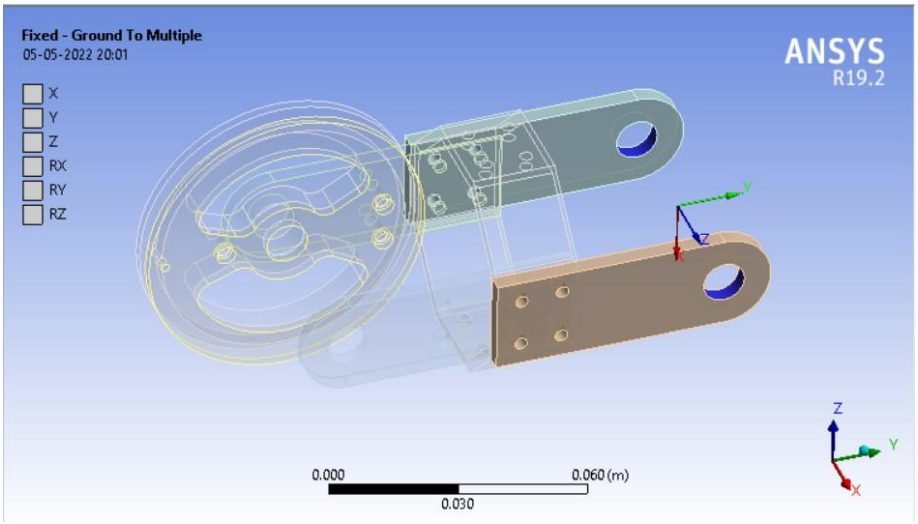

Contact Constraint- One end of fork Fixed to Ground:

Fig 40- Constraints FEA

Contact Constraints between winch and fork components – Body to Body fixed contact:

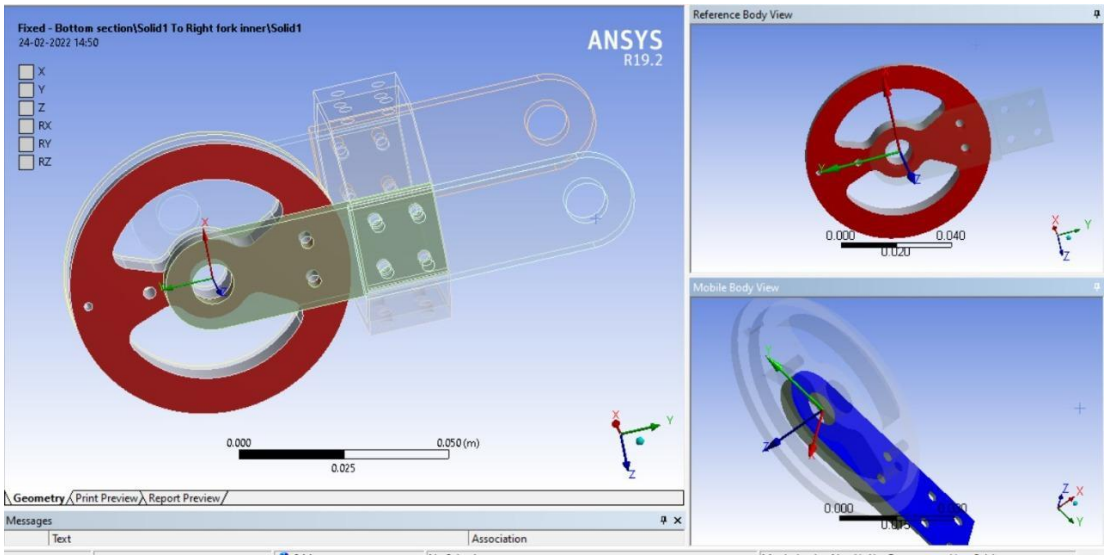

Fig 41 and 42- Moment on eye

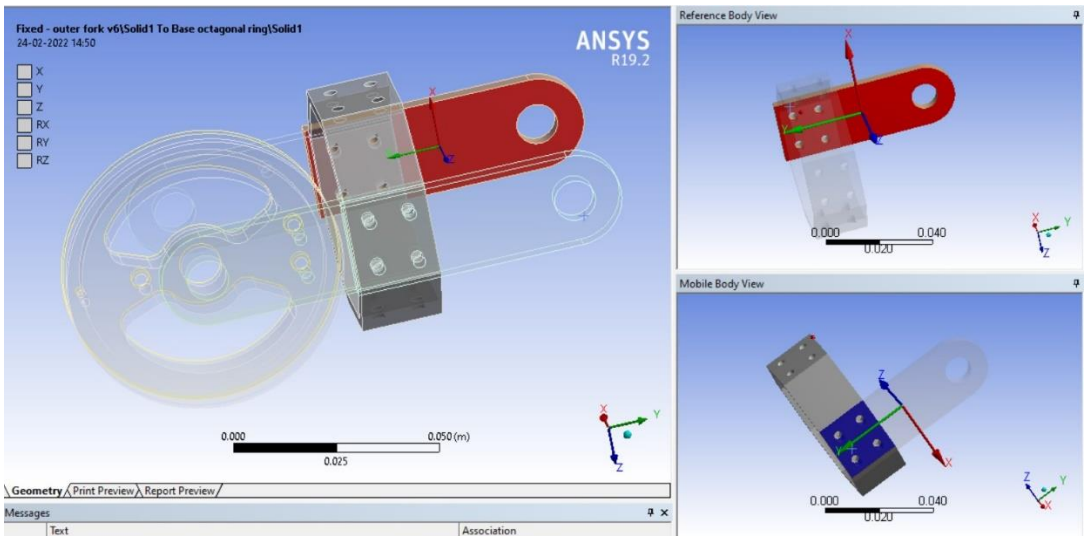

Meshing: Fine Tetrahedral Mesh

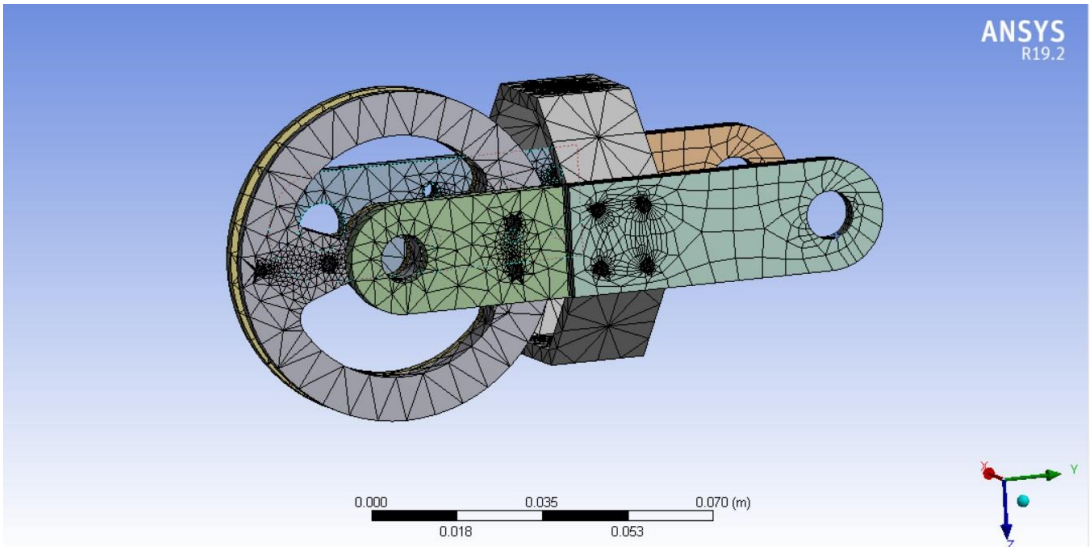

CASE: Bending at critical joint due to the weight of the remaining 7 joints:

SPECIFICATION	VALUE
Material	PLA(Polylactic Acid)
Contacts	Fixed joint between Winch and Forks
Fixed Support	Body to Ground contact at one end of fork
Mesh Type	Fine, Tetrahedral
Force Position/ Direction	At the axis of other end of fork in the downward direction.
Force Magnitude	15 N

Force: 15N

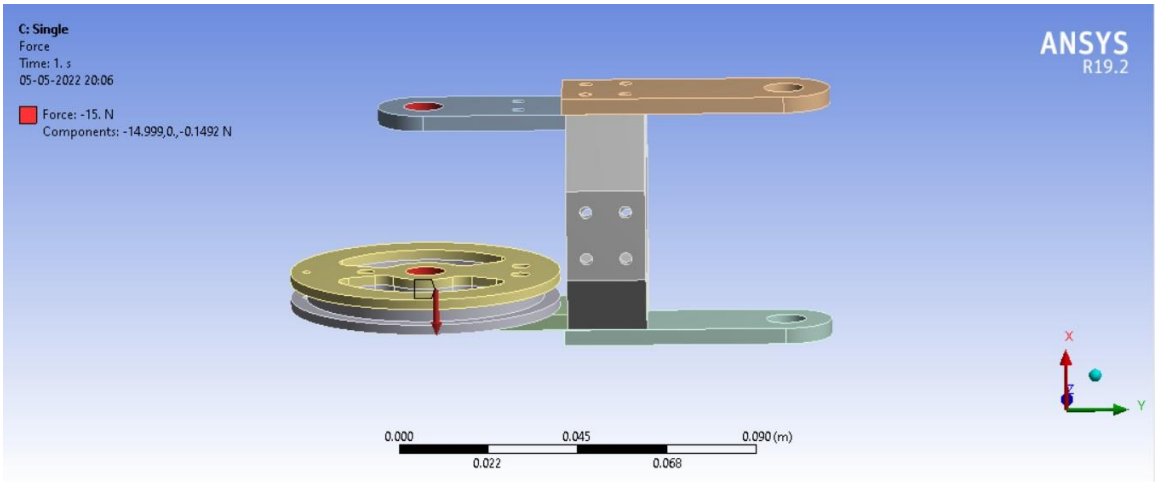

Fig 43 Force on winch

Total Deformation:

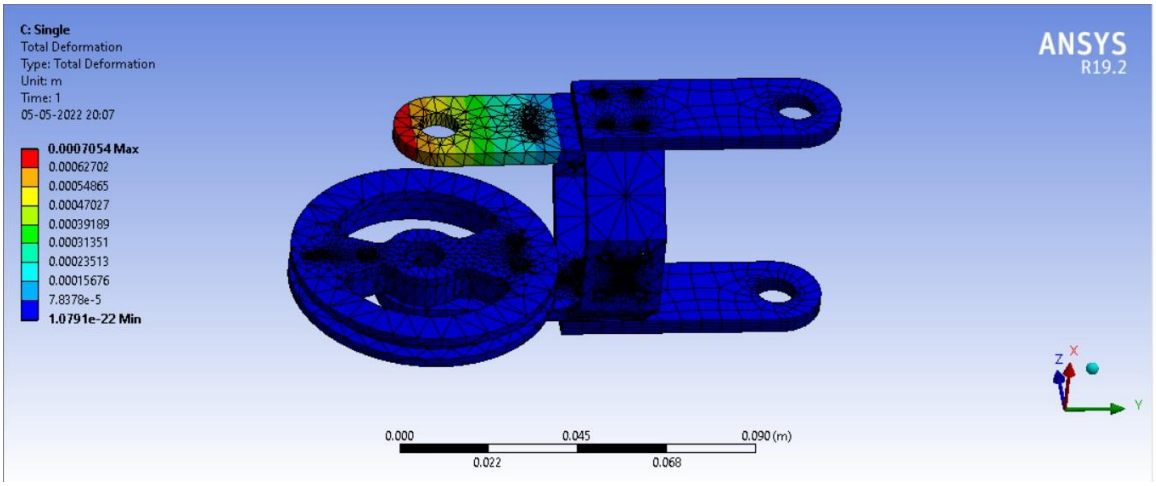

Maximum Principal Stress:

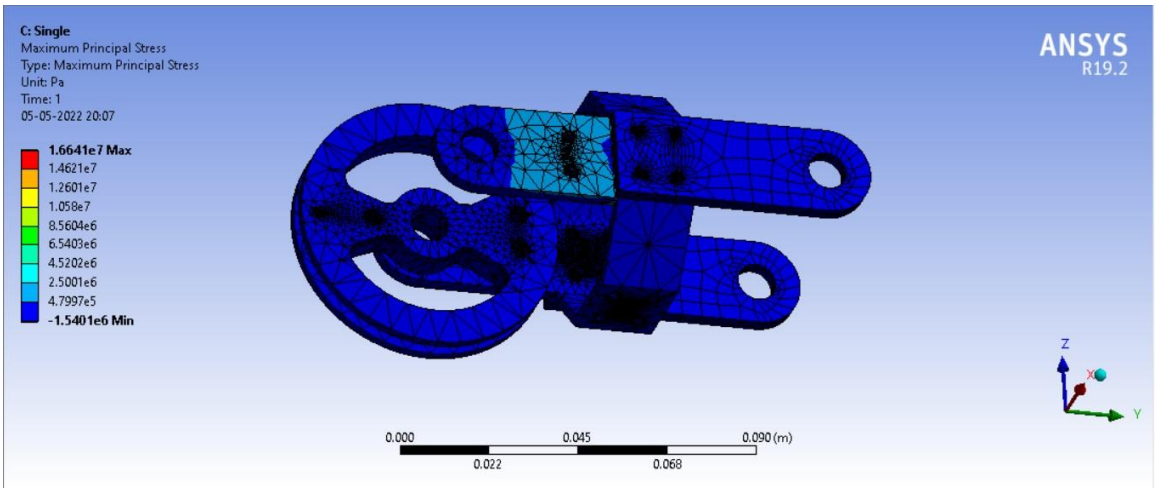

Fig 44- Maximum Principal Stress

Output:

SPECIFICATION	VALUE
Max. Deformation	0.705 microns
Maximum Principal Stress	4.5 MPa

Conclusion: Safe

CASE: Moment at Joint due to tendon actuation:

SPECIFICATION	VALUE
Material	PLA(Polylactic Acid)
Contacts	Fixed joint between Winch and Forks
Fixed Support	Body to Ground contact at one end of fork
Mesh Type	Fine, Tetrahedral
Moment Position/ Direction	About the axis of winch
Moment Magnitude	0.6 Nm

Moment: 0.6Nm

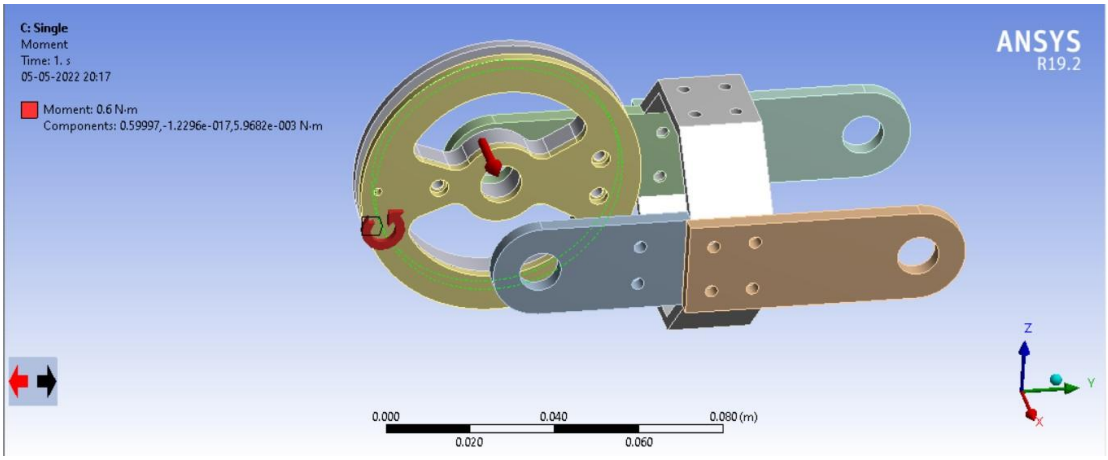

Fig 45- Forces on eye

Maximum Principal Stress:

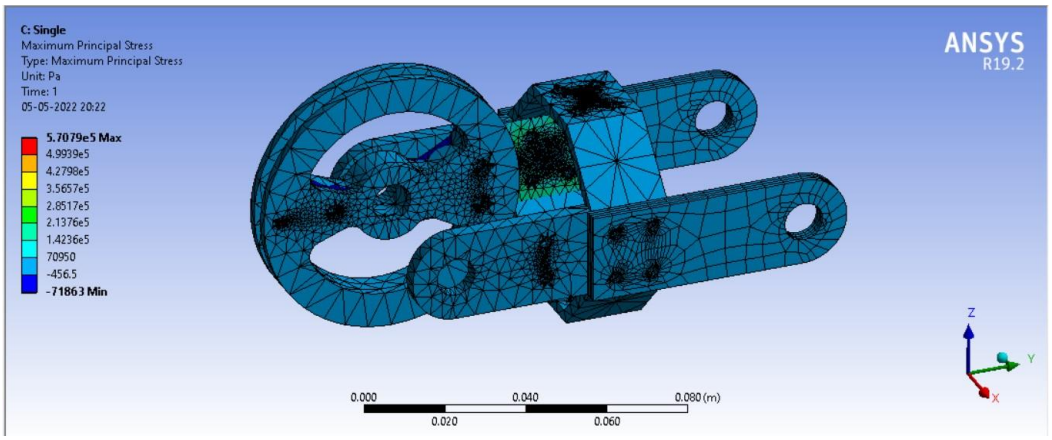

Fig 46- Meshing of Fork

Total Deformation:

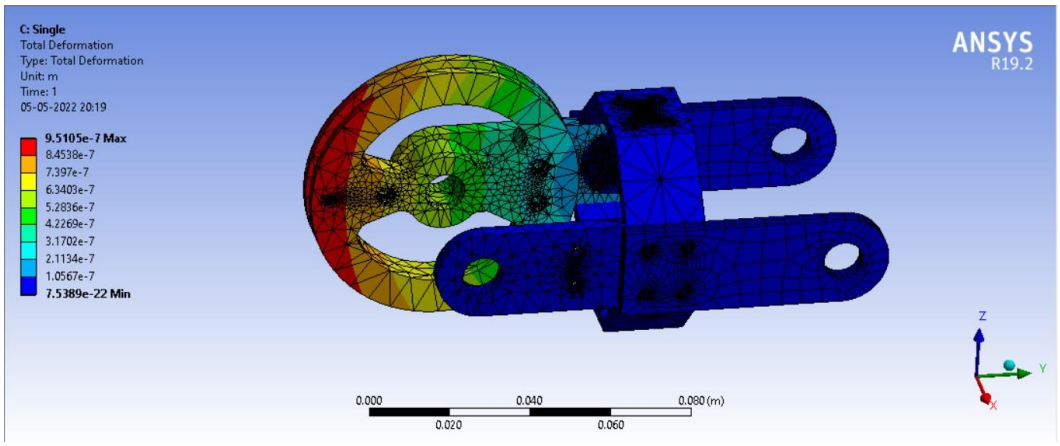

Output

SPECIFICATION	VALUE
Max. Deformation	0.95 microns
Maximum Principal Stress	0.5 MPa

Conclusion: Safe

CASE: Tension in the joint during tendon actuation:

SPECIFICATION	VALUE
Material	PLA(Polylactic Acid)
Contacts	Fixed joint between Winch and Forks
Fixed Support	Body to Ground contact at one end of fork
Mesh Type	Fine, Tetrahedral
Force Position/ Direction	Along the direction of the fork length
Force Magnitude	20 N

Force: 20N

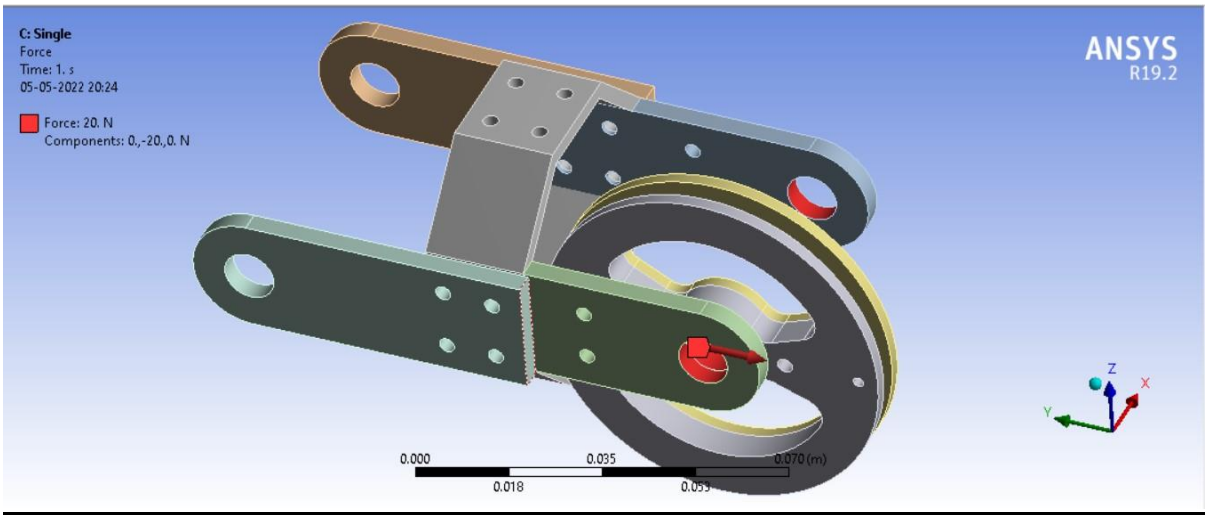

Fig 47- Perpendicular force on eye

Total Deformation:

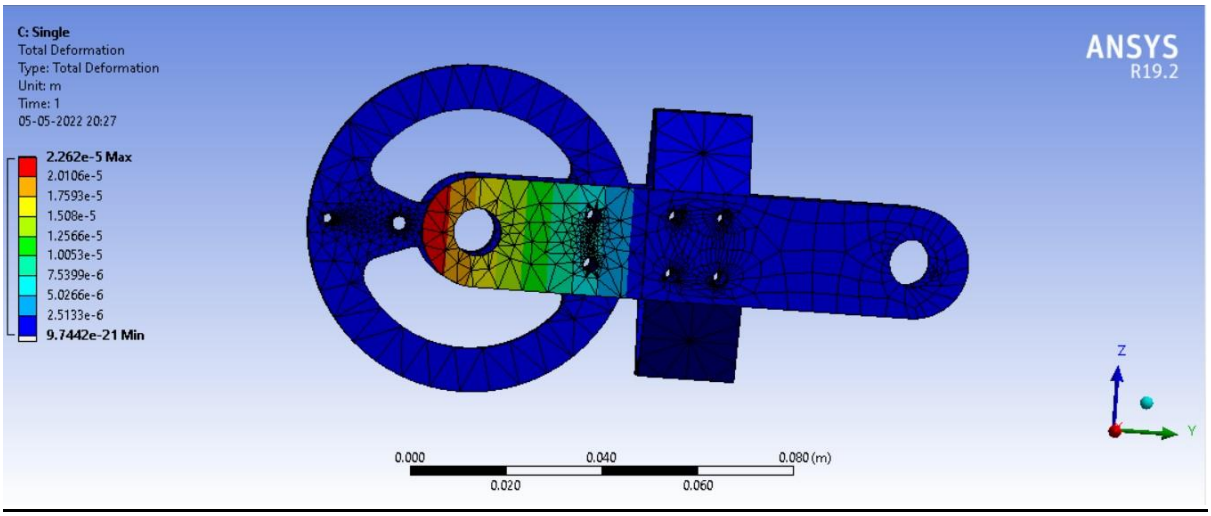

Fig 47- Total Deformation in FEA

Maximum Principal Stress:

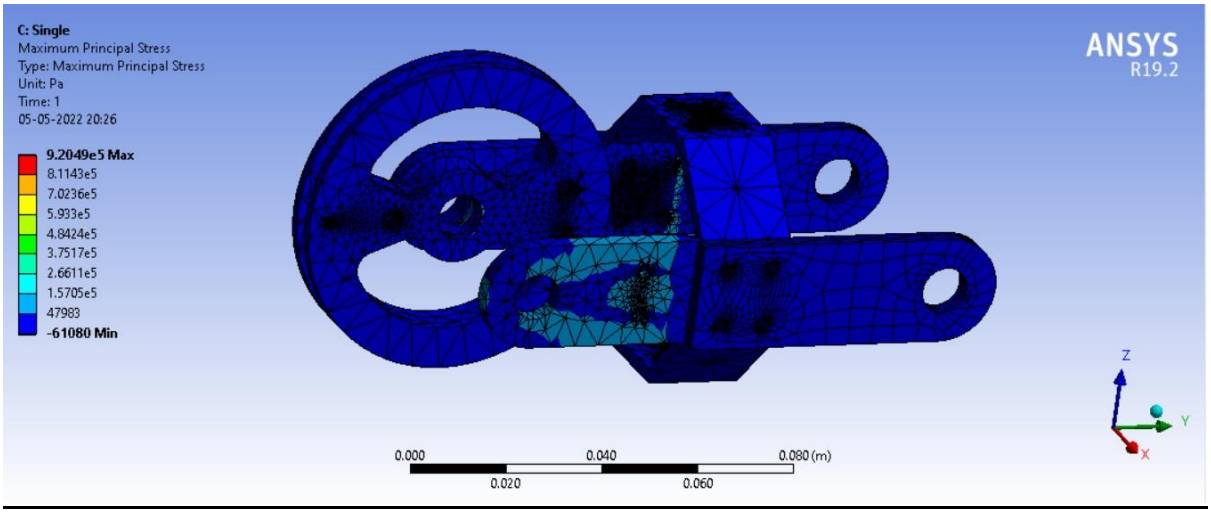

Fig 49-Maximum Principal Stress

Output

SPECIFICATION	VALUE
Max. Deformation	22 microns
Maximum Principal Stress	0.92 MPa

Conclusion: Safe

Multibody Static Analysis:

Bending at the critical joint due to the weight of remaining joints:

SPECIFICATION	VALUE
Material	PLA(Polylactic Acid)
Contacts	Revolute Joint between winch of one joint and fork of the next joint
Fixed Support	Body to Ground contact at the fork of the first joint
Mesh Type	Fine, Tetrahedral
Force Position/ Direction	At the axis of fork of the last joint in the downward direction.
Force Magnitude	Rb = 14.7 ~ 15 N

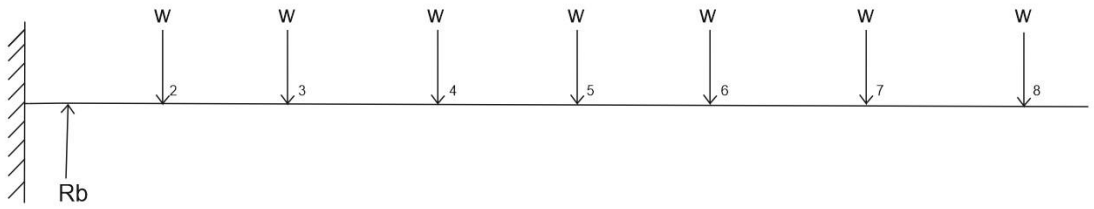

Free Body Diagram for bending case

w = Weight of one joint

Joint Assembly:

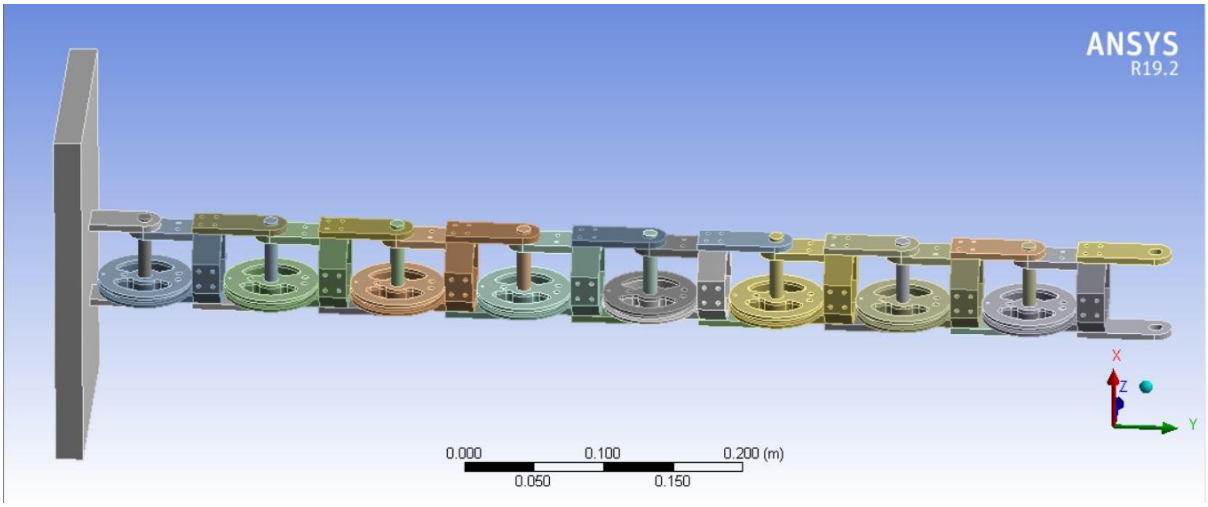

Contact Constraint: Body to ground on both ends to prevent rotation and analyse the stress

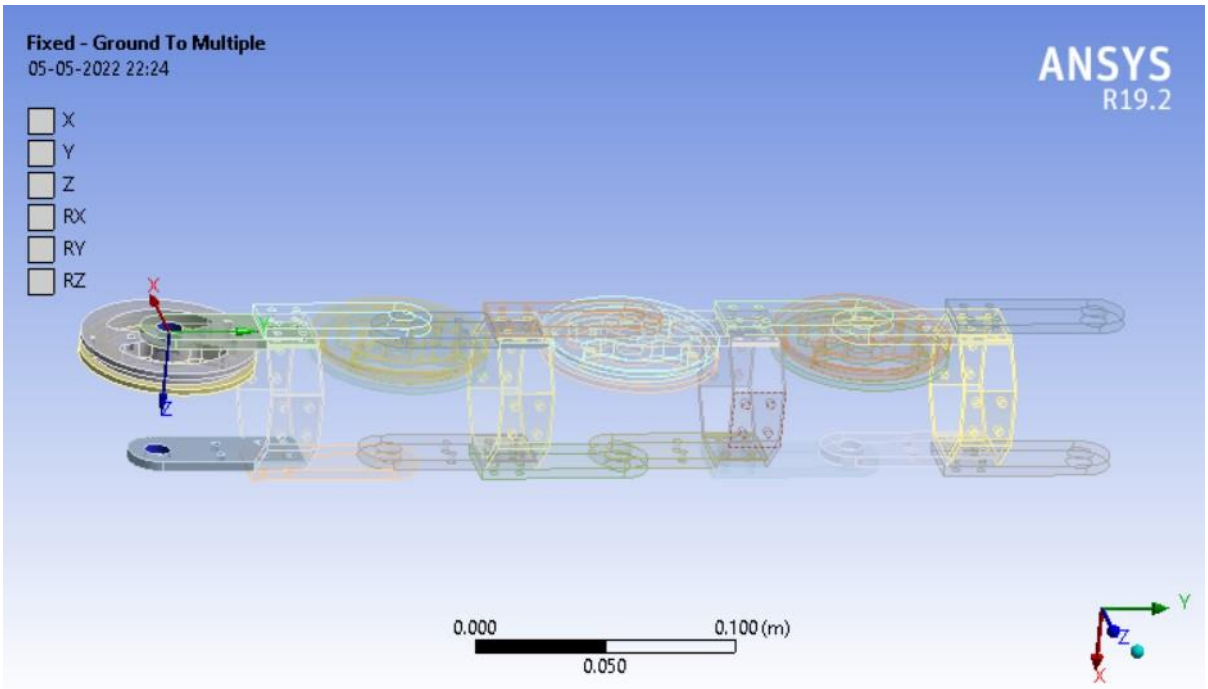
Fixed - Ground To Multiple
05-05-2022 22:24
ANSYS
R19.2
X
Y
Z
RX
RY
RZ
0.000
0.100 (m)
0.050

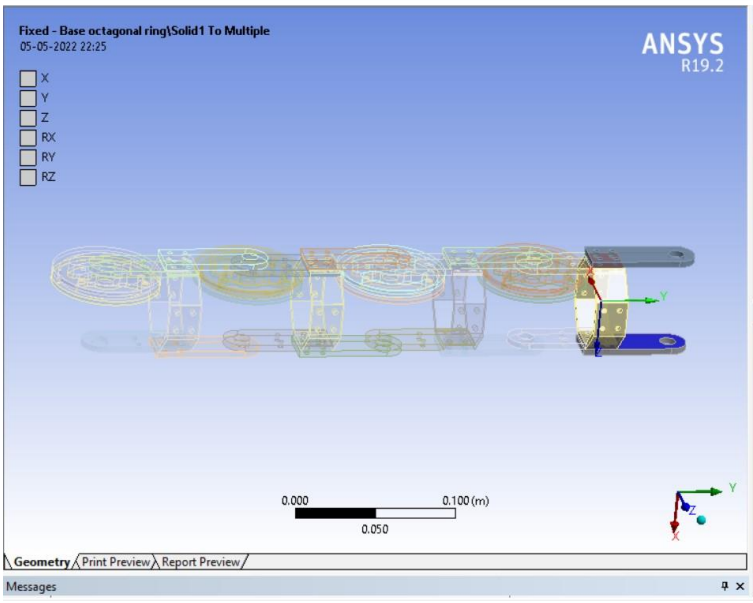
Fixed - Base octagonal ring\Solid1 To Multiple
05-05-2022 22:25
ANSYS
R19.2
X
Y
Z
RX
RY
RZ
0.000
0.100 (m)
0.050
Geometry
Print Preview
Report Preview
Messages

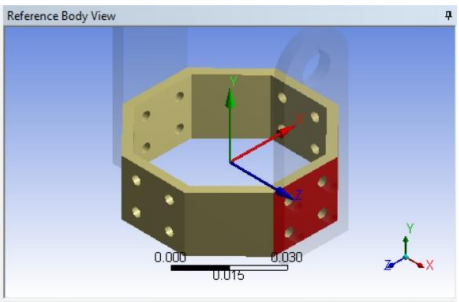
Reference Body View
0.000
0.030
0.015

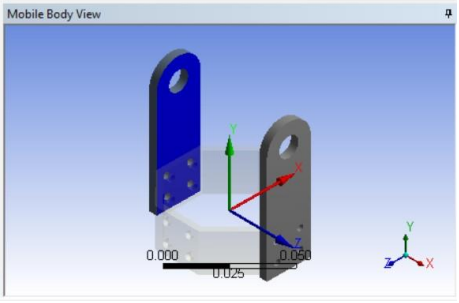
Mobile Body View
0.000
0.050
0.025

Meshing:

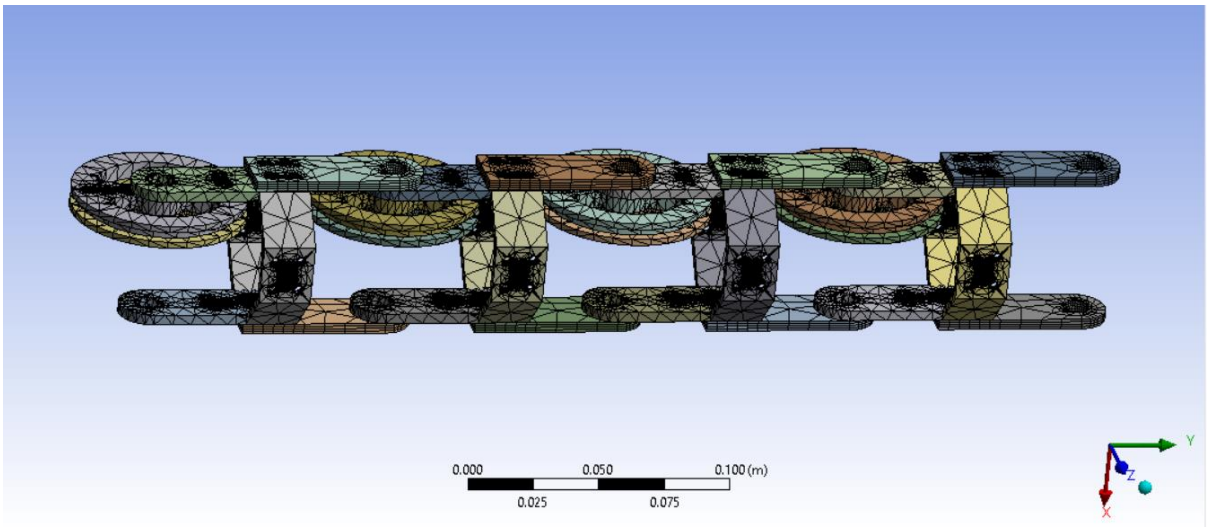

Fig 50- Meshing of Arm

Force: 15N

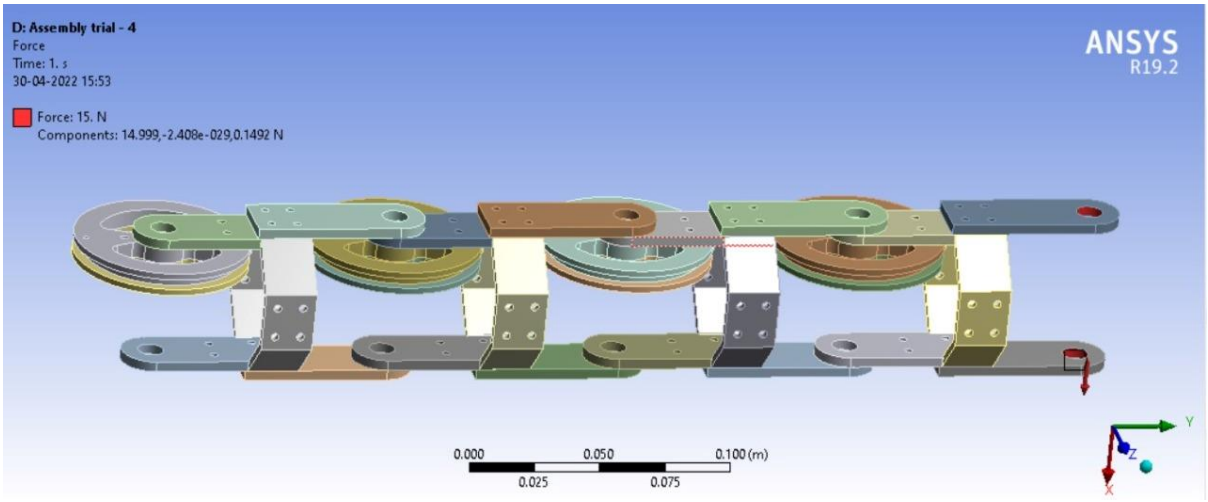

Fig 51- Total Deformation of Arm

Total Deformation:

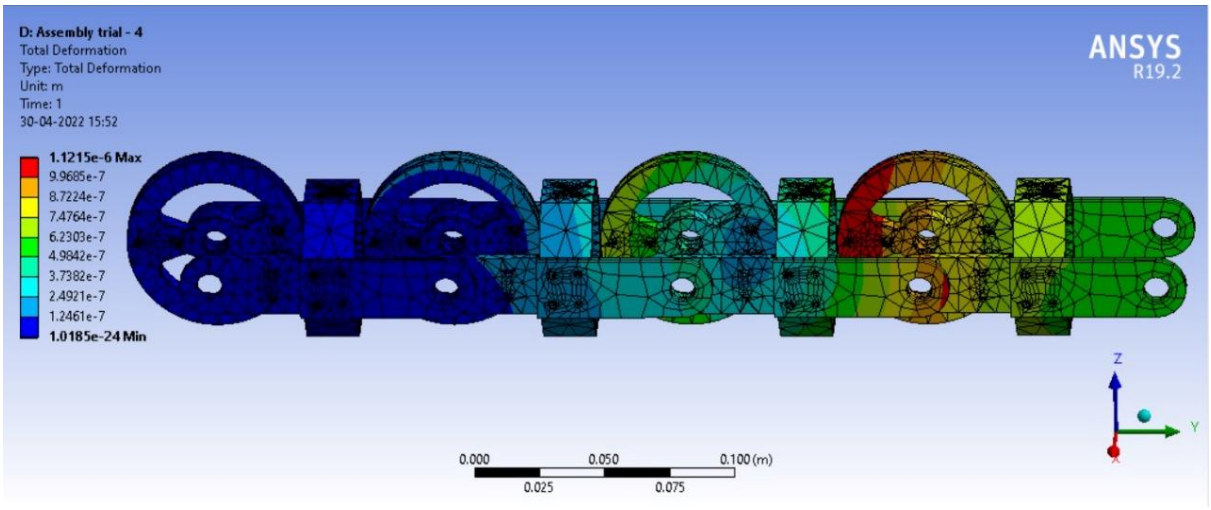

Maximum Principal Stress:

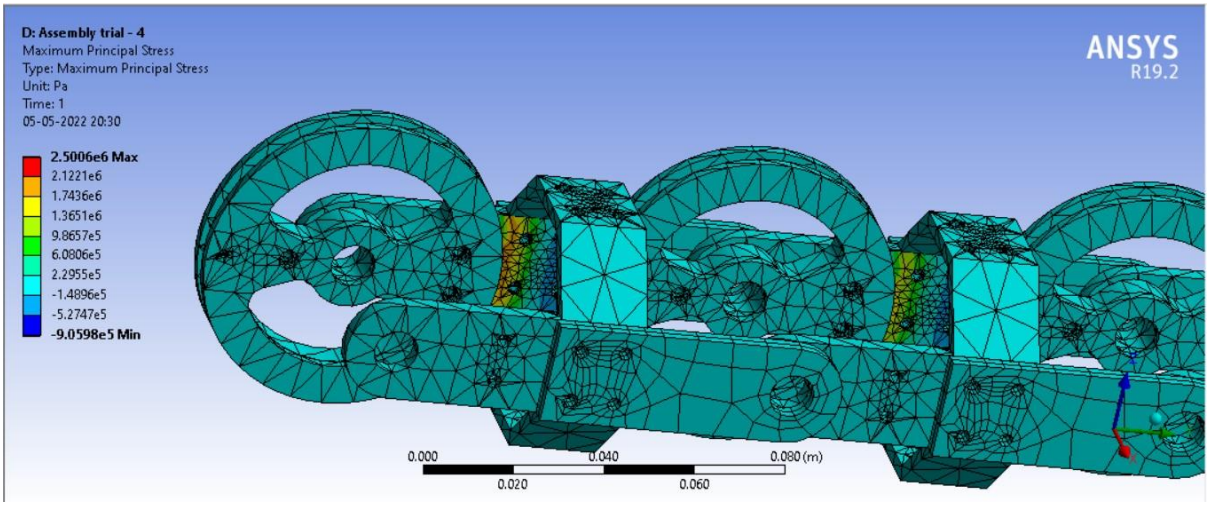

Fig 52- Meshing of arm

Output:

SPECIFICATION	VALUE
Max. Deformation	1.12 microns
Maximum Principal Stress	2.5 MPa

Conclusion: Safe

CHAPTER 5- Testing and Validation

Actuation and control assembly-

The entirety of the mechanism is driven by five components in a sequence: -

COMPUTER

↓

ARDUINO UNO

↓

CNC SHIELD A4988

↓

DRV 8255 STEPPER MOTOR DRIVER

↓

NEMA 17 STEPPER MOTOR

1.**ARDUINO UNO-**

Arduino is used to control actuation. Inputs are given as 'Action code' <degrees> <rpm>, Where actuation code is TT for Turntable and JT for joint

Arduino UNO is a low-cost, flexible, and easy-to-use programmable open-source microcontroller board that can be integrated into a variety of electronic projects. This board can be interfaced with other Arduino boards, Arduino shields, Raspberry Pi boards and can control relays, LEDs, servos, and motors as an output.

Arduino UNO features AVR microcontroller Atmega328, 6 analogue input pins, and 14 digital I/O pins out of which 6 are used as PWM output.

Fig 53-Arduino UNO

This board contains a USB interface i.e. A USB cable is used to connect the board with the computer and Arduino IDE (Integrated Development Environment) software is used to program the board.

The unit comes with 32KB flash memory that is used to store the number of instructions while the SRAM is 2KB and EEPROM is 1KB.

The operating voltage of the unit is 5V which projects the microcontroller on the board and its associated circuitry operates at 5V while the input voltage ranges between 6V to 20V and the recommended input voltage ranges from 7V to 12V.

Arduino UNO Components

The Arduino UNO board contains the following components and specifications:

ATmega328: This is the brain of the board in which the program is stored.

Ground Pin: there are several ground pins incorporated on the board.

PWM: the board contains 6 PWM pins. PWM stands for Pulse Width Modulation, using this process we can control the speed of the servo motor, DC motor, and brightness of the LED.

Digital I/O Pins: there are 14 digital (0-13) I/O pins available on the board that can be connected with external electronic components.

Analogue Pins: there are 6 analogue pins integrated on the board. These pins can read the analogue sensor and can convert it into a digital signal.

AREF: It is an Analog Reference Pin used to set an external reference voltage.

Reset Button: This button will reset the code loaded into the board. This button is useful when the board hangs up, pressing this button will take the entire board into an initial state.

USB Interface: This interface is used to connect the board with the computer and to upload the Arduino sketches (Arduino Program is called a Sketch)

DC Power Jack: This is used to power up the board with a power supply.

Power LED: This is a power LED that lights up when the board is connected with the power source.

Micro SD Card: The UNO board supports a micro SD card that allows the board to store more information.

3.3V: This pin is used to supply 3.3V power to your projects.

5V: This pin is used to supply 5V power to your projects.

VIN: It is the input voltage applied to the UNO board.

Voltage Regulator: The voltage regulator controls the voltage that goes into the board.

SPI: The SPI stands for Serial Peripheral Interface. Four Pins 10(SS), 11(MOSI), 12(MISO), 13(SCK) are used for this communication.

TX/RX: Pins TX and RX are used for serial communication. The TX is a transmit pin used to transmit the serial data while RX is a receive pin used to receive serial data.

Arduino UNO Pinout

There is a range of Arduino boards available in the market but the Arduino UNO is the most common board used in the electronic industry. The following figure shows the Arduino UNO Pinout for better understanding:

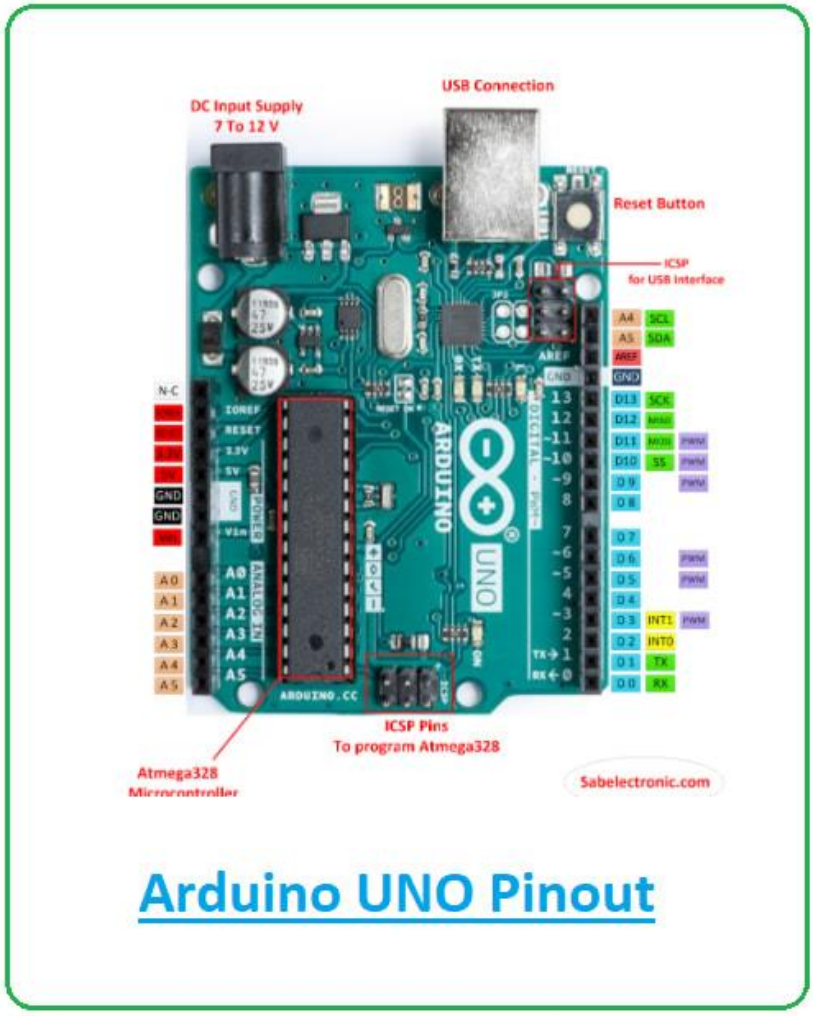

Fig 54- Arduino UNO pinout

Arduino Code

```
// This program rotates the motors for each rotor front and rear
// in clockwise or anticlockwise direction. It is made specifically
// to rotate the Stepper motors for the robotic arm.

// After connecting new Arduino, go to "Tools" - "Port" and it will
// find and set the correct port. Select the one which is connected to Arduino.

// table gear ratio driven to driving => 4:1
#define TABLE_RATIO 1

// defines pins numbers for base for speed
const int stepPin_table = 2;
// Direction PIN for rotating base
const int dirPin_table = 5;
```

```
// defines pins numbers for driving motor for speed
const int stepPin_jt = 3;
// Direction PIN for driving motor
const int dirPin_jt = 6;


// For DRV8825 a HIGH on pin 8 DISABLES the driver and
// LOW on this pin 8 ENABLES the driver.
const int enPin = 8;

// Each step for a stepper motor is 1.8 degrees.
// This makes 360 degrees / 1.8 degrees == 200 steps for one rotation.
// With 100 (M0 M1 M2) jumper setting, the motor moves (1.8) degrees per step.
// This means it needs 200 * 32 == 6400 steps per rotation.

String inpval = "";
String temp_str;
int table_deg;
int table_speed;

void rotateMotor(int degrees, float speed_rpm, const int ratio, const int stepPin, const int
dirPin){
  int steps;
  steps = ratio * degrees * (6400 / 360);

  if (degrees < 0){
    // Clockwise rotation
    digitalWrite(dirPin, LOW);

    steps = -1 * steps;
    }
  else if (degrees >= 0){
    // Anti Clockwise rotation
    digitalWrite(dirPin, HIGH);
    }

  unsigned int step_delay;
  if (speed_rpm > 0) {
    // formula: ((10^6 x 360) / (6400*step_delay*2))/6 = rpm
    step_delay = (3600000)/(64 * 12 * speed_rpm * ratio);
    Serial.println("Steps: " + String(steps));
    Serial.println("Delay: " + String(step_delay));

    for(int x = 0; x < steps; x++){
      digitalWrite(stepPin, HIGH);
      delayMicroseconds(step_delay);
      digitalWrite(stepPin, LOW);
      delayMicroseconds(step_delay);
      }
```

```
  }
 }


void setup() {

 Serial.begin(9600);

 // Sets the two pins as Outputs
 pinMode(stepPin_table,OUTPUT);
 pinMode(dirPin_table,OUTPUT);

 // Sets the two pins as Outputs
 pinMode(stepPin_jt,OUTPUT);
 pinMode(dirPin_jt,OUTPUT);

 pinMode(enPin,OUTPUT);
 digitalWrite(enPin,LOW);    // enable driver
}

void loop() {
 Serial.println("Command:");
 while (Serial.available() == 0)
 { }  //Wait for user input
 inpval = Serial.readString();

 // Serial format is TT <degrees> <rpm>
 // TT for turntable degrees +ve for CCW and -ve for CW
 table_deg = 0;
 table_speed = 20; // default values

 if (inpval.startsWith("TT") && (inpval.indexOf('<') != inpval.lastIndexOf('<')) ){

  temp_str = inpval.substring( inpval.indexOf('<')+1, inpval.indexOf('>'));
  table_deg = temp_str.toInt();
  temp_str = inpval.substring( inpval.lastIndexOf('<')+1, inpval.lastIndexOf('>'));
  table_speed = temp_str.toInt();
  Serial.println("Degrees: " + String(table_deg) + ", Speed(rpm): " + String(table_speed));
  rotateMotor(table_deg, table_speed, TABLE_RATIO, stepPin_table, dirPin_table);
  }
 else if (inpval.startsWith("JT") && (inpval.indexOf('<') != inpval.lastIndexOf('<')) ){

  temp_str = inpval.substring( inpval.indexOf('<')+1, inpval.indexOf('>'));
  table_deg = temp_str.toInt();
  temp_str = inpval.substring( inpval.lastIndexOf('<')+1, inpval.lastIndexOf('>'));
  table_speed = temp_str.toInt();
  Serial.println("Degrees: " + String(table_deg) + ", Speed(rpm): " + String(table_speed));
  rotateMotor(table_deg, table_speed, TABLE_RATIO, stepPin_jt, dirPin_jt);
  }
```

```
  else{
    Serial.println("Err: Invalid Input");
    }


  delay(500);
}
```

2. CNC SHIELD A4988-

CNC Shield V3.0 can be used as drive expansion board for engraving machine, 3D printer and other devices. There're 4 slots in the board for stepper motor drive modules, can drive 4 stepper motors, and each step stepper motor only need two IO port, that is to say, 6 IO ports can quite well to manage three stepper motor, it's very convenient to use. After insert CNC Shield V3.0 into OSOYOO Basic board, and installed GRBL firmware then you can quickly DIY a CNC engraving machine.

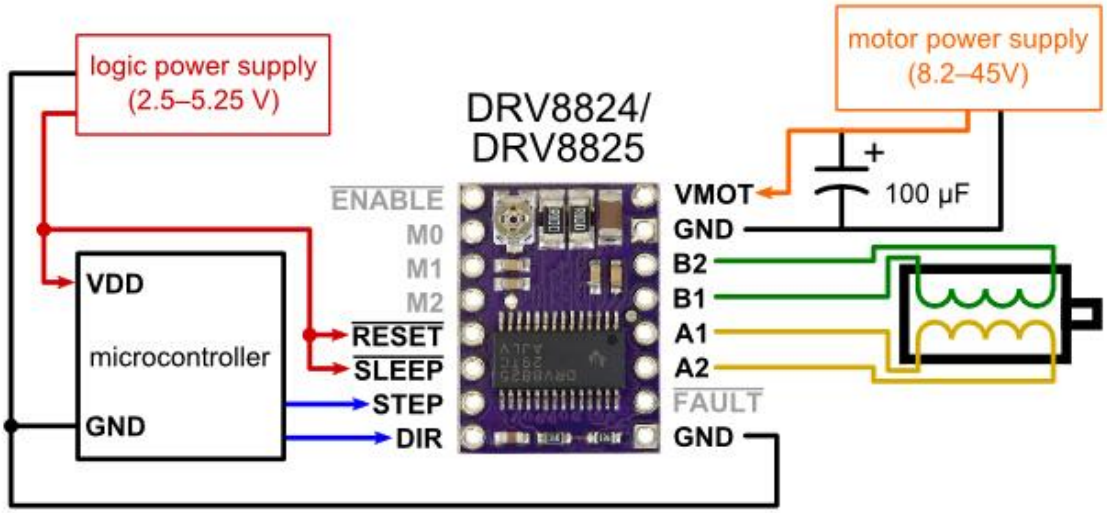

Minimal wiring diagram for connecting a microcontroller to a DRV8824/DRV8825 stepper motor driver carrier (full-step mode).

3.DRV 8255 STEPPER MOTOR DRIVER

This driver is a carrier board or breakout board for a DRV8825 stepper motor driver. This stepper motor driver lets you control one bipolar stepper motor at up to 2.2 A output current per coil Here are some of the driver's key features:

- Simple step and direction control interface
- Six different step resolutions: full-step, half-step, 1/4-step, 1/8-step, 1/16-step, and 1/32-step
- Adjustable current control lets you set the maximum current output with a potentiometer, which lets you use voltages above your stepper motor's rated voltage to achieve higher step rates
- Intelligent chopping control that automatically selects the correct current decay mode (fast decay or slow decay)
- 45 V maximum supply voltage
- Built-in regulator (no external logic voltage supply needed)
- Can interface directly with 3.3 V and 5 V systems
- Over-temperature thermal shutdown, over-current shutdown, and under-voltage lockout
- Short-to-ground and shorted-load protection
- 4-layer, 2 oz copper PCB for improved heat dissipation
- Exposed solderable ground pad below the driver IC on the bottom of the PCB
- Module size, pinout, and interface match those of our A4988 stepper motor driver carriers in most respects (see the bottom of this page for more information)

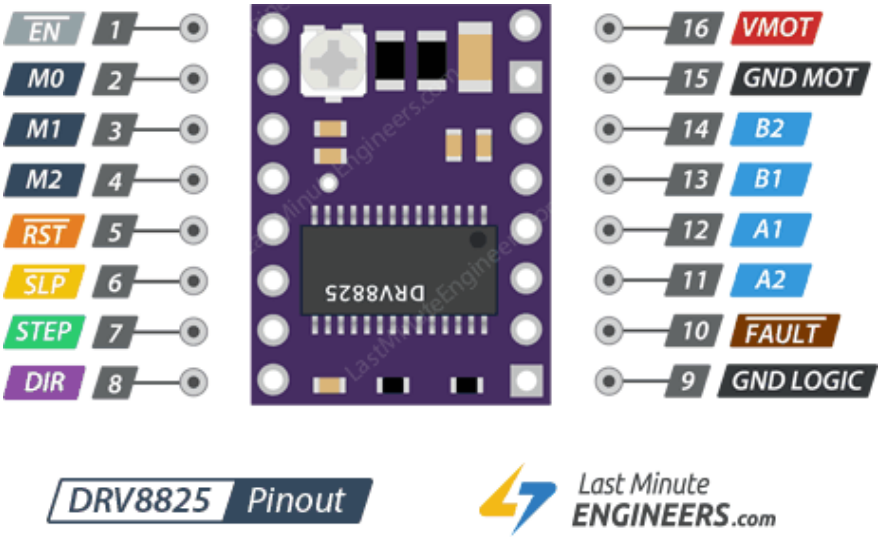

DRV8825 Pinout

Last Minute ENGINEERS.com

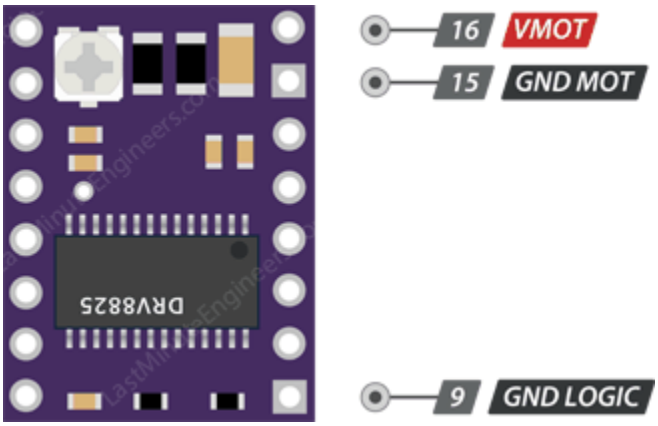

4.NEMA 17 STEPPER MOTOR WITH 1.8 STEP ANGLE

The stepper motors move in precisely repeatable steps, hence they are the motors of choice for the machines requiring precise position control. The Nema17 4.2 kg-cm Stepper motor can provide 4.2 kg-cm of torque at 1.7A current per phase.

The motor's position can be commanded to move or hold in one position with the help of Stepper Motor Drivers. The Nema17 4.2 kg-cm Stepper motor provides excellent response to starting, stopping, and reversing pulses from the stepper motor driver.

They are very useful in various applications, especially those which demand low speed with high precision. Many machines such as 3D Printers, CNC Router and Mills, Camera Platforms, XYZ Plotters, etc.

It is a brushless DC motor, so the life of this motor is dependent upon the life of the bearings. The position control is achieved by a simple Open Loop control mechanism so it doesn't require complex electronic control circuitry.

The motor's shaft has been machined for good grip with a pulley, drive gear, etc. and especially avoiding stall or slip.

1. The input pulse decides the rotation angle of the motor.
2. High accuracy of around 3 to 5% a step.
3. It provides good starting, stopping, and reversing.
4. Control of this motor is less costly because of the exclusion of complex control circuitry.
5. The speed is proportional to the frequency of the input pulses.

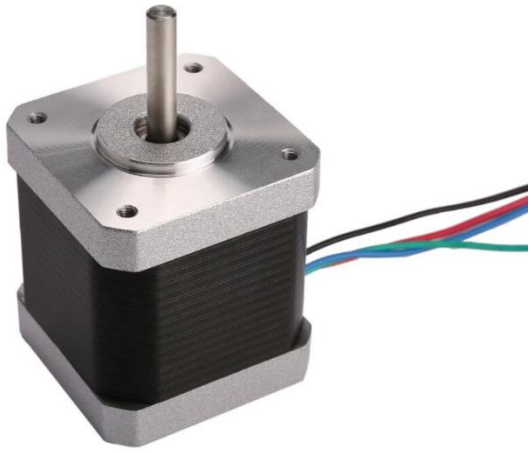

Fig 58- NEMA Stepper motor

5. KEVLAR WIRES-

After successful completion of our mini project(which included designing and prototyping a tension cable driven robotic arm module), we observed that the tension cables used to drive the robotic arm had a noticeable amount of slack in them, which in turn affected the robot accuracy at the output. To combat this problem , we are using Kevlar wires in our new design. Kevlar wires have the following advantages over other materials-

1. At its core Kevlar is an extremely lightweight, yet strong synthetic polymer that is weaved into a material that is 5 times stronger than steel when the weight is equal. Kevlar has an incredibly high tensile strength that is 8 times stronger than steel wire.
2. Kevlar fibre is a Para-aramid fibre with tensile strength of about 3,620 MPa and relative density of 1.44
3. It is slightly stronger at low temperatures. At higher temperatures the tensile strength is immediately reduced by about 10–20%, and after some hours the strength progressively reduces further.

Chapter 4- Actuation and control assembly

DH Parameters which govern the inverse kinematics of the arm-

Frames of reference of robot arms are represented using Denavit Hartenberg parameters. Invented by Jacques Denavit and Richard S. Hartenberg, these conventions use coordinate frames to describe the joints between two links so that one transformation is assigned with the joint, [Z], and the second is set with the link [X].
The series of coordinate transformations form the kinematic equation of the arm.

[T]=[Z1][X1][Z2][X2]...[Xn-1][Zn][Xn],
Where [T] is the transformation locating the end-link.

To determine the coordinate transformations [Z] and [X], the joints connecting the links are modelled as hinged or sliding joints, each of which has a unique line S in space that forms the joint axis and defines the relative movement of the two links. A typical serial robot is characterized by a sequence of six lines Si, i = 1,...,6, one for each joint in the robot. For each series of lines Si and Si+1, there is a common normal line Ai,i+1. The six joint axes Si and five common normal lines Ai,i+1 form the kinematic skeleton of the typical six degrees of freedom serial robot. Denavit and Hartenberg introduced the convention that Z coordinate axes are assigned to the joint axes Si, and X coordinate axes are assigned to the common normal Ai,i+1.

Where [Z]=

$$\begin{bmatrix} \cos\theta i & -\sin\theta i & 0 & 0 \\ \sin\theta i & \cos\theta i & 0 & 0 \\ 0 & 0 & 1 & di \\ 0 & 0 & 0 & 1 \end{bmatrix}$$

Where θi is the rotation around, and di is the slide along the Z-axis—either of the parameters can be constants depending on the robot's structure. Under this convention, the dimensions of each link in the serial chain are defined by the screw displacement around the common normal Ai,i+1 from the joint Si to Si+1, which is given as

[X]=

1	0	0	r i,i+1
0	cos **α**i,i+1	-sin	0
0	sin **α**i,i+1	**α**i,i+1	0
0	0	sin **α**i,i+1	1
		0	

The following four transformation parameters are known as D–H parameters: • d: offset along the previous z to the common normal • Θ: angle about the previous z, from old x to new x • r: length of the common normal. In revolute joint, this is the radius about previous z • α: angle about common normal, from old z-axis to new z-axis

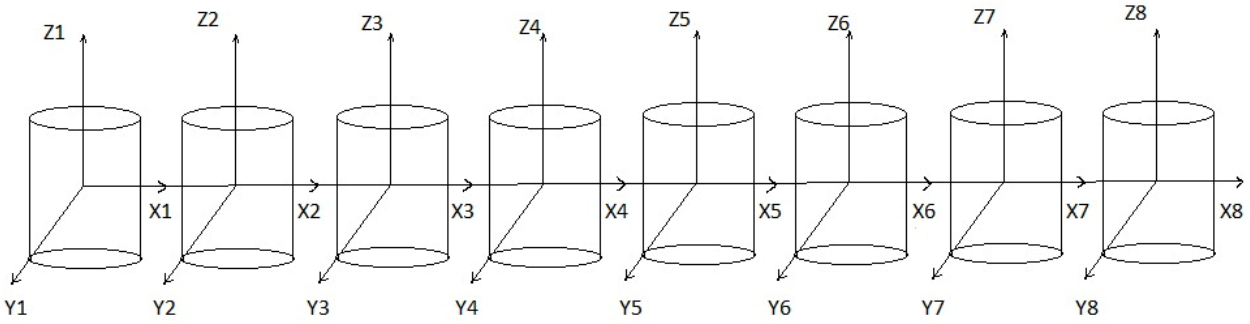

Hence for following system, the transform matrix is

Link	a_{i-1}	α_{i-1}	d_i	Θ_i	Range
1	l	0	0	Θ_1	0 to 180
2	l	0	0	Θ_2	-90 to 90
3	l	0	0	Θ_3	-90 to 90
4	l	0	0	Θ_4	-90 to 90
5	l	0	0	Θ_5	-90 to 90
6	l	0	0	Θ_6	-90 to 90
7	l	0	0	Θ_7	-90 to 90
8	l	0	0	Θ_8	-90 to 90

$T^0_8 = T^0_1\, T^1_2\, T^2_3\, T^3_4\, T^4_5\, T^5_6\, T^6_7\, T^7_8$

This transform matrix can be visualized in a python script to understand the work envelope and the work area accessible to the robot arm. It also allows to calculate cartesian location from joint angles.

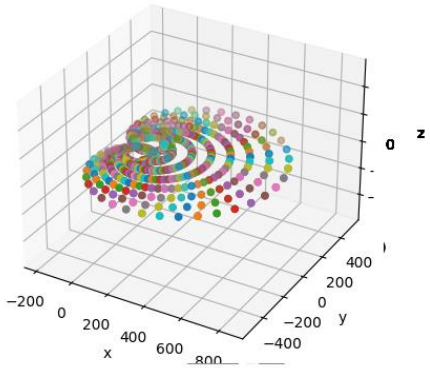

Inverse Kinematics

The end effector position in cartesian is often more useful than joint angle space for reach.
This reach calculation can be done using the inverse kinematics , which focuses on mapping end effector position to the joint space.
This generally is a complex problem as, unlike forward kinematics, a unique solution does not exist. Multiple solutions may be available in some cases while in some cases , no solutions may exist.

Generally, for a planar arm with more than 3 segments, analytical solutions become complex to solve. Hence, numerical methods may be far more optimal to achieve the necessary results. These use a Newton Raphson method based iterative solver to arrive to a required solution. This solver iterates random values till it reaches a point of convex in the graph.
Each iteration aims at reducing the error to a smaller value till it lies within an acceptable error margin. The calculation is performed by taking Jacobian of present and previous value, thus calculating position of end effector for required pose.

The flow of the inverse kinematics is given in the figure.

Thus, it is possible to calculate the angles for required pose.

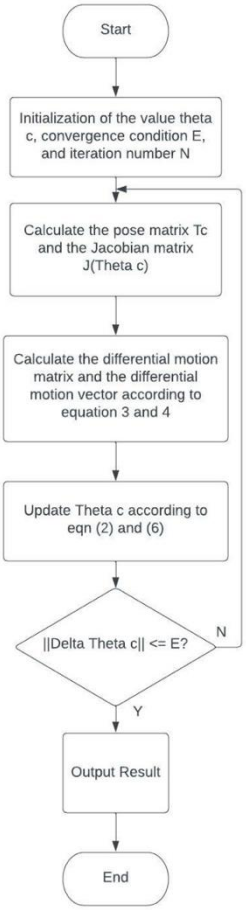

Values	End effector coordinates		Joint Angle values
	X coordinate	Y coordinate	
Initial	255	-255	-40, -30, -35, -20
Target	375	0	0,0,0,0

The actuation and position of actuator step by step with actuation from joint 1 to joint 4
In given table above an example of actuation is given. The Inverse kinematic algorithm utilizes present location and target location to calculate joint angles iteratively.

Step	Joint angle actuation (degrees)	X coordinate	Y coordinate
1-2	+40	320	-145
2-3	+30	365	-40
3-4	+35	0	380

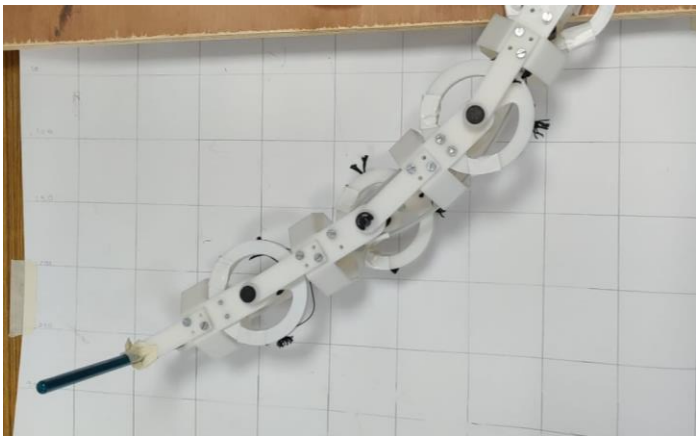

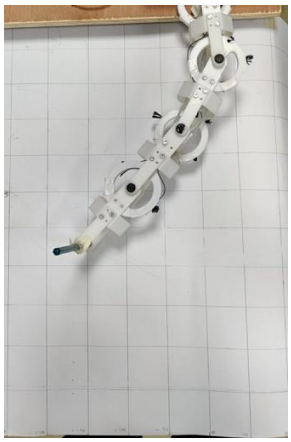

Figure 1 (left) Arm at initial position (right) step 1-2 (joint 1 actuated)

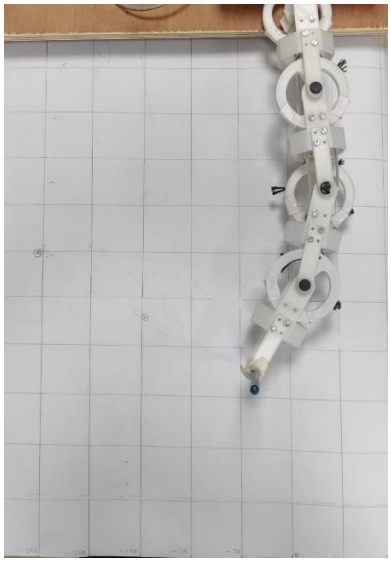

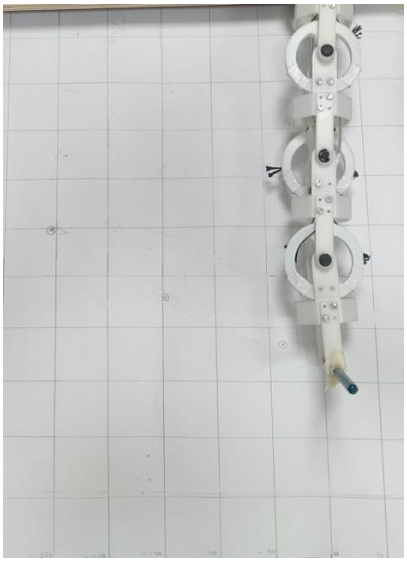

Figure 2 (Left) step 2-3 (joint 3 actuated) (Right) step 3-4 (joint 4 actuated)

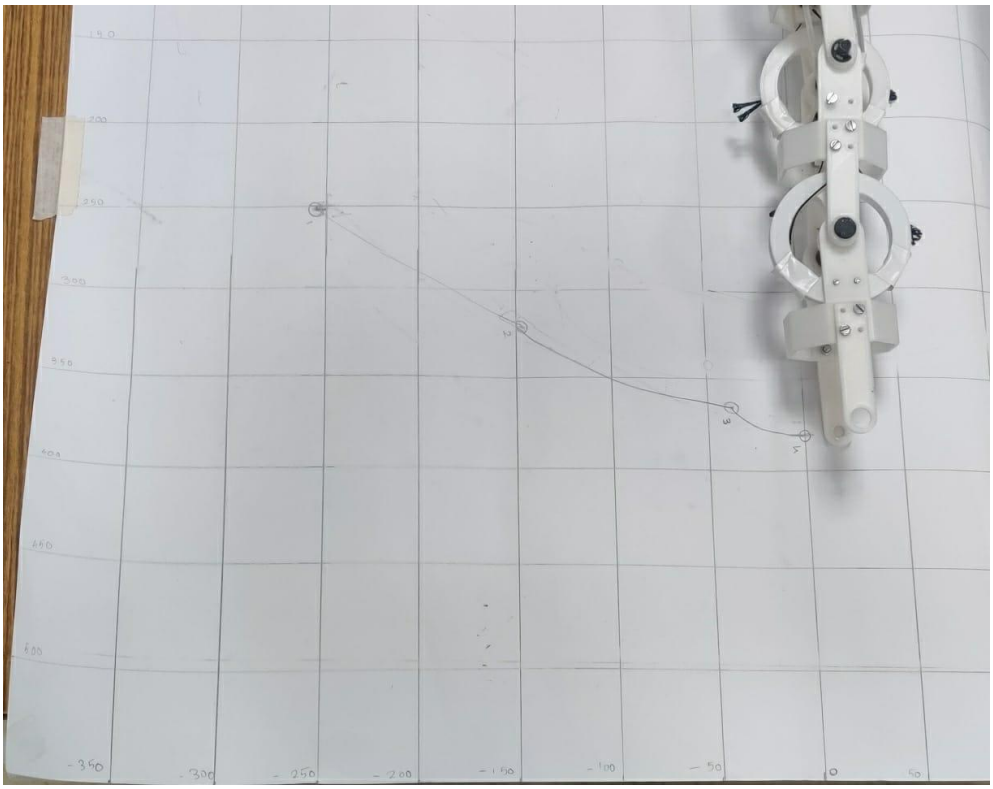

Figure 3 Complete traversed path

Stage 4 Prototyping

Introduction to the 3D printer in use-

Creality Ender 3 S1 printer- Some features of this printer are-

Molding technology: FDM

Printer dimensions: 487 x 453 x 622 mm

Build size: 220 x 220 x 270 mm

Type of Extruder: “Sprite” Direct Extruder

Leveling method: Manual leveling

Nozzle temperature: ≤ 260℃

Hotbed temperature: ≤ 100℃

This 3D printer allows you to print intricate shapes made of PLA with high precision and accuracy. We used the printer to 3D print the different components of the arm assembly as well as the mechanical multiplexer as well as the actuation assembly.

1. Components were Fabricated using 3D printing and CNC acrylic cutting.

2. Testing was done for various loading conditions, positions, angles, accuracy etc.

3. Mathematical model of Forward and Inverse Kinematics was developed for simulations and autonomous control.

4. Optimization of control algorithm and automatic operation development.

Testing and Validation:

Prototype assembly:

The prototype is currently assembled for validation of system and ensure if system can perform motion commands. 4 Modules were assembled and tests related to motion tests, positional accuracy and angular accuracy (for single module) are tested for the following.

Path traversed by end effector is plotted using a pencil to plot how it travels. A 5 x 5 cm matrix of lines is used to measure positional accuracy.

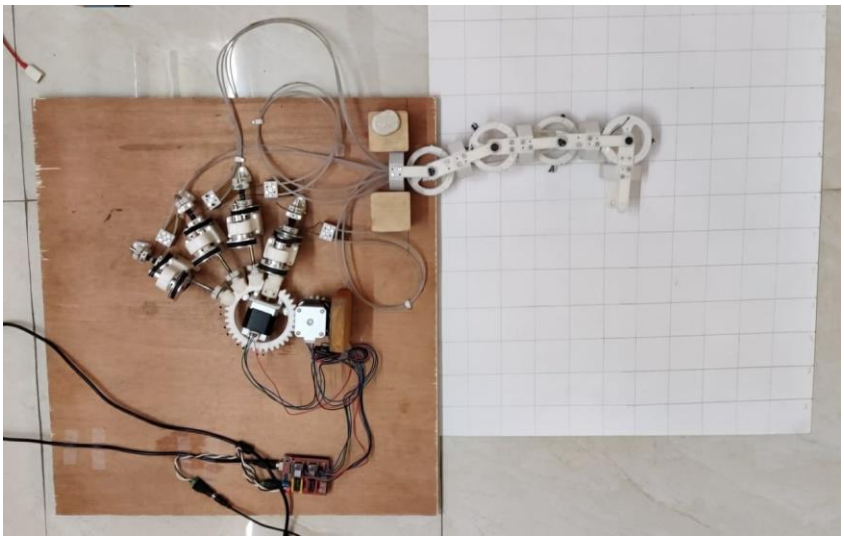

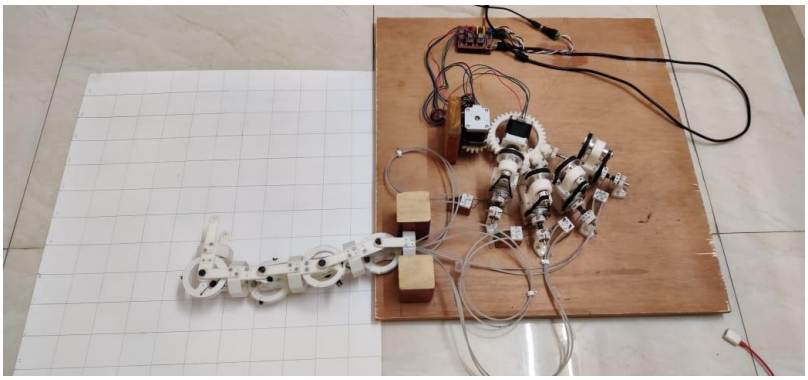

I. Motion tests

Motion tests were performed to confirm ability of the arm to move through required angles and perform action of motions required.

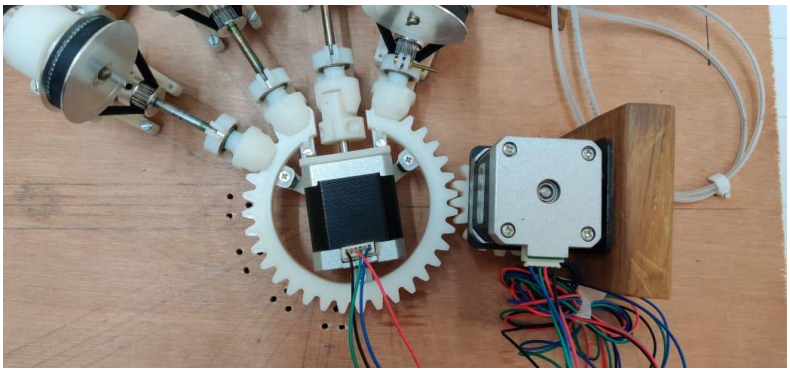

Figure 4 The multiplexer selecting joint 2 for actuation

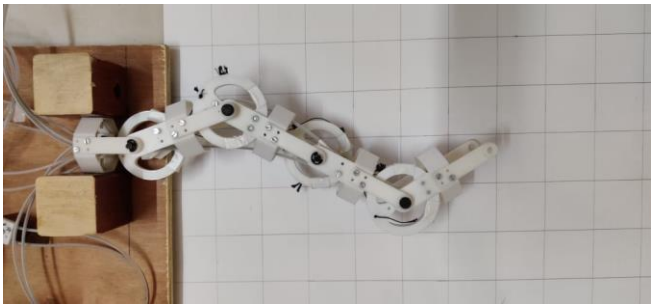
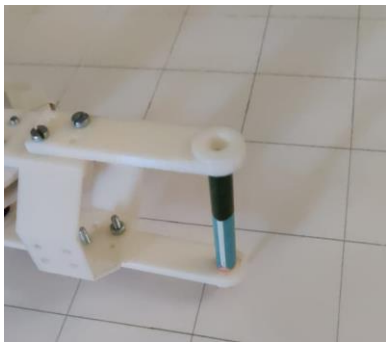

Figure 5 Initial position of arm

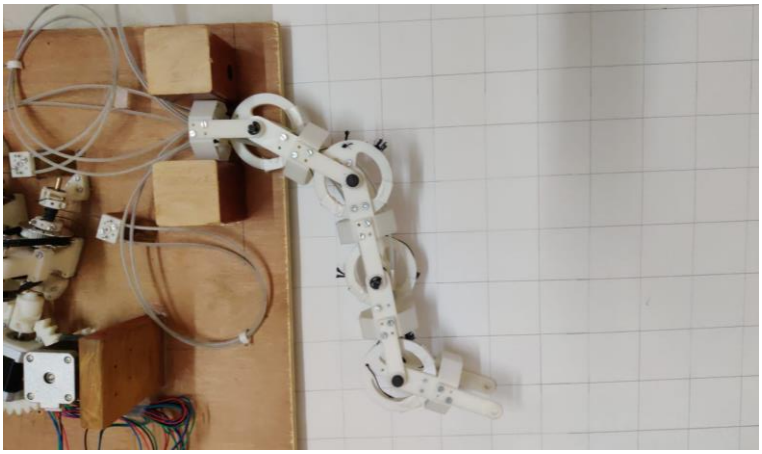
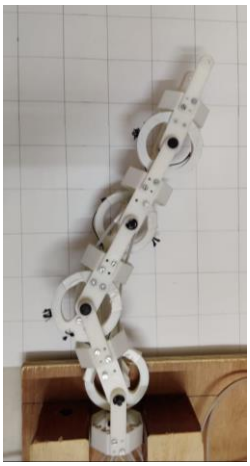

Figure 6 Final position of arm

Arm was actuated to test the mechanical multiplexer joint selection and joint rotation. Arm was able to travel the required angles without any problems.

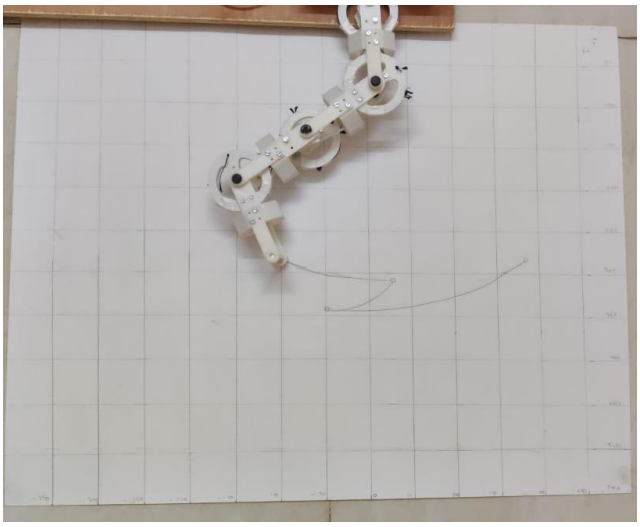

Figure 7 Path tracing of the robot arm.

II. Single actuator angular Accuracy test:

Initially, tests were performed to check accuracy of joint angle for one joint. Results for measurements are as follows.

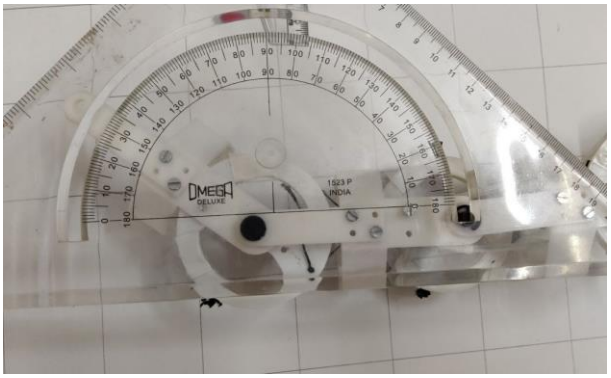

Test Results:

Clockwise is Negative, Counterclockwise is positive

Sr. No.	Input Value of angle (degrees)	Measured value of angle (degrees)				Error
		Reading 1	Reading 2	Reading 3	Average	
1	0	0	1	-1	0	0
2	30	30	32	28	30.6	0.6
3	44	46	44	48	45.3	0.3
4	60	62	64	58	61	1
5	74	72	72	76	73	-1
6	90	90	88	88	89.3	-1.3

The test results show the arm has a resolution of 2 degrees with a variation of +/- 1 degree. This variation is within acceptable range for robot arm in the sewage cleaning application.

Positional accuracy test:

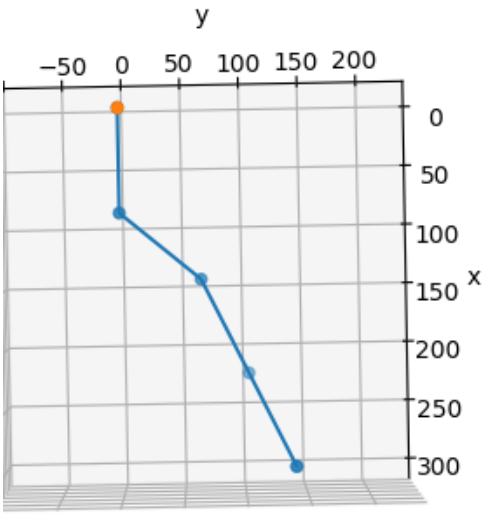

Figure 8 Position of end efffector in Forward kinematic simulation vs position of end effector in actual value

No.	Axis	Position (calculated) (mm)	Position (Measured) (mm)	Error(mm) = True value - Measured
1	X	302	292	-10
	Y	148	156	-8
2	X	0	2	2
	Y	300	296	4

The measurements show the arm has an positional accuracy in the range of +/- 10 mm.
This may be due to following factors:

1. Error in the joint angle of actuators getting magnified
2. Slackness in cable due to inconsistencies.
3. Measurement errors in the system
4. Step loss in the Stepper motors due to high force.
5. Friction of Tendons in Bowden tubes
6. Extension of Kevlar in the Bowden tubes.

CHAPTER 6- CONCLUSION

Summary of Progress

- As an improvement to our previous design, we have started and completed working on the design of a mechanical multiplexer as a limb selector for our arm. We have finished the design and FEA analysis of the multiplexer.

- We went through two different iterations of models of the mechanical multiplexer involving components like a sliding linear mechanism, a geared reducer mechanism, but finally decided on using a shaft based locking mechanism for the required reduction as it offers the most simple and manageable design with good accuracy.

- We will be using a Bowden cable mechanism to actuate the limbs with satisfactory precision.

- We have decided to replace the hollow universal joint (used in mini project) with a simple joint (knuckle type) actuated with a pulley mechanism.

Market Survey

Mechanical Multiplexer BOM

Cost estimation				
Description	Material	Qty.	Rate (Rs.)	Cost(Rs.)
Flex Kwik bond	Liquid bond	1	50	50
M3 screws 20mm long	SS	40	2	80
M3*50mm bolt and nut set	SS	15	3.933333	59
M2*8mm socket head cap bolt and nut set	SS	12	16.53333	198.4
M3 screws 30mm long	SS	80	2	160
M5 Rods 75mm long	SS	10	6	60
GT2 timing pulley 60 teeth 6mm width	Aluminium	16	249	3984
GT2 timing pulley 20 teeth 6mm width	Aluminium	16	100	1600
GT2 timing belt 6mm width	Rubber	16	149	2384
Radial Ball bearing (5 x 16 x 5)	SS 625zz	48	33.75	1620
Shielded radial ball bearing (8 x 19 x6)	SS 698zz	4	49.75	199
M3*15mm hex standoff female to female spacer	Nylon	25	2.6	65
M3 Nylock nuts	SS and nylon rubber	50	3.76	188
M2*8mm CSK countersunk Philips head screw	SS	50	2.38	119
M3 screws 20 mm long	SS	40	2	80
M3 screws 10 mm long	SS	30	1.5	45
M3 Nut	SS	42	1	42
M2 Screws 10 mm long	SS	32	4	128
Metal pins 6mm	CI	8	4	32
Nylon Tube 10 m ID 1.5 mm	Nylon	300	2	600
1Kg PLA Filament	PLA	1	1224	1224
Kevlar Tendon cable 100 feet	Kevlar	800	1	800
Plywood base 2x2 feet	Wood	224	1	224
NEMA 17 Stepper 5.6 kgf-cm bipolar type		2	700	1400
Arduino Uno		1	900	900
A4988 CNC shield		1	200	200
DRV 8825 Stepper driver		2	300	600
4 Pin stepper cable		2	20	40
M3 Nylon standoff spacers 15 mm length	Nylon	10	16	160
3 mm ID washers	Steel	50	0.5	25
Total				**17266.4**

Possible Improvements:

- Addition of a Potentiometer/optical encoder for better accuracy
- Initiation of closed loop feedback system for better dimensional precision
- Mounting of cameras/ other aid for visual inspection

Future Scope

Since our model is extremely light, sturdy, flexible and maneuverable, It has the following applications-

1. Could be used with a camera for visual inspection of disaster-stricken areas like the aftermath of earthquakes, which are inaccessible to human intervention. This search operation could help save human lives.
2. Has the potential to be used underwater to explore the ocean.
3. Could be used for mining applications, such as metal detection, finding cracks and faults in mines.
4. If fitted with the appropriate equipment, it could be used in the construction of tunnels and underground passages.

Conclusion

We have designed and prototyped a light and compact robotic tentacle mechanism which is simple to implement. The easy folding feature of the model allows it to be transported easily. We hope to explore more possibilities and uses of this mechanism with addons like a camera for computer vision, or fingers for gripping and other sensors.

In the report we have discussed the design and parameters required for design of the multiplexer, the requirements related to quantization of the input from multiplexer and the design of the arm to operate with the bowden tubes.

Further, dh table, forward kinematics and inverse kinematics using python was used to verify results from the prototype and the actual device and the ideal values. These results show promising utility of this arm and further development can lead to greater accuracy and higher reliability.

References-

[1] Design and Modelling of a Minimally Serial Robot, IEEE Robotics and Automation Letters (Volume: 5, Issue: 3, July 2020) Actuated . Yotam Ayalon, Lior Damti and David Zarrouk

https://ieeexplore.ieee.org/document/9126155

[2] Super Dragon: A 10 m-long Coupled Tendon-driven Articulated Manipulator Gen Endo1, Atsushi Horigome2 and Atsushi Takata1

IEEE Robotics and Automation Letters (Volume: 4, Issue: 2, April 2019) https://ieeexplore.ieee.org/document/8624267

[3] Design of Tendon-Driven Manipulators

Lung-Wen Tsai Professor, Mechanical Engineering Department and Institute for Systems Research, University of Maryland, College Park, MO 20742 Fellow ASM Published Online: June 1, 1995

https://asmedigitalcollection.asme.org/mechanicaldesign/article-abstract/117/B/80/432260/Design-of-Tendon-Driven-Manipulators?redirectedFrom=fulltext

[4] Kinematic comparison of surgical tendon-driven manipulators and concentric tube manipulators Zheng Lia,∗ , Liao Wub , Hongliang Renc , Haoyong Yuc

Mechanism and Machine TheoryVolume 107, January 2017, Pages 148-165 https://www.sciencedirect.com/science/article/abs/pii/S0094114X16302580

[5] A Review of Motion Planning Algorithms for Robotic Arm Systems Shuai Liu[0000-0001-6939-494X] and Pengcheng Liu[0000-0003-0677-4421] https://eprints.whiterose.ac.uk/168146/1/LR_7.pdf

[6] A General Mechanical Model for Tendon-Driven Continuum Manipulators

Federico Renda, Student Member, IEEE and Cecilia Laschi, Member, IEEE

https://www.researchgate.net/publication/239763442_A_general_mechanical_model_for_tendon-driven_continuum_manipulators

[7] SIMBA: Tendon-Driven Modular Continuum Arm with Soft Reconfigurable Gripper Anand Kumar Mishra1,2*, Emanuela Del Dottore1,2, Ali Sadeghi1, Alessio Mondini1 and Barbara Mazzolai1

https://www.frontiersin.org/articles/10.3389/frobt.2017.00004/full

[8] Physical Human-Robot Interaction with a Lightweight, Elastic Tendon Driven Robotic Arm Modeling, Control, and Safety Analysis

https://d-nb.info/1107769965/34

[9] Design of a Weight-compensated and Coupled Tendon-driven Articulated Long-reach Manipulator

Atsushi Horigome1, Gen Endo2, Koichi Suzumori2 and Hiroyuki Nabae2

https://link.springer.com/chapter/10.1007/978-3-319-49058-8_60

[10] Design of Modular Re-configurable Robotic System for Construction and DigitalFabrication Milica Vujović Aleksandar Rodićlija Stevanović https://link.springer.com/chapter/10.1007/978-3-319-49058-8_60

[11] Design of Modular Re-configurable Robotic System for Construction and Digital Fabrication

Milica Vujovic Mihajlo Pupin Institute,Aleksandar RodićMihajlo Pupin Institute,Ilija StevanovicUniversity of Belgrade Mihailo Pupin Institute

https://www.researchgate.net/figure/Hyper-redundant-tendon-driven-robot-manipulator-3_fig2_311098885

[12] Kinematics Rapid Modeling Method of Tendon-Driven Robotic Mechanisms Using the Tendon-Routing Matrix and Equivalent Radius Matrix https://www.researchgate.net/figure/ACTIVE-TENDON-DRIVEN-BY-AN-ACTUATOR_fig2_303481715

[13] A Hybrid Electromagnetic and Tendon-Driven Actuator for Minimally Invasive Surgery. Haochen Wang, Saihui Cui, Yao Wang and Chengli Song

https://go.gale.com/ps/i.do?id=GALE%7CA638435913&sid=googleScholar&v=2.1&it=r&linkaccess=abs&issn=20760825&p=AONE&sw=w&userGroupName=anon%7E9fed6f73

[14] Mechatronic design and genetic-algorithm-based MIMO fuzzy control of adjustable-stiffness tendon-driven robot finger https://ms.copernicus.org/articles/9/277/2018/

[15] Kinematic and compliance analysis for tendon-driven robotic mechanisms with flexible tendons

Sun-LaiChangaJyh-JoneLeebHome-CheYenb

https://www.sciencedirect.com/science/article/abs/pii/S0094114X05000066

[16] Comparison of typical 3D printing materials http://2015.igem.org/wiki/images/2/24/CamJIC-Specs-Strength.pdf

[17] https://github.com/lanius/tinyik

[18] https://github.com/kubakos/forward-kinematics

Assembly drawing

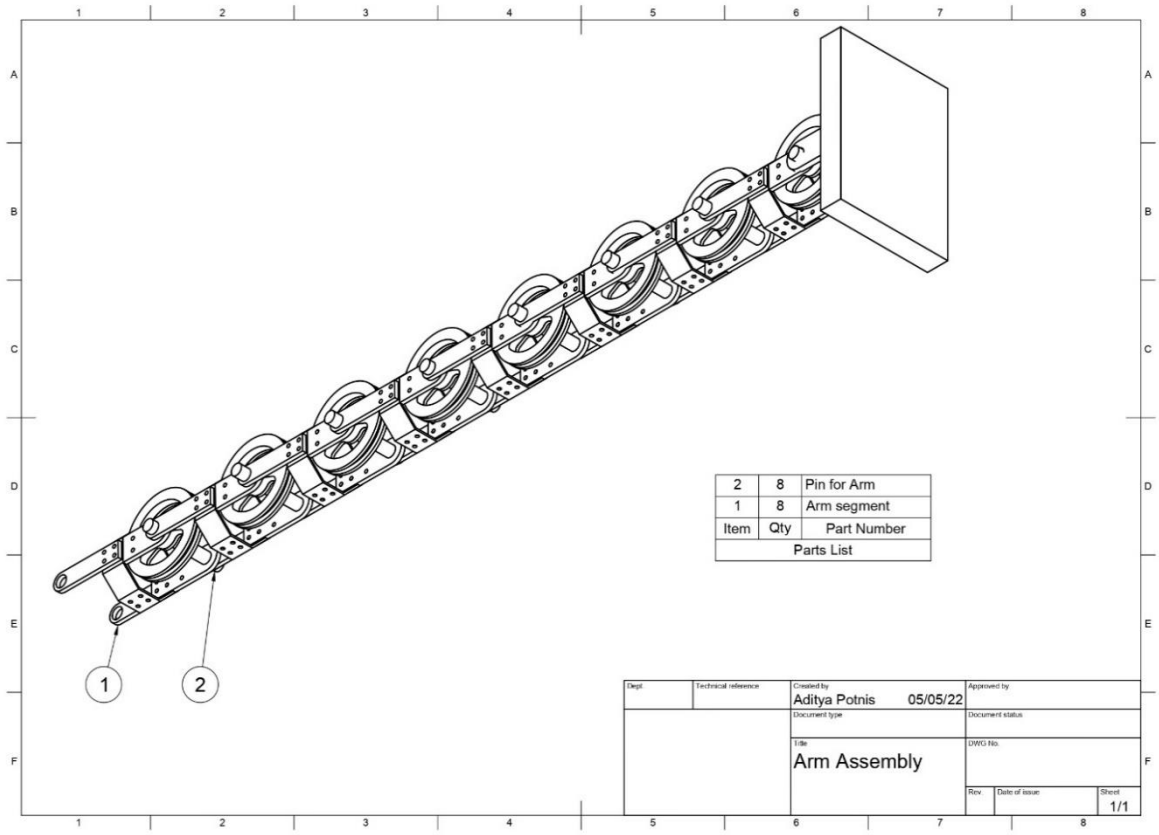

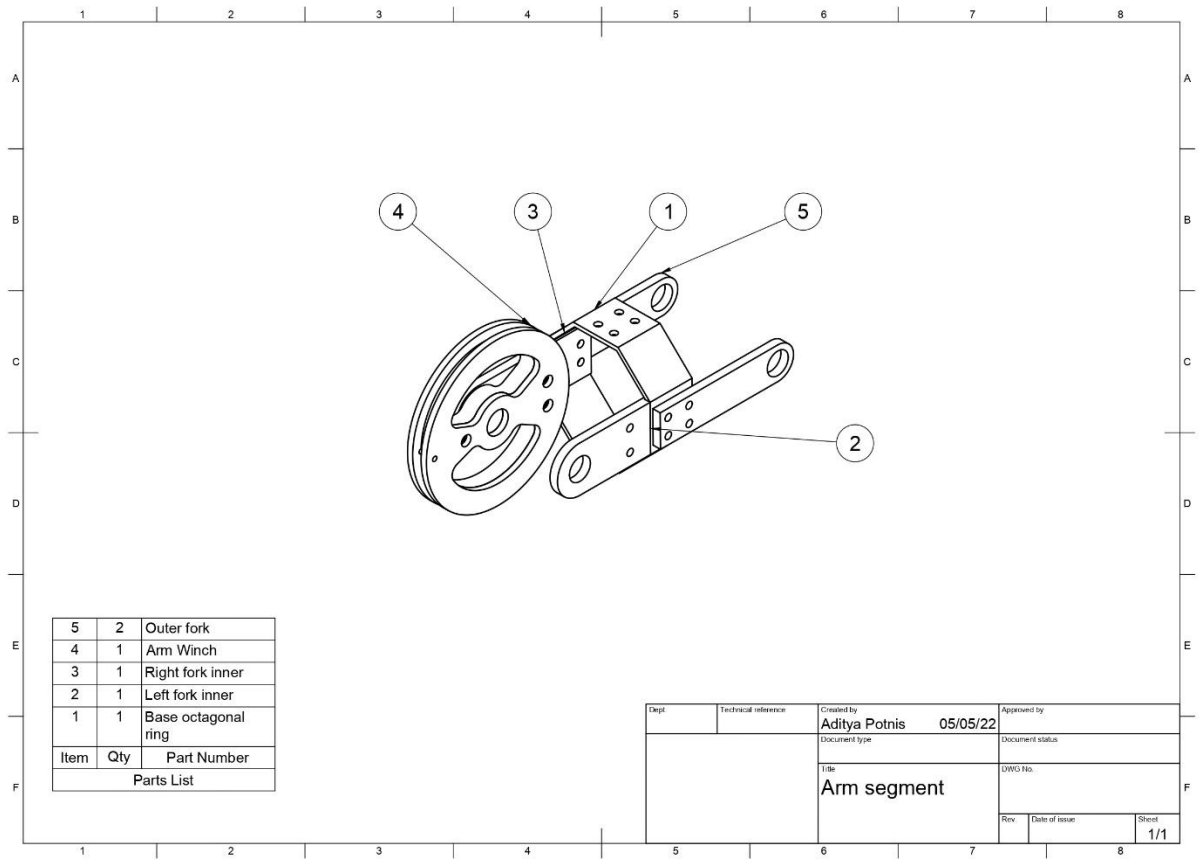

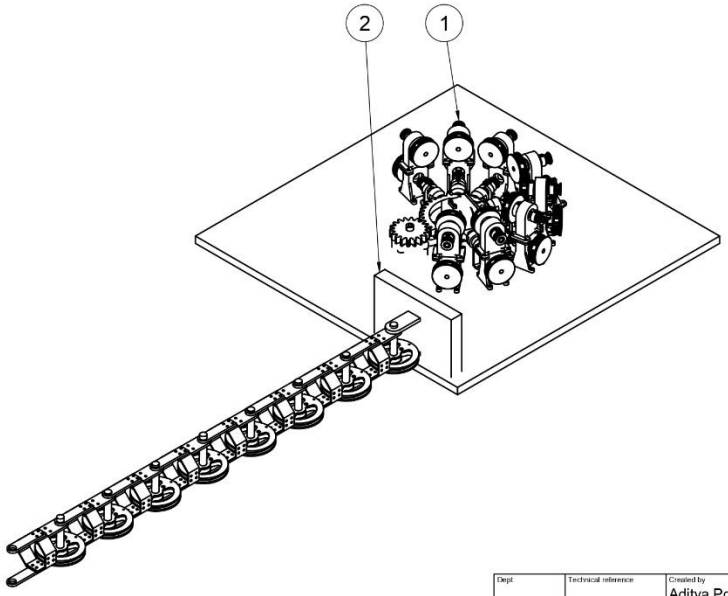

Item	Qty	Part Number
2	1	Arm Assembly
1	1	Multiplexer

Parts List

Dept	Technical reference	Created by: Aditya Potnis 05/05/22	Approved by
		Document type	Document status
		Title: Full assembly	DWG No.
			Rev. / Date of issue / Sheet: 1/1

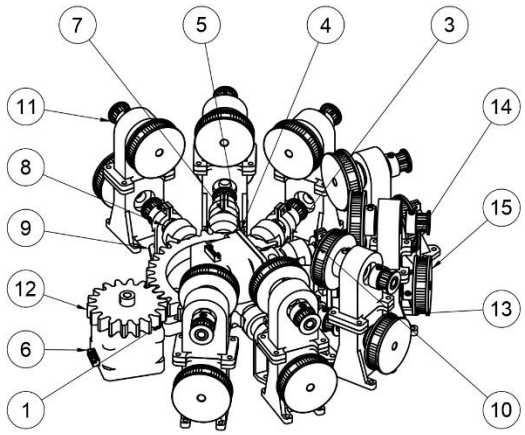

Item	Qty	Part Number
1	1	RA_Spider
2	1	Component1
3	1	Hand
4	1	Ring2
5	1	Nema 17 Mount
6	2	NEMA 17
7	8	Knob
8	8	Rod 6mm
9	9	Bearing Mount
10	1	SKF_625_2Z
11	16	GT2_20T
12	1	Pinion 2
13	8	Compund reducer lower mount
14	8	Compound reducer upper mount
15	16	GT2_Pully_60T_6 mm

Parts List

Dept	Technical reference	Created by: Aditya Potnis 05/05/22	Approved by
		Document type	Document status
		Title: Multiplexer	DWG No.
			Rev. / Date of issue / Sheet: 1/1

Appendix 2) Python code

tf.py (used for forward kinematics)

```
#!/usr/bin/env python3
from math import radians, sin, cos
import numpy as np


class HomogeneousMatrix(object):
    # Creates a homogeneous matrix.

    def __init__(self):
        # [0,0] - [2,2] rotation
        # [0,3] - [2,3] position
        # [3,0] - [3,2] perspective parameters
        # [3,3] scale factor

        self.matrix = np.identity(4)

    def __getitem__(self, key):
        return self.matrix[key]

    def get(self):
        return self.matrix

    def roll(self, angle_X):
        # Rotates the homogeneous matrix by angle_X by the X axis

        rolled_by = np.identity(4)
        rolled_by[1, 1] = cos(radians(angle_X))
        rolled_by[1, 2] = -(sin(radians(angle_X)))
        rolled_by[2, 1] = sin(radians(angle_X))
        rolled_by[2, 2] = cos(radians(angle_X))

        self.matrix = np.dot(self.matrix, rolled_by)

    def pitch(self, angle_Y):
        # Rotates the homogeneous matrix by angle_Y by the Y axis

        pitched_by = np.identity(4)
        pitched_by[0, 0] = cos(radians(angle_Y))
        pitched_by[0, 2] = sin(radians(angle_Y))
        pitched_by[2, 0] = -(sin(radians(angle_Y)))
        pitched_by[2, 2] = cos(radians(angle_Y))

        self.matrix = np.dot(self.matrix, pitched_by)
```

```
def yaw(self, angle_Z):
    # Rotates the homogeneous matrix by angle_Z by the Z axis

    yawed_by = np.identity(4)
    yawed_by[0, 0] = cos(radians(angle_Z))
    yawed_by[0, 1] = -(sin(radians(angle_Z)))
    yawed_by[1, 0] = sin(radians(angle_Z))
    yawed_by[1, 1] = cos(radians(angle_Z))

    self.matrix = np.dot(self.matrix, yawed_by)

def set_pos(self, posX, posY, posZ):
    # Sets the position of the homogeneous matrix

    self.matrix[0, 3] = posX
    self.matrix[1, 3] = posY
    self.matrix[2, 3] = posZ

def set_perspective(self, X, Y, Z):
    # Sets the perspective parameter of the homogeneous matrix

    self.matrix[3, 0] = X
    self.matrix[3, 1] = Y
    self.matrix[3, 2] = Z

def set_scale(self, scale):
    # Sets the scale parameter of the homogeneous matrix

    self.matrix[3, 3] = scale

def set_a(self, a):
    # Sets the 'a' parameter of the DH convention

    self.matrix[0, 3] = a

def set_alpha(self, alpha):
    # Sets the 'alpha' parameter of the DH convention

    self.roll(alpha)

def set_d(self, d):
    # Sets the 'd' parameter of the DH convention

    self.matrix[2, 3] += d

def set_theta(self, theta):
    # Sets the 'theta' parameter of the DH convention

    self.yaw(theta)
```

```
    def set_parent(self, parent):
        self.matrix = np.dot(parent, self.matrix)
```

Plotter.py (Used for plotting forward kinematics)

```
#!/usr/bin/env python3
# https://stackoverflow.com/questions/13685386/matplotlib-equal-unit-length-with-equal-aspect-ratio-z-axis-is-not-equal-to

from tf import HomogeneousMatrix
from mpl_toolkits.mplot3d import Axes3D
import matplotlib.pyplot as plt
from matplotlib import cm
import numpy as np


def set_axes_equal(ax):
    '''Make axes of 3D plot have equal scale so that spheres appear as spheres,
    cubes as cubes, etc..  This is one possible solution to Matplotlib's
    ax.set_aspect('equal') and ax.axis('equal') not working for 3D.

    Input
      ax: a matplotlib axis, e.g., as output from plt.gca().
    '''

    x_limits = ax.get_xlim3d()
    y_limits = ax.get_ylim3d()
    z_limits = ax.get_zlim3d()

    x_range = abs(x_limits[1] - x_limits[0])
    x_middle = np.mean(x_limits)
    y_range = abs(y_limits[1] - y_limits[0])
    y_middle = np.mean(y_limits)
    z_range = abs(z_limits[1] - z_limits[0])
    z_middle = np.mean(z_limits)

    # The plot bounding box is a sphere in the sense of the infinity
    # norm, hence I call half the max range the plot radius.
    plot_radius = 0.5*max([x_range, y_range, z_range])

    ax.set_xlim3d([x_middle - plot_radius, x_middle + plot_radius])
    ax.set_ylim3d([y_middle - plot_radius, y_middle + plot_radius])
    ax.set_zlim3d([z_middle - plot_radius, z_middle + plot_radius])

data_list = []
# --- Robotic Arm construction ---
#   Joint Angle variables
a = 96    # Link length

q1, q2, q3 = 0, 0, 0
q4, q5, q6 = 0, 0, 0
q7, q8 = 0, 0
```

```
#   ---------------------

for q1 in range(-90, 91, 2):
    q2 = q1
    q3 = q1
    q4 = q1
    q5 = q1
    q6 = q1
    q7 = q1
    q8 = q1



    base = HomogeneousMatrix()
    joint1 = HomogeneousMatrix()
    joint2 = HomogeneousMatrix()
    joint3 = HomogeneousMatrix()
    joint4 = HomogeneousMatrix()
    joint5 = HomogeneousMatrix()
    joint6 = HomogeneousMatrix()
    joint7 = HomogeneousMatrix()
    joint8 = HomogeneousMatrix()

    joint1.set_a(a)
    joint1.set_theta(q1)


    joint2.set_a(a)
    joint2.set_theta(q2)

    joint3.set_a(a)
    joint3.set_theta(q3)

    joint4.set_a(a)
    joint4.set_theta(q4)

    joint5.set_a(a)
    joint5.set_theta(q5)

    joint6.set_a(a)
    joint6.set_theta(q6)

    joint7.set_a(a)
    joint7.set_theta(q7)

    joint8.set_a(a)
    joint8.set_theta(q8)

    # ---------------------------------
```

```
    joint1.set_parent(base.get())
    joint2.set_parent(joint1.get())
    joint3.set_parent(joint2.get())
    joint4.set_parent(joint3.get())
    joint5.set_parent(joint4.get())
    joint6.set_parent(joint5.get())
    joint7.set_parent(joint6.get())
    joint8.set_parent(joint7.get())

    # Prepare the coordinates for plotting

    X = [base[0, 3], joint1[0, 3],
        joint2[0, 3], joint3[0, 3],
        joint4[0, 3], joint5[0, 3],
        joint6[0, 3], joint7[0, 3],
        joint8[0, 3]]
    Y = [base[1, 3], joint1[1, 3],
        joint2[1, 3], joint3[1, 3],
        joint4[1, 3], joint5[1, 3],
        joint6[1, 3], joint7[1, 3],
        joint8[1, 3]]
    Z = [base[2, 3], joint1[2, 3],
        joint2[2, 3], joint3[2, 3],
        joint4[2, 3], joint5[2, 3],
        joint6[2, 3], joint7[2, 3],
        joint8[2, 3]]

    # Plot

    ax = plt.axes(projection='3d')
    # ax.set_aspect('equal')
    ax.plot3D(X, Y, Z)
    ax.scatter(X, Y, Z)
    ax.scatter(X[0], Y[0], Z[0]) # origin point

    ax.set_xlabel('x')
    ax.set_ylabel('y')
    ax.set_zlabel('z')
    data_list.append((X, Y, Z))
    set_axes_equal(ax)
    plt.savefig(str(q5) + '.png')

def final_plot(data_list, name):
    ax = plt.axes(projection='3d')
    # ax.set_aspect('equal')
    ax.set_xlabel('x')
    ax.set_ylabel('y')
    ax.set_zlabel('z')
    for row in data_list:
        ax.scatter(row[0], row[1], row[2])
```

```
for row in data_list:
    ax.scatter(row[0], row[1], row[2])


set_axes_equal(ax)


plt.show()
plt.savefig(name)
```